AN INVESTIGATION INTO THE POTENTIAL OF NFM, DEG AND TEG AS REPLACEMENT SOLVENTS FOR NMP IN SEPARATION PROCESSES

Mark Williams-Wynn

[BSc. (Eng)]

Submitted in partial fulfilment of the requirements for the degree of Master of Science in the School of Chemical Engineering at the University of KwaZulu-Natal

UNIVERSITY OF KWAZULU-NATAL

January 2012

Supervisors: Prof. D. Ramjugernath
Dr P. Naidoo

Preface

The work presented in this dissertation was performed in the Thermodynamics Research Unit laboratories in the School of Chemical Engineering at the University of KwaZulu-Natal from January 2011 to December 2011. The work was supervised by Professor D. Ramjugernath and Doctor P. Naidoo.

This dissertation is submitted as a requirement for the degree of MSc. in Chemical Engineering. All of the work presented in this dissertation is original, unless otherwise stated, and this work has not (in whole or in part) been previously submitted to any tertiary institute as part of a degree.

_____

Mark Williams-Wynn

As supervisor of this candidate, I approve this dissertation for submission:

_____ _____

Professor D. Ramjugernath Doctor P. Naidoo

Acknowledgements

- All glory to my Lord, Jesus Christ. Colossians 3 vs. 17.

- An acknowledgement of the assistance and guidance of the supervisors of the research undertaken, Prof. Deresh Ramjugernath and Dr Paramespri Naidoo, is necessary.

- The financial support of the National Research Foundation (NRF) is acknowledged.

- The help and advice of the Thermodynamics Research Unit's laboratory technicians, Mr Lindenkosi Mkize and Mr Ayanda Khanyile, and the School of Chemical Engineering's workshop staff, Mr Leon Augustyn and Mr Ken Jack was greatly appreciated.

- An acknowledgement of Dr Prashant Reddy, Mr Jim Chiyen and Mr Kaniki Tumba is required for their assistance with understanding the experimental procedures for gas-liquid chromatography.

Abstract

Optimisation attempts within the petrochemical industry have led to interest in alternate solvents. The most widely used commercial solvents for the separation of hydrocarbons, by extractive distillation, are N-methylpyrrolidone and sulfolane. There has also been reference made to other solvents, such as N-formylmorpholine and the ethylene glycols [mono-, di-, tri- and tetra], being used. The alternate solvents proposed for this study were N-formylmorpholine, triethylene glycol and diethylene glycol. Infinite dilution activity coefficients, γ^{∞}, provided a means of comparing the ease of separation of the different solutes using different solvents in extractive distillation.

There is a substantial database of γ^{∞} measurements for systems involving N-methylpyrrolidone and hydrocarbons. A fairly large data set of γ^{∞} values of hydrocarbons in N-formylmorpholine has also been measured. Very little work has been conducted on the γ^{∞} values of hydrocarbons in either diethylene glycol or triethylene glycol.

Gas liquid chromatography is one of the more common methods used to measure γ^{∞}. To enable the measurement of γ^{∞} at higher temperatures, a pre-saturator was installed prior to the column. This ensured that the carrier gas entering the column was saturated with solvent and prevented the elution of solvent from the column.

The γ^{∞} values of 25 solutes; including n-alkanes, alk-1-enes, alk-1-ynes, alcohols and aromatics; were measured at temperatures of 333.15, 348.15 and 363.15 K. The γ^{∞} measurements in N-formylmorpholine were used to verify this experimental set up and technique. Once the experimental set up had been proven, γ^{∞} in N-methylpyrrolidone, triethylene glycol and diethylene glycol were measured. Selectivities and capacities, at infinite dilution, of several solute combinations in the four solvents were then compared. In a few of these separation cases, the alternative solvents appeared to have better separation performance than N-methylpyrrolidone.

The γ^{∞} values of three of the solutes in N-formylmorpholine and N-methylpyrrolidone were also measured using the novel cell design and measurement procedure suggested by Richon. It was found that this new technique required further development for the case of volatile solvents, since the results obtained using this technique did not compare favourably with the literature data.

Contents

1. Preface iii
2. Acknowledgements v
3. Abstract vii
4. Contents ix
5. List of figures xiii
6. List of tables xvii
7. List of photographs xix
8. Nomenclature xxi
1. Introduction 1
   1.1 Extractive distillation 2
      1.1.1 Industrial applications 3
      1.1.2 Solvent screening 3
   1.2 Infinite dilution activity coefficient 4
   1.3 Systems for comparison 4
2. Literature review of techniques 7
   2.1 Measurement techniques 7
      2.1.1 Extrapolation from VLE data 8
      2.1.2 Ebulliometry 8
      2.1.3 Gas-liquid chromatography 8
      2.1.4 Inert gas stripping 8
      2.1.5 Headspace gas chromatography 9
   2.2 Gas-liquid chromatography 9
      2.2.1 Background 9
      2.2.2 Method 9
      2.2.3 Pre-saturators 10
   2.3 Dilutor cell technique 12
      2.3.1 Background 12
      2.3.2 Method 15
3. Equipment description and operation 17
   3.1 Gas-liquid chromatography 17

3.1.1 Shimadzu GC-2014 and AOC 20i+s 19
3.1.2 Bubble flow meter 20
3.1.3 Reference stream pre-saturation 21
3.1.4 Pre-saturators 22
3.1.5 Column length 25
3.1.6 Column preparation 27
3.1.7 Operational procedure 28
3.1.8 Experimental uncertainties 29
3.2 Dilutor cell technique 30
3.2.1 Operational procedure 32
3.2.2 Experimental uncertainties 33
4. Theory 35
4.1 Infinite dilution activity coefficient 35
4.1.1 Prediction 36
4.2 Gas-liquid chromatography 36
4.2.1 Everett (1965) 37
4.2.2 Laub and Pecsok 38
4.2.3 Correlations for physical properties 38
4.3 Inert gas stripping 45
5. Literature data 47
5.1 N-formylmorpholine 47
5.2 N-methylpyrrolidone 54
5.3 Triethylene glycol 59
5.4 Diethylene glycol 62
6. Results and discussion 63
6.1 Calibrations 63
6.2 Gas-liquid chromatography 64
6.2.1 Uncertainty analysis 65
6.2.2 Experimental method 65
6.2.3 Hexadecane test system 68
6.2.4 N-formylmorpholine test system 71
6.2.5 N-methylpyrrolidone 80
6.2.6 Triethylene glycol 85
6.2.7 Diethylene glycol 89

6.3 Dilutor cell technique 91
6.3.1 Uncertainty analysis 91
6.3.2 N-formylmorpholine 91
6.3.3 N-methylpyrrolidone 94
6.3.4 Experimental method 96
6.3.5 Viability of technique 98
6.4 Selectivities and capacities 98
6.4.1 Cyclohexane/benzene 100
6.4.2 n-Heptane/cyclohexane 101
6.4.3 n-Heptane/toluene 102
6.4.4 n-Hexane/hex-1-ene 103
6.4.5 Hex-1-ene/hex-1-yne 104
6.4.6 n-Hexane/benzene 105
6.4.7 Benzene/methanol 106
7. Conclusions 107
8. Recommendations 109
9. References 111
10. Appendix A 119
11. Appendix B 121
12. Appendix C 123
13. Appendix D 125
14. Appendix E 129

List of figures

Figure 2-1: Generalised configuration of a gas-liquid chromatography experimental set up 10

Figure 2-2: Dilutor flask as proposed by Leroi et al. (1977) 13

Figure 2-3: Dilutor cell proposed by Richon et al. (1980) 14

Figure 2-4: Generalised dilutor cell configuration 15

Figure 3-1: Schematic of gas-liquid chromatography set up 18

Figure 3-2: Schematic of a Shimadzu TCD 19

Figure 3-3: Approach to equilibrium in the vapour phase against height of N-methylpyrrolidone as a function of helium bubble diameter 24

Figure 3-4: Recorded output from the thermal conductivity detector of the Shimadzu GC-2014, for propan-1-ol in N-methylpyrrolidone at 333.2 K using the 1m column 26

Figure 3-5: Recorded output from the thermal conductivity detector of the Shimadzu GC-2014, for propan-1-ol in N-methylpyrrolidone at 363.2 K, using the 0.3m column 26

Figure 3-6: Experimental set up for measurement of infinite dilution activity coefficients using inert gas stripping 30

Figure 4-1: The second virial coefficient as a function of temperature for n-hexane 39

Figure 4-2: The second virial coefficient as a function of temperature for benzene 40

Figure 4-3: The second virial coefficient as a function of temperature for ethanol 40

Figure 4-4: The second virial coefficient as a function of temperature for ethanol 42

Figure 4-5: Molar volume and extrapolated partial molar volumes at infinite dilution of (2) for the binary system; benzene (1) and N-methylpyrrolidone (2) at various temperatures 45

Figure 5-1: Literature $\ln(\gamma^{\infty})$ for n-hexane (1) in NFM (3) 49

Figure 5-2: Literature $\ln(\gamma^{\infty})$ for cyclohexane (1) in NFM (3) 49

Figure 5-3: Literature $\ln(\gamma^{\infty})$ for hex-1-ene (1) in NFM (3) 50

Figure 5-4: Literature $\ln(\gamma^{\infty})$ for benzene (1) in NFM (3) 50

Figure 5-5: Literature $\ln(\gamma^{\infty})$ for n-hexane (1) in NMP (3) 55

Figure 5-6: Literature $\ln(\gamma^{\infty})$ for cyclohexane (1) in NMP (3) 55

Figure 5-7: Literature $\ln(\gamma^{\infty})$ for hex-1-ene (1) in NMP (3) 56

Figure 5-8: Literature $\ln(\gamma^{\infty})$ for benzene (1) in NMP (3) 56

Figure 5-9: Literature $\ln(\gamma^{\infty})$ for n-heptane (1) in TEG (3) 59

Figure 5-10: Literature $\ln(\gamma^{\infty})$ for n-octane (1) in TEG (3) 60

Figure 5-11: Literature ln(γ^{∞}) for benzene (1) in TEG (3) 60

Figure 6-1: Temperature calibration for the Pt-100. 63

Figure 6-2: Residuals for the calibration of the Pt-100 64

Figure 6-3: Vapour pressure as a function of temperature 66

Figure 6-4: Measured ln(γ^{∞}) including error bars and literature ln(γ^{∞}) against 1000/T for n-hexane (1) in hexadecane (3) 68

Figure 6-5: Measured ln(γ^{∞}) including error bars and literature ln(γ^{∞}) against 1000/T for cyclohexane (1) in hexadecane (3) 68

Figure 6-6: Measured ln(γ^{∞}) including error bars and literature ln(γ^{∞}) against 1000/T for benzene (1) in hexadecane (3) 69

Figure 6-7: Measured ln(γ^{∞}) including error bars and literature ln(γ^{∞}) against 1000/T for n-hexane (1) in N-formylmorpholine (3) 71

Figure 6-8: Measured ln(γ^{∞}) including error bars and literature ln(γ^{∞}) against 1000/T for cyclohexane (1) in N-formylmorpholine (3) 71

Figure 6-9: Measured ln(γ^{∞}) including error bars and literature ln(γ^{∞}) against 1000/T for hex-1-ene (1) in N-formylmorpholine (3) 72

Figure 6-10: Measured ln(γ^{∞}) including error bars and literature ln(γ^{∞}) against 1000/T for benzene (1) in N-formylmorpholine (3) 72

Figure 6-11: Sensitivity of the infinite dilution activity coefficient of various solutes in N-formylmorpholine at 333.2 K to variations of 10% in various parameters 78

Figure 6-12: Measured ln(γ^{∞}) and literature ln(γ^{∞}) against 1000/T for n-hexane (1) in N-methylpyrrolidone (3) 80

Figure 6-13: Measured ln(γ^{∞}) and literature ln(γ^{∞}) against 1000/T for cyclohexane (1) in N-methylpyrrolidone (3) 81

Figure 6-14: Measured ln(γ^{∞}) and literature ln(γ^{∞}) against 1000/T for hex-1-ene (1) in N-methylpyrrolidone (3) 81

Figure 6-15: Measured ln(γ^{∞}) and literature ln(γ^{∞}) against 1000/T for benzene (1) in N-methylpyrrolidone (3) 82

Figure 6-16: Measured ln(γ^{∞}) and literature ln(γ^{∞}) against 1000/T for n-heptane (1) in triethylene glycol (3) 85

Figure 6-17: Measured ln(γ^{∞}) and literature ln(γ^{∞}) against 1000/T for benzene (1) in triethylene glycol (3) 85

Figure 6-18: Elution of n-hexane from N-formylmorpholine at 333 K; natural logarithm of initial signal over signal as a function of time 92

Figure 6-19: ln(γ^{∞}) against 1000/T for n-hexane (1) in N-formylmorpholine (2) 92

Figure 6-20: ln(γ^{∞}) against 1000/T for n-heptane (1) in N-formylmorpholine (2) 93

Figure 6-21: ln(γ^{∞}) against 1000/T for cyclohexane (1) in N-formylmorpholine (2) 93

Figure 6-22: ln(γ^{∞}) against 1000/T for n-hexane (1) in N-methylpyrrolidone (2). 95

Figure 6-23: ln(γ^{∞}) against 1000/T for n-heptane (1) in N-methylpyrrolidone (2) 95

Figure 6-24: ln(γ^{∞}) against 1000/T for cyclohexane (1) in N-methylpyrrolidone (2) 96

Figure 6-25: Selectivities of various solvents against temperature for the combination of cyclohexane (1) and benzene (2) 100

Figure 6-26: Selectivities of various solvents against temperature for the combination of n-heptane (1) and cyclohexane (2) 101

Figure 6-27: Selectivities of various solvents against temperature for the combination of n-heptane (1) and toluene (2) 102

Figure 6-28: Selectivities of various solvents against temperature for the combination of n-hexane (1) and hex-1-ene (2) 103

Figure 6-29: Selectivities of various solvents against temperature for the combination of hex-1-ene (1) and hex-1-yne (2) 104

Figure 6-30: Selectivities of various solvents against temperature for the combination of n-hexane (1) and benzene (2) 105

Figure 6-31: Selectivities of various solvents as a function of temperature for the combination of benzene (1) over methanol (2) 106

List of tables

Table 1-1: Industrial applications of extractive distillation..... 3
Table 1-2: Combinations for which the performance of various solvents in extractive distillation was compared..... 5
Table 3-1: Experimental uncertainties for gas-liquid chromatography technique..... 29
Table 3-2: Experimental uncertainties for dilutor cell technique..... 33
Table 5-1: Techniques and temperatures utilised for previous γ^{∞} measurements in NFM..... 47
Table 5-2: Excess enthalpy and standard deviation of various solutes in NFM from regression of literature data..... 51
Table 5-3: Literature Values for γ^{∞} in NFM..... 52
Table 5-4: Techniques and temperatures utilised for previous γ^{∞} measurements in NMP..... 54
Table 5-5: Excess enthalpy and standard deviation of various solutes in NMP from regression of literature data..... 57
Table 5-6: Literature Values for γ^{∞} in NMP..... 58
Table 5-7: Techniques and temperatures utilised for previous γ^{∞} measurements in TEG..... 59
Table 5-8: Infinite dilution activity coefficient data for various solutes in TEG..... 61
Table 5-9: Techniques and temperatures utilised for previous γ^{∞} measurements in DEG..... 62
Table 5-10: Infinite dilution activity coefficients for various solutes with DEG at 298.15 K.... 62
Table 6-1: Solvents used; with their refractive index (measured and literature) and their measured purity..... 66
Table 6-2: Measured γ^{∞} data, literature γ^{∞} data and percentage error with respect to literature data for the systems of several hydrocarbon solutes in hexadecane..... 70
Table 6-3: Measured γ^{∞} and percentage error from literature data for the hydrocarbon solutes in N-formylmorpholine..... 73
Table 6-3 cont.: Measured γ^{∞} and percentage error from literature data for the hydrocarbon solutes in N-formylmorpholine..... 74
Table 6-4: Comparison of results calculated using the equation of Everett (1965) and the equation of Laub and Pecsok (1978) for selected solutes in N-formylmorpholine..... 76
Table 6-5: Measured γ^{∞} and percentage error from literature data for the hydrocarbon solutes in N-methylpyrrolidone..... 83

Table 6-6: Measured γ^{∞} and percentage error from literature data for the hydrocarbon solutes in triethylene glycol..... 86
Table 6-7: Measured γ^{∞} and calculated error of measurement of hydrocarbon solutes in diethylene glycol. 89
Table 6-8: Values of the infinite dilution activity coefficient of three solutes in N-formylmorpholine at 333 K measured utilising the dilutor cell technique..... 94
Table 6-9: Values of the infinite dilution activity coefficient of three solutes in N-methylpyrrolidone at 333 K measured utilising the dilutor cell technique. 94
Table 6-10: Effect of vapour volume on the infinite dilution activity coefficient for n-hexane and n-heptane in NMP. 97
Table 6-11: Selectivities of NFM, NMP, TEG and DEG for several hydrocarbon combinations at 333.2K. 98
Table 6-12: Selectivities of NFM, NMP, TEG and DEG for several hydrocarbon combinations at 348.2K. 99
Table 6-13: Selectivities of NFM, NMP, TEG and DEG for several hydrocarbon combinations at 363.2K. 99
Table 6-14: Capacities, k_i, of the various solvents for benzene. 100
Table 6-15: Capacities of the various solvents for cyclohexane 101
Table 6-16: Capacities of the various solvents for toluene 102
Table 6-17: Capacities of the four solvents for hex-1-ene 103
Table 6-18: Capacities of the four solvents for hex-1-yne 104
Table 6-19: Capacities of the four solvents for methanol 106
Table A-1: Special atomic and structural diffusion volumes for use in the FSG equation proposed by Fuller et al. (1966). 120
Table C-1: Critical properties for the solutes and for helium used for the calculation of the infinite dilution activity coefficients.. 123
Table C-2: Vapour pressure correlation constants 124
Table D-1: Comparison of three equations of state..... 125

List of photographs

Photograph 2-1: New dilutor cell for the measurement of infinite dilution activity coefficients by inert gas stripping, proposed by Richon (2011a). 14

Photograph 3-1: Gas-liquid chromatography set up 17

Photograph 3-2: Bubbles from the ¼ inch tubing distributor 25

Photograph 3-3: Bubbles from the 0.05mm capillary tube distributor..... 25

Nomenclature

α_i	SRK parameter
$\alpha_{i,j}$	Relative volatility/Interaction parameter
γ_i	Activity coefficient
μ	Dipole moment [deBye]
v_L	Kinematic viscosity of liquid [m^2s^{-1}]
v_t	Atomic or structural diffusion volume
φ_i	Fugacity coefficient
τ	Ratio for P_i^0 correlation
τ_G	Approach to equilibrium
τ_{ij}	UNIQUAC parameter
ω_i	Acentric factor
A	Parameter (regressed)/Antoine's equation parameter/EOS parameter
a	Parameter (EOS)/P_i^0 correlation parameter
B	Parameter (regressed)/Antoine's equation parameter/EOS parameter
B_{ij}	Second virial interaction coefficient [m^3mol^{-1}]
b	Parameter (EOS)/P_i^0 correlation parameter
C	Antoine's equation parameter
C	Pressure correlation parameter
D	Helium gas flow (Dilutor method) [m^3s^{-1}]
$D_{i,j}^G$	Diffusion coefficient of i in gas j [m^2s^{-1}]
d	P_i^0 correlation parameter
E	P_i^0 correlation parameter
F	P_i^0 correlation parameter
$f^{(i)}$	Function i
f_i	Fugacity, pure species i
$\hat{f}_i$	Fugacity, species i in solution
$\bar{G}_i^E$	Excess Gibbs energy [$J.mol^{-1}$]
h	Path length of bubbles in solution [m]
h_i	Signal magnitude [V]
H_i^E	Excess enthalpy of component i [$J.mol^{-1}$]
$I_{C\,i,j}$	Interaction ionisation potential [$J.mol^{-1}$]
J_2^3	Column pressure correction factor

K_i	Vapour/liquid equilibrium ratio
k_i	Capacity
M_L	Molecular mass of solvent [kg.mol^{-1}]
m_i	SRK slope of temperature dependence
$N_{i,j}$	Number of carbon atoms for McGlashan & Potter equation.
n_i	Number of moles [mol]
P_c	Critical Pressure [Pa]
P_i	Pressure [Pa]
P_i^0	saturated vapour pressure [Pa]
q	Pure component molecular structure constant (area)
q'	Modified pure component molecular structure constant (area)
q_i	Volumetric flow rate [m^{3}s^{-1}]
R	Ideal gas constant [J.mol^{-1}K^{-1}]
R_b	Bubble radius [m]
r	Pure component molecular structure constant (size)
$S_{ij,s}$	Selectivity of component i over component j, in solvent s
S	GC peak area
T	Temperature [K]
t_R	Retention time (GLC) [s]
t	Time (dilutor method) [s]
u^∞	Limiting speed of bubbles [m.s^{-1}]
V	Volume [m^3]
V_G	Vapour phase volume [m^3]
$V_g^{0°C}$	Specific retention volume corrected to 0°C [m^3]
V_L	Solvent (liquid) volume [m^3]
V_N	Solute retention volume [m^3]
v	Molar volume [m^3.mol^{-1}]
$v\infty$	Partial molar volume at infinite dilution [m^3.mol^{-1}]
w_L	Mass of solvent [kg]
x	Ratio for P_i^0 correlation
x_i	Liquid molar fraction
y_i	Vapour molar fraction
Z	Compressibility
Z_{RA}	Spencer and Danner parameter

Subscripts

c	Critical property
f	Bubble flow meter
g	Unretained component
in	Inlet
L	Liquid phase
o	Outlet
ov	Corrected flow rate
r	Reduced property
s	Solvent
v	Uncorrected flow rate
w	Water

Superscripts

E	Excess property
id	Ideal solution
l	Liquid
v	Vapour
∞	Property at infinite dilution
0	Saturated property
*	Molar property

CHAPTER 1

Introduction

In the consumer driven world, a diverse range of chemicals is necessary for the supply of products with which to provide for the demand of consumers. Improved processes are continually required in order to provide larger volumes of commodities at lower prices. The separation of chemicals is one of the more energy intensive processes found in the chemical industry. It is therefore of importance that either new, more efficient processes are developed, or that existing processes are optimised.

In the petrochemical industry, the production of pure organic components requires their separation from streams containing a number of classes of organic compounds. The nature of petroleum, both crude and synthetic, means that any given petroleum process stream could contain a large number of components (Ahmad et al., 2010). This further complicates the separation, and the initial design is based upon the separation of the key components. These key components are usually the most difficult to separate, and must be identified prior to the design phase.

The separation of hydrocarbons is often performed by distillation. To accurately design any distillation process, accurate thermodynamic models are a necessity. Parameters for the thermodynamic models are most often obtained by the regression of very precise vapour-liquid equilibrium (VLE) data. This VLE data is obtained by meticulous measurement techniques.

When the pure components have boiling points that are in close proximity, or form azeotropes, the separation cannot be performed utilising conventional distillation techniques. The separation of these petrochemicals is most often performed by advanced distillation techniques, such as extractive or pressure swing distillation (Seader and Henley, 2006). Extractive distillation improves the separation of the components by adding a high boiling solvent near to the top of the column, to entrain one to the components (Schult et al., 2001).

For extractive distillation, the solvent (entrainer) is chosen based on a number of criteria. These were given in detail by Schult et al. (2001). The solvent must have a high selectivity and

capacity as well as a relative volatility that is much lower than that of the components being separated. Other important characteristics of the solvent include ease of separation from the solutes and good thermal stability. This allows for repeated use of the solvent. The physiochemical properties of the pure solvents are also of importance, as these affect the economics of the plant operation. The solvents that were considered in this investigation were previously found to exhibit the desired properties, and are therefore suited to extractive distillation (Wauquier et al., 1995).

N-methylpyrrolidone (NMP) and N-formylmorpholine (NFM) have both been commonly employed in the industrial separation of aliphatics from aromatics or in the separation of C_4 fractions (Weidlich et al., 1987). Little description of the use of the ethylene glycols as solvents was available in literature.

In recent investigations, the use of co-solvents has become popular. Krummen and Gmehling (2004) investigated the use of water as a co-solvent with NMP and NFM. They found that the presence of water lead to an increase in the selectivity of the solvent, but a decrease in its capacity. Mahmoudi and Lotfollahi (2010) measured liquid-liquid equilibrium for a mixed solvent system of sulfolane and N-formylmorpholine, and although this was for a solvent extraction system, it depicted the current interest being shown in the use of solvent mixtures.

The measurement of VLE data is very time consuming, as it must be extremely accurate. The key components for which VLE measurements need to be performed for a given system are therefore first selected by a screening process. This is done by considering the infinite dilution activity coefficients of a large number of solutes in the solvents of interest. The measurement of the infinite dilution activity coefficients is far quicker than VLE measurements, which allows a large number of components to be considered. The infinite dilution activity coefficients are used in order to provide a rough prediction as to how the separation will be affected by the addition of the solvent (Schult et al., 2001).

This project is of industrial importance, as the experimental set up and procedure used in this work was also used to provide SASOL with measured infinite dilution activity coefficients, which would allow for the improvement and optimisation of extractive distillation processes currently in use.

1.1 Extractive distillation

Extractive distillation makes use of changes in the thermodynamic properties of solutes when entrained by a solvent, to improve the separation of different solutes (Seader and Henley, 2006). The most widely used solvents are N-methylpyrrolidone and sulfolane. Wauquier et al. (1995)

and Mokhtari and Gmehling (2010) also made reference to the use of other polar solvents. These less commonly used solvents include N-formylmorpholine and the ethylene glycols [mono-, di-, tri- and tetra-].

The entrainers that are utilised for extractive distillation have a much lower vapour pressure than the components being separated. They are added near to the top of the distillation column. Ruiz et al. (1997) and Schult et al. (2001) include the need for good selectivity, high miscibility with the feed and good stability among other criteria for solvents to be used in extractive distillation.

1.1.1 Industrial applications

Seader and Henley (2006) provided a list of separations of key components which are performed industrially by extractive distillation. A number of other systems for which extractive distillation has been used were given by other authors (see footnote to Table 1-1).

A wide range of entrainers has been used to perform these separations. Several of the mixtures applicable to this study are listed below in Table 1-1. These separations constitute a small portion of the possible applications of extractive distillation.

Table 1-1: Industrial applications of extractive distillation

Key components in feed mixture	Common solvents
benzene/cyclohexane	aniline [a], N-methylpyrrolidone [c], dimethyl phalate [c], furfural [d],
benzene/hexane	N-formylmorpholine [e]
cyclohexane/heptane	aniline [a], phenol [a]
toluene/heptane	aniline [a], N-methylpyrrolidone [b], phenol [a]

a (Seader and Henley, 2006); b (Steltenpohl et al., 2005); c (van Dyk and Nieuwoudt, 2005); d (Villaluenga and Tabe-Mohammadi, 2000); e (Diehl et al., 2005).

1.1.2 Solvent screening

Zeotropic behaviour is required for all the streams exiting the extractive distillation column. The solvent is added to increase the relative volatility of the key components in the system, and thereby enable easier separation (Gmehling and Mollmann, 1998). If the light key (more volatile) component is defined as component (1) and the heavy key (less volatile) component as component (2); the relative volatility of the key components would be described by:

$$\alpha_{12} = \frac{K_1}{K_2} = \frac{\gamma_1 P_1^o}{\gamma_2 P_2^o}$$

(1–1)

From Equation 1-1, it can be observed that to alter the relative volatility (at constant temperature), the activity coefficient of either one or both of the components must be altered. This is because the vapour pressures are dependent on temperature and are composition independent. Determination of the activity coefficient therefore gives good indication as to the performance of a particular solvent for a separation.

In this study, the performance of NMP, NFM, diethylene glycol (DEG) and triethylene glycol (TEG) as solvents for extractive distillation was investigated at temperatures greater than those that have been measured previously.

1.2 Infinite dilution activity coefficient

Infinite dilution activity coefficients (IDACs) are commonly used as a means of pre-screening the performance of different solvents for a large number of solutes (Schult et al., 2001). The IDACs can be used to estimate the selectivity of the solvent for one solute over another and the capacity of the solvent for a particular solute at infinite dilution.

A microscopic perspective of the solutes at infinite dilution views each solute molecule as being completely surrounded by solvent molecules. The solute is therefore at its greatest non-ideality at this point, because all interactions of the solute are with the solvent (Krummen & Gmehling, 2004). It is because of the high costs of separation at higher purities that these measurements are of great value.

1.3 Systems for comparison

The large number of systems for which the infinite dilution activity coefficient could be measured in a short time period meant that there would be a vast number of combinations that could be considered. The comparison of all possible combinations was, however, impractical, and a smaller number of combinations had to be chosen. These combinations were chosen based on the difficulty of separation utilising conventional techniques. Included in this list were the combinations for which extractive distillation is currently used, which are listed in Table 1-1.

The combinations for which the performance of the various solvents was compared are listed in Table 1-2. Combinations that are not listed here can also be investigated, using the measured data given in Chapter 6.

Table 1-2: Combinations for which the performance of various solvents in extractive distillation was compared.

Combination	Reason for inclusion
cyclohexane/benzene	Currently separated using extractive distillation, relative volatility very near to 1, forms an azeotrope [a]
n-heptane/cyclohexane	Currently separated using extractive distillation
n-heptane/toluene	Currently separated using extractive distillation
n-hexane/hex-1-ene	Relative volatility close to 1
hex-1-ene/hex-1-yne	Relative volatility close to 1
hexane/benzene	Currently separated using extractive distillation
benzene/methanol	Forms an azeotrope [b]

[a] (Villaluenga and Tabe-Mohammadi, 2000); [b] (Nagata, 1969).

blank page

CHAPTER 2

Literature review of techniques

The infinite dilution activity coefficient (γ_i^{∞}) can be measured by either direct or indirect methods.

Indirect methods include extrapolation directly from measured vapour liquid equilibrium (VLE) data or by calculation from dilute thermodynamic data (Kojima et al., 1997). These methods have not always provided accurate results and some of the methods are lengthy, due to the sheer bulk of measurements required for the accurate determination of a value.

A number of non-analytical methods cannot be clearly distinguished as either direct or indirect techniques. These techniques use the measurement of minute deviations in equilibrium conditions with very small changes in composition (Dohnal, 2005). These changes are made within the dilute region, but minor extrapolation is still required to obtain the infinite dilution activity coefficient. Techniques that fall within this category include ebulliometry and tensimetry.

2.1 Measurement techniques

A substantial number of direct measurement techniques have been developed for the measurement of γ^{∞}'s. These were classified into five different groups by Dohnal, although this is not an exhaustive classification of the methods. The categories given by Dohnal were:

- Gas-liquid chromatography (GLC)
- Inert gas stripping method (dilutor cell technique)
- Headspace gas analysis method
- Static mass balance method
- Distillation methods

The more common techniques are expounded below.

2.1.1 Extrapolation from VLE data

The extrapolation of data from VLE data requires the measurement of a complete set of isothermal P-x-y data in order to determine a single γ^{∞} value (Fischer and Gmehling, 1996). Due to the large volumes of data which are required for the determination of a single data point, these methods are not generally used for the sole purpose of determining the infinite dilution activity coefficient, but rather, γ^{∞} is determined using this method for systems for which VLE data is available.

2.1.2 Ebulliometry

Ebulliometry measures the difference between the boiling point of a pure solvent and very dilute mixtures (Thomas et al., 1982). It uses the gradient of the temperature with the change in concentration to determine the infinite dilution activity coefficient. It requires highly accurate control of the pressure, which must be held constant. The ebulliometry design of Thomas et al. allowed for up to five systems to be measured simultaneously. Even with the ability to measure multiple systems simultaneously, this method remained slow, with a single set of measurements requiring as much as 8 hours.

2.1.3 Gas-liquid chromatography

Gas-liquid chromatography utilises the retention time of the solute through the stationary solvent to determine γ^{∞} (Everett, 1965). It provides rapid measurement (Gruber et al., 1998) and can be adapted as a technique for low-boiling solvents by the addition of a pre-saturator (Kojima et al., 1997). The column preparation, however, is difficult and time consuming (Letcher et al., 2001).

2.1.4 Inert gas stripping

This method utilises the analysis of variation with time of the composition of a vapour phase. The vapour phase is created by the stripping of a highly diluted liquid mixture with a constant flow of inert gas (Gruber et al., 1998). It is based on the assumption of equilibrium between the gas phase leaving the stripping cell and the liquid phase (Leroi et al., 1977). These measurements were originally highly sensitive and time consuming (Kojima et al., 1997), but novel techniques have been developed which have simplified and accelerated the dilutor technique, rendering it user friendly (Richon, 2011a).

2.1.5 Headspace gas chromatography

Headspace gas chromatography uses the measurement of the changes in the composition of the vapour phase, which is in equilibrium with a solution of a low solute concentration, when solvent is added to the solution (Kojima et al., 1997). It requires the calibration of the detector outputs for all of the components (Weidlich and Gmehling, 1985), but the measurement of γ^{∞} is as easy for mixed solvents as for pure solvents. The γ^{∞} of reactive solute/solvent mixtures can also be measured (Kojima et al., 1997)

2.2 Gas-liquid chromatography

Gas-liquid chromatography (GLC) makes use of the retention time of a solute through a column, to determine the infinite dilution activity coefficient. The column contains a liquid solvent supported on an inert solid. A carrier gas is employed to transport the solute through the column. Interactions between the solute and the solvent, which are described by the activity coefficient, cause the retention of the solute. The comparison of the retention time of the solute to the retention time of an inert component is used to determine the activity coefficient. Compared with the amount of solvent present in the column, the amount of solute which is injected is negligible, and the measurement is therefore performed at conditions that approximate infinite dilution.

2.2.1 Background

The use of GLC for the determination of γ^{∞} was first suggested in the 1950's, and improved throughout the 1960's (Dohnal, 2005). These improvements included the derivation of improved calculations for the determination of the infinite dilution activity coefficient from experimental data by authors such as Everett (1965) and Cruickshank et al. (1966). Dohnal noted that comprehensive accounts of the theory and practice of gas-liquid chromatography have been presented by Letcher (1975) and by Conder and Young (1979). According to Dohnal, the GLC method has not been altered much in the last 30 years, with the major changes being the integration of new technologies, such as new on-line gas chromatographs, into the existing technique.

2.2.2 Method

To obtain accurate measurements, the column must be prepared with a solvent of very high purity (Weidlich and Gmehling, 1985). Due to the nature of chromatography, solutes of high purity are not necessary as separation of different components will occur within the column (Letcher et al., 2001).

The experimental set up for GLC, as shown in Figure 2-1, is simple; it provides rapid measurements and only requires small volumes of the solvent and the solutes (Zhang et al., 2003).

In conventional gas-liquid chromatography, a constant flow rate of carrier gas is passed through a gas chromatograph fitted with a packed column. At a time of zero, a minuscule volume of solute is injected and vaporised into the carrier gas stream. This stream passes through the column and on to the detector. The detector is usually either a thermal conductivity detector (TCD) or a flame ionisation detector (FID). The time taken for the solute to pass through the column in comparison with the time taken by an inert component is used to calculate the infinite dilution activity coefficient. The activity coefficient is also dependent on the flow rate of the carrier gas, which is measured by means of an external flow meter. The inert component is usually a gas, for which the interactions with the solvent are small enough to be approximated to not having occurred.

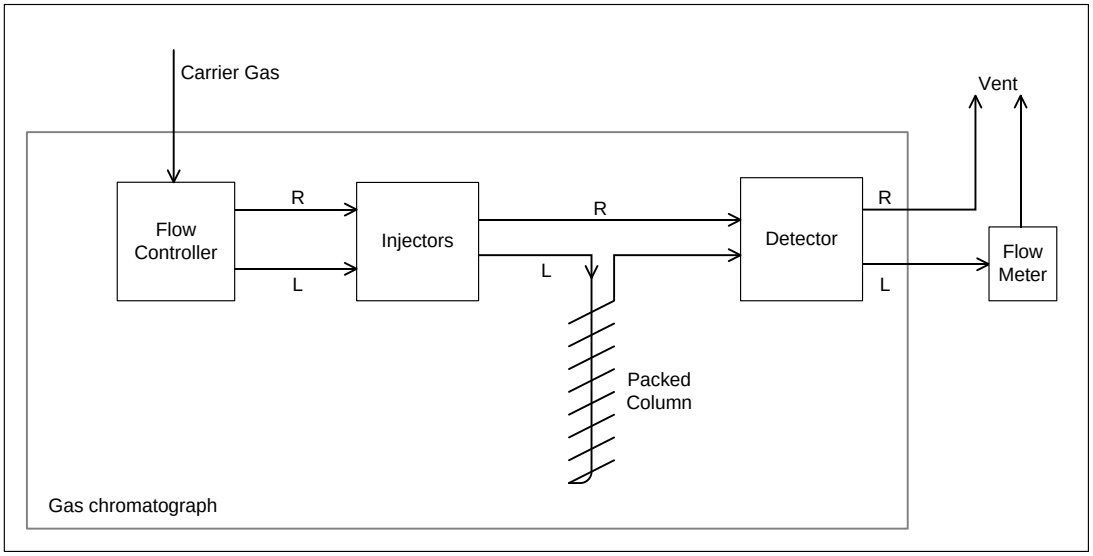

Figure 2-1: Generalised configuration of a gas-liquid chromatography experimental set up, including reference carrier gas stream. The flow controller, injectors, packed column and detectors are all housed within a commercially available gas chromatograph. An additional flow meter is used to obtain accurate flow readings of the exhaust gas stream.

2.2.3 Pre-saturators

A major disadvantage in the use of conventional GLC was the limit in the temperature range. This range was further reduced when performing measurements for solvents that had significant vapour pressures, as elution of the solvent would then occur (Kwantes & Rijinders, 1958). Kwantes and Rijinders therefore proposed the use of pre-saturators for the carrier gas, to ensure that elution of solvent from the column did not affect the measurements. The mass of solvent in

the column was held constant by ensuring complete saturation of the carrier gas prior to its entry into the column.

Weidlich et al. (1987) reviewed two common methods of pre-saturating the carrier gas. The first method was suggested by Pescar and Martin (1966), and utilised a column that was identical to the column used for measurements. The solvent in this column was used to saturate the carrier gas with the solvent. A problem with this approach was the small amount of solvent available in the pre-saturation column, which meant that it had to be replaced regularly (Weidlich et al., 1987).

The second method, which was proposed by Shaffer and Daubert (1969) was the use of 'wash-bottle' cells filled with the liquid solvent, through which the carrier gas was bubbled. These bubbles were produced by a gas distributor. The bubble column method had the disadvantage of having a shorter distance of solvent through which the carrier gas travelled. If a bubble column was utilised, a heating coil was required prior to the first pre-saturator, to ensure that the carrier gas was at the correct temperature prior to entering the cell (Knoop et al., 1989). The bubble column approach was utilised by Weidlich et al., who did not use any packing in their pre-saturators. It was also used by Knoop et al., but many authors utilised packing in the bubble columns to increase the interfacial contact surface and the contact time.

In the earlier uses of GLC with pre-saturation, a reference stream had to be used to provide a baseline, to which the actual measurement could be compared. This reference stream also required pre-saturation, to prevent over-saturation of the output signal from the detector due to detection of the solvent in only one stream. Over-saturation of the signal would lead to the solutes passing through the column undetected. Both Knoop et al. and Zhang et al. (2003) utilised a single carrier gas stream, which was firstly heated to the correct temperature and saturated with the solvent before passing through the reference detector. Once this stream exited the detector, it was tempered and re-saturated, before the solute was injected and the stream passed through the GLC column.

From this configuration, it was deduced that complete saturation of the reference carrier gas with the solvent was not required, but the saturation of this stream was simply to prevent saturation of the detector output signal. Complete saturation of the carrier gas was only required for the stream which would pass through the GLC column, as this would prevent the loss of solvent from the column.

Weidlich et al. stated that, at elevated temperatures, the pre-saturators did not provide complete saturation of the carrier gas, and there was still weight loss from the column. This bleed of solvent from the column was exacerbated by the drop in pressure that occurred across the

column (Weidlich et al., 1987 and Knoop et al., 1989). In order to minimise this problem both authors kept the pressure drop over the column as low as possible. This was be done by ensuring that the carrier gas flow rate remained low and that the column was not too tightly packed. The bleed of solvent from the column was accounted for in calculations by the interpolation of the mass of the solvent in the column. The mass was obtained by regular weighing of the column (Knoop et al., 1989). This approach was feasible because the elution rate was low, and therefore the mass of solvent in the column could be approximated as constant for each solute.

2.3 Dilutor cell technique

The use of the dilutor cell technique, also known as the inert gas stripping technique was proposed, by Leroi et al. (1977), to measure infinite dilution activity coefficients. The technique makes use of the variation, with time, of the concentration of a solute in the gas phase. This variation is measured by the detector of a gas chromatograph and used to determine the infinite dilution activity coefficient. The gas phase is created by stripping solute from a highly diluted solution by the bubbling of a constant flow rate carrier gas through the solution. With a flow of the carrier gas through the solution, the concentration of the solute in liquid phase and therefore in the vapour phase decreased. It is this 'decay rate' that is useful for the determination of the infinite dilution activity coefficient.

2.3.1 Background

The original dilutor cell technique, as proposed by Leroi and co-workers focused predominately on involatile solvents. The experimental work used to verify the technique focused on temperatures close to ambient temperature. They suggested that at this temperature, the solvents investigated could be approximated as involatile, as they had vapour pressures of lower than 1mmHg. There was therefore no need for pre-saturation of the carrier gas.

2.3.1.1 Volatile solvents

When infinite dilution activity coefficients in volatile solvents were measured, the original dilutor cell technique did not provide accurate results. This was due to the steady decrease in the number of moles of solvent in the cell. The pre-saturation of the carrier gas with the solvent was therefore proposed by Dolezal and co-workers (1981). This pre-saturation technique was further developed by Dolezal and Holub (1985).

Their pre-saturator was of a similar design to the dilutor cell, and the solvent was of the same composition as of that in the dilutor cell. This so-called 'double cell technique' (DCT) was used

by Krummen et al. (2000) and by Krummen and Gmehling (2004) for their measurements of the infinite dilution activity coefficients of hydrocarbons in various solvents. Their solvents were both pure and mixtures.

2.3.1.2 Improved cell designs

The original dilutor cell proposed by Leroi et al. (1977) made use of a fritted glass disk to disperse the carrier gas in small diameter bubbles through the solvent. Their design is shown in Figure 2-2.

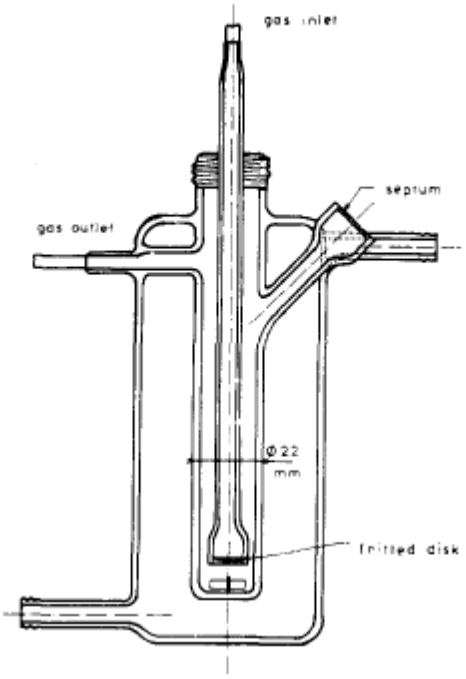

Figure 2-2: Dilutor flask as proposed by Leroi et al. (1977)

The use of a fritted disk allowed bubbles of different sizes to form. Some of the bubbles that formed were extremely tiny, but others were too large for adequate mass transfer from the liquid phase to the vapour phase (Richon et al., 1980). The accuracies of the measurements were therefore compromised, as equilibrium was not always attained.

Richon and co-workers therefore proposed a new equilibrium cell, in which the fritted glass disk was replaced with a number of capillaries (Figure 2-3). These capillaries allowed gas bubbles of equal size to form at their ends. The constant generation of fine bubbles of less than 2 mm in diameter meant that equilibrium between the liquid and vapour phases was assured. The calculation of the required rise height developed by Richon is given in Chapter 3.1.4.1. The new equilibrium cell was built with a concentric inlet/outlet to prevent the entrainment of liquid, while keeping the vapour phase volume in the cell to a minimum.

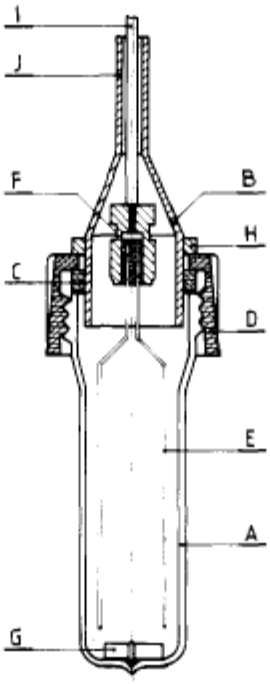

Figure 2-3: Dilutor cell proposed by Richon et al. (1980). A, glass still body; B, concentric inlet/outlet; C, gasket; D, plug; E, capillaries; F, Teflon seal; G, magnetic stirrer; H, metallic ring to adjust the depth of the collector in the still; I, tube for carrier gas inlet; J, gas outlet.

A number of revisions to the structure of the dilutor cell have since been made, although these were, for the most part, made for specialised applications, and not to improve the design developed by Richon et al. (1980).

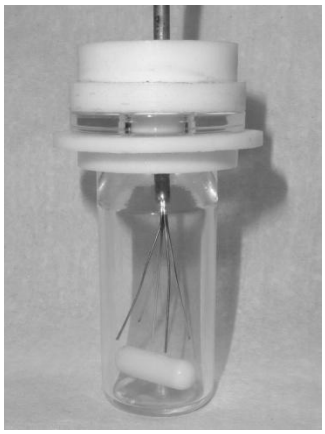

Photograph 2-1: New dilutor cell for the measurement of infinite dilution activity coefficients by inert gas stripping, proposed by Richon (2011a).

The design utilised by George (2008) was modified by Richon (2011a) by the alteration of the cell opening back to a tapered concentric opening. This reduced the vapour volume, while preventing entrainment of the solvent by the carrier gas. This new design is shown in Photograph 2-1.

2.3.2 Method

The infinite dilution activity coefficient is highly dependent on the temperature of measurement. The stripping gas therefore required temperature adjustment to the correct temperature prior to entering the dilutor cell. In most of the more recent cell developments, the gas distributor has been capillary tubes (George, 2008). A large surface area, sufficient contact time and good dispersion of the bubbles of carrier gas are required in order for the solute in the gas phase to equilibrate with the solute in the liquid phase (Leroi et al., 1977).

A schematic of a generalised dilutor cell set up was shown in Figure 2-4. The flow controller and the detector of a gas chromatograph have often been employed to control the flow of carrier gas and to measure the solute concentrations. Other than the matter of charging and discharging the dilutor cell, the dilutor cell method has been found to be much simpler than other methods of infinite dilution activity coefficient measurements (Richon, 2011a).

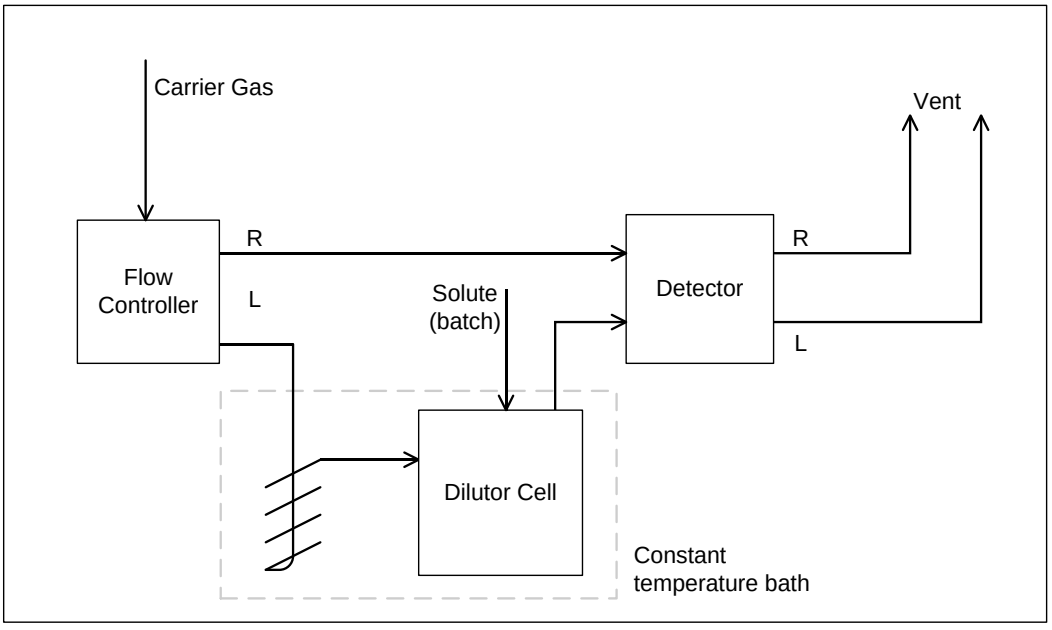

Figure 2-4: Generalised dilutor cell configuration. Left and right carrier gas required for detector 'bridge'.

Along with the improved cell design, Richon also proposed a novel procedure for the dilutor cell technique. This new procedure offers improvements to the dilutor cell technique in terms of speed, accuracy and simplicity. It allowed for the addition of solute directly into the cell filled with the solvent, whereas previous methods required the preparation of a new solution for every measurement. This permitted the re-use of the solvent for multiple measurements which greatly accelerated the turn-around time between individual measurements.

blank page

CHAPTER 3

Equipment description and operation

Two techniques were utilised to measure the infinite dilution activity coefficients of various hydrocarbons in organic solvents. The description of the set up of the equipment for each of the experimental methods, along with the operational procedures for each of the techniques is detailed in this chapter.

3.1 Gas-liquid chromatography

The experimental procedure for the measurement of infinite dilution activity coefficients using the gas-liquid chromatography method has been documented in detail by Tumba (2010) as well as by Letcher (2001), but the addition of the pre-saturators required small alterations to the experimental technique.

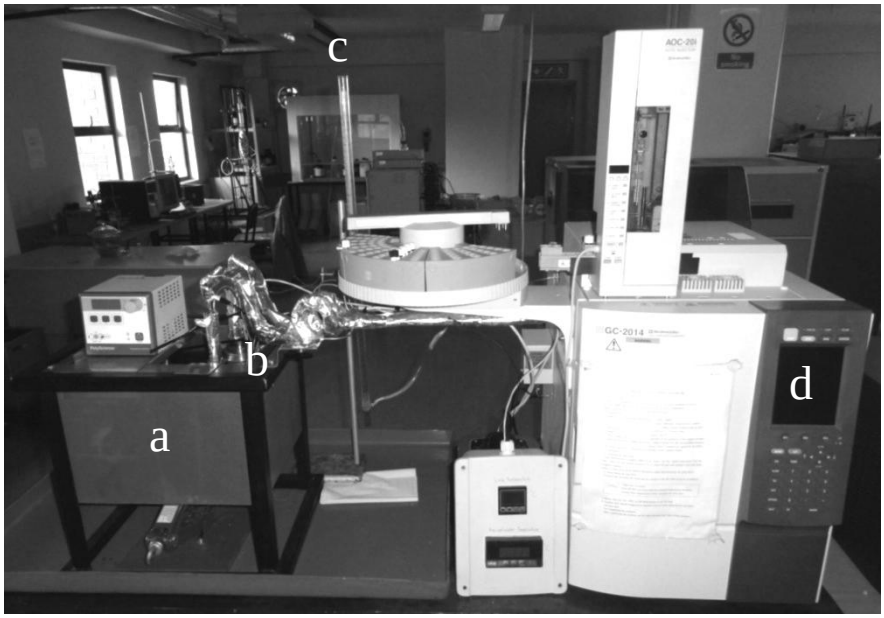

Photograph 3-1: Gas-liquid chromatography set up. a, silicon oil bath; b, pre-saturators; c, bubble flow meter; d, Shimadzu GC-2014 gas chromatograph

Photograph 3-1 and Figure 3-1 show the modified configuration of the gas chromatograph used for gas-liquid chromatography. The modification added a pre-saturator line to the existing gas-liquid chromatography set up. The previous GLC set up was housed entirely within a Shimadzu

GC-2014 gas chromatograph. The set up was altered so as to allow for the measurement of gas-liquid chromatography with or without the pre-saturator cells.

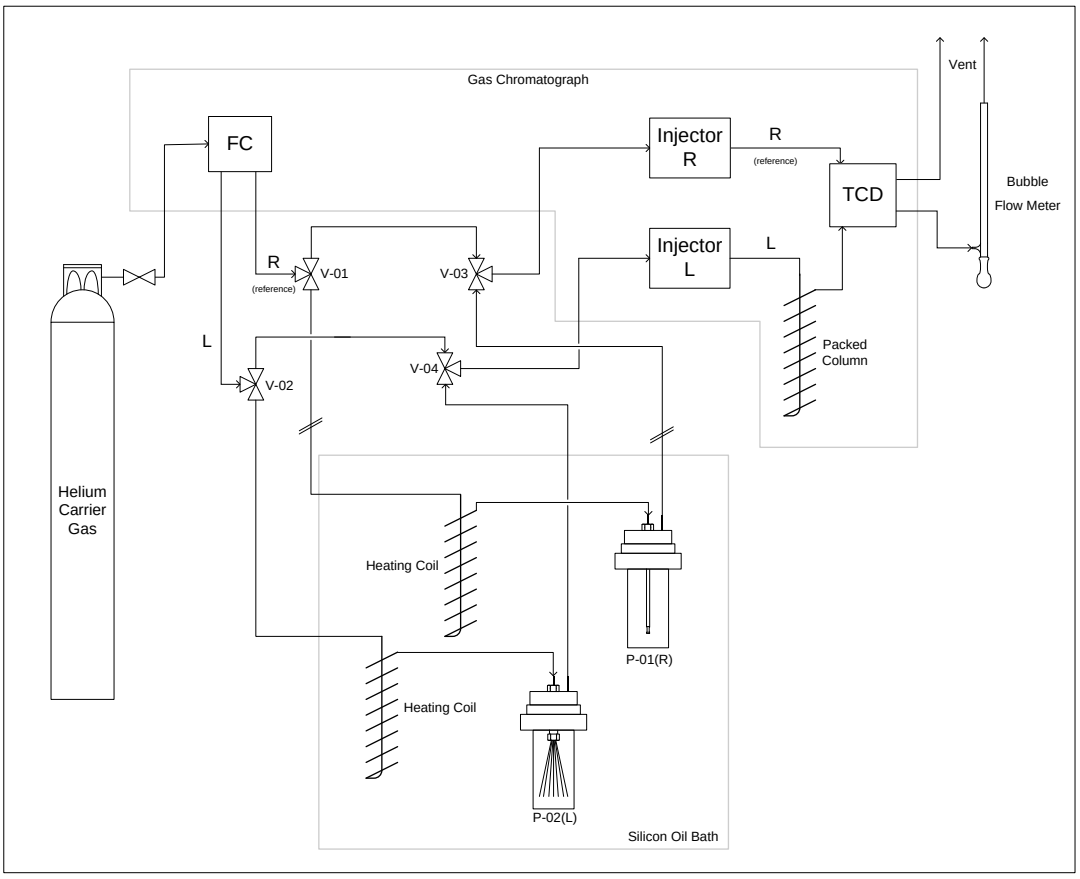

Figure 3-1: Schematic of gas-liquid chromatography set up, including pre-saturation lines (based upon the experimental set up of Weidlich et al. (1987) and Knoop et al. (1989)).

The carrier gas flow-rate was set using the flow controller of the gas chromatograph. After this, it was passed through a three way valve, V-02, to a heating coil and then to the pre-saturator. The carrier gas was bubbled through capillary tubes into the solvent in the pre-saturators, after which it was returned to the injector through the three way valve, V-04.

The solute was introduced into the gas stream by the auto-injector, in which it was vaporised and then passed through the column. Small sample injection volumes of between 0.2 and 0.4µl were used, with smaller injection volumes being used for solutes with faster retention times and the larger injection volumes being for solutes with longer retention times. 0.4µl volumes were required as lengthy retention times tended to allow the solute peak areas to spread out more, making it more difficult to detect a peak. A mole fraction of solute less than 10^{-3} was considered small enough to be at infinite dilution (Richon, 2011a).

Once through the column, the carrier gas flowed through the detector (TCD) and then through the bubble flow meter, with which the flow rate was measured. The injector and the detector

were set to a temperature of 548.15 K to ensure that no condensation of solvent occurred on these vital pieces of equipment.

3.1.1 Shimadzu GC-2014 and AOC 20i+s

The Shimadzu GC-2014 is a high performance gas chromatograph, with the option to fit a number of different detectors. The most commonly used detectors in the GC-2014 are the thermal conductivity detector (TCD) and the flame ionization detector (FID), as these are best suited to organic compounds. Shimadzu Scientific Instrumentation (2011) recommended the use of the TCD for inorganic gases as well as for concentrated organic compounds, and the FID for the detection of organic compounds with hydrogen-carbon bonds. For this experimental work, the TCD was used to detect the solutes, as it provided sufficiently sensitive detection capabilities, while remaining simple to operate.

The thermal conductivity detector exploits the change in thermal conductivity of a gas with change in its composition to detect increased concentrations of solutes in the carrier gas passing over it. The detection is performed using a Wheatstone bridge wiring configuration (Mitov and Petrov, 1995 and Shimadzu Asia Pacific Pty. Ltd., 2006). As the thermal conductivity of the gas passing over one of the arms changed, the resistance in that arm changed, creating a potential difference, which could be measured (Johnson, 2006). A reference stream of pure carrier gas was required to balance the detector bridge. The schematic of the Shimadzu TCD is given in Figure 3-2.

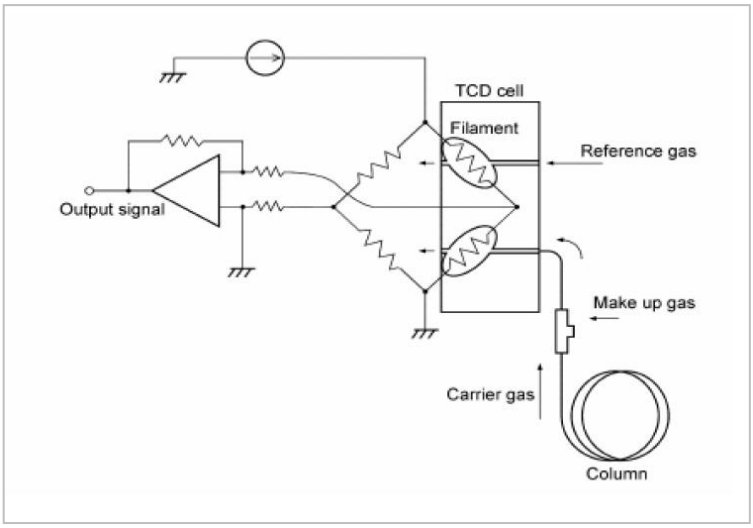

Figure 3-2: Schematic of a Shimadzu TCD given by (Shimadzu Asia Pacific Pty. Ltd., 2006)

Helium gas, supplied by Afrox was used as the carrier gas in this experimental work. Helium has previously been shown to be a superior gas than nitrogen for GLC measurements using thermal conductivity detectors (Knoop et al., 1989).

Knoop and co-workers stated that helium has the greatest known thermal conductivity, and therefore if the gas passing the cell was not pure helium, its thermal conductivity would decrease. If a gas with a lower thermal conductivity were to flow over the 'left hand side' of the TCD, the temperature of that arm would increase, due to lower heat dissipation. This increase in temperature would cause a corresponding increase in resistance, using the same principle as used by resistance-temperature detectors (Johnson, 2006). The increase in resistance would cause the voltage in this arm to decrease (with constant current). The TCD calculates the potential difference caused by the change in gas composition by subtracting the voltage in the 'left hand' arm from that in the reference arm.

The flow rate of the two carrier gas streams was controlled by the GC-2014's advanced flow controller. This gave an extremely steady gas flow rate, and therefore a high level of repeatability of the retention times (Shimadzu Scientific Instruments, 2011). The advanced controller had the ability to maintain a constant gas flow rate even when there were changes in the downstream pressure drop.

The column holding the solvent on the inert support was housed inside the oven of the Shimadzu GC-2014. This oven was specified to have an accuracy of 1% of the set value (in K), with a maximum deviation from the set-point of 2°C.

The Shimadzu GC-2014 was modified by the addition of an AOC 20i+s auto-injector and auto-sampler. These allowed for the automation of the injection process, and thereby the automation of the measurement of the retention times. This automation increased the precision of the measurements, and therefore also improved the repeatability, as errors due to human reaction time were removed. The process did not, however, become completely automated, as manual measurements were still required for other parameters.

The gas chromatograph set the inlet pressure to the column based on the sum of the pressure drop across the column and the atmospheric pressure at the discharge. The pressure drop across the column was measured and displayed by the gas chromatograph. The atmospheric pressure for calculation purposes was measured using a Mensor DPG 2400 digital barometer.

3.1.2 Bubble flow meter

Shimadzu claimed that the advanced flow controller gave sufficiently accurate gas flow rates to eliminate the requirement of a bubble flow meter (Shimadzu Scientific Instruments, 2011). The temperature at which the volumetric flow-rate was set was not given. The claim was therefore examined by the measurement of the flow rate of helium exiting the gas chromatograph by means of a bubble flow meter. The measured value was compared with the set-point of the flow

controller. The gas flow rate was found to be highly repeatable, but with an offset from the flow controller set-point. This offset could have been the change in the volume due to expansion from the temperature at which the flow was set. Because of this uncertainty, the bubble flow meter could not be eliminated from the experimental set up.

The bubble flow meter consisted of a 100ml cylinder with a small volume of soapy water in a bulb at the base. Bubbles were driven along its length by the flow of the gas exiting the detector through the flow meter. The time which it took a bubble to flow through the column was used to determine the flow rate. This measurement technique provided a high degree of accuracy, particularly if the time taken for the bubble to traverse the length of the cylinder was lengthy, as this minimised any effect of reaction times.

The flow rate measured by the bubble flow meter had to be corrected for temperature and for the water vapour added by the solution in the bulb of the flow meter. The temperature of operation of the flow meter was therefore measured in order to account for the expansivity of helium with temperature, as well as to calculate the fraction of water vapour in the saturated helium.

3.1.3 Reference stream pre-saturation

Initially, both the column and the reference streams were saturated with the solvent by their passing through separate coils and pre-saturators. The use of a saturated reference carrier gas flow was made by Knoop and co-workers (1989), as well as by Schult and co-workers (2001). Weidlich and co-workers (1987), however, did not include the saturation of the reference carrier gas. The assumption that the pre-saturation of the reference line carrier gas was simply to prevent saturation of the detector signal was made. The modern online GC's are able to deal with this, due to their larger response ranges. Modern gas chromatographs also have the ability to zero the output signal.

The layout of the experimental set up for these measurements was changed to the configuration shown in Figure 3-1 on p. 16. This prevented slugs of solvent from passing directly from the pre-saturator of the reference stream to the TCD. These slugs of solvent would pass through the reference side of the TCD when vaporised and could cause large negative peaks. This complicated the procedure of determining the retention times from the peaks.

The manner in which the potential difference across the two arms of the TCD was calculated meant that if the composition of the gas flowing over the reference arm changed, the TCD would show this by measuring a negative potential difference. This observation was used to determine that the erratic negative peaks being produced by the TCD were due to changes in the

concentration of the solvent in the reference stream. These changes in concentration were most likely due to the movement of solvent along the line in liquid plugs, which were vaporised at the detector.

There were three options available to prevent these peaks. The first option was to not saturate the reference carrier gas with the solvent, but rather to send pure helium to the detector. The offset caused by the different compositions over the different arms was then compensated for by adding an offset to the measured potential difference. The second option was to add a small amount of packing into the reference line, to prevent slugs of solvent from moving along the line to the detector. The final option was the frequent 'baking' of the injectors and detector, by increasing their temperature to the maximum while operating at a high flow-rate of 'dry' carrier gas. This option was initially used, but it treated the symptoms by removing any excess solvent from the lines, rather than actually removing the cause of the problem. The second alternative was deemed to be unnecessary, and the option not to saturate the carrier gas with solvent was preferred. After this alteration had been performed, the inverted peaks did not re-appear.

3.1.4 Pre-saturators

From the flow-controller of the Shimadzu GC-2014, the gas firstly passed through a $1/8^{th}$ inch pre-heater coil. This heating coil was 3m in length and was immersed in a silicon oil bath which was held by a Polyscience 8206 heating circulator at the temperature at which the measurements were being made. The length of the coils was based on the length of coil used by Knoop and co-workers (1989) in their experimental set up.

From the pre-heat coil, the gas was bubbled through the solvent by a gas distributor. Two different gas distributors were trialled. Further discussion on these techniques can be found in Section 3.1.4.2. The design of the pre-saturators was based on the design of Tumba (2010) for his inert gas stripping set up, and had a volume of 50 cm^3. The volume of solvent inside the pre-saturator had to be kept approximately constant. Over time, with the evaporation of the solvent and subsequent drop in the solvent height, the saturation of the carrier gas was no longer sufficient and the mass of solvent in the column was found to decrease. Once more solvent was added into the cell; the mass was again found to remain steady.

Polyscience (2011) claimed that their Polyscience 8206 heating circulator had a temperature stability of ±0.05°C with an accuracy of ±0.5°C, although they did not state what fluid was used in the bath for these specifications. The Polyscience 8206 heating circulator had a minimum temperature of operation + 5°C above ambient temperature, up to a maximum temperature of

150°C. The stability was high due to a circulating pump, which could operate at up to 12*l*/min, allowing for good circulation of the liquid in the bath.

The lines transferring the carrier gas from the pre-saturator cells to the injector port of the Shimadzu GC-2014 were maintained at a constant temperature by a jacketed nichrome wire, which was wrapped around the tube, along its length. A voltage was applied across this wire by a variable voltage transformer, so as to maintain the tubing at the system temperature. The tubing was insulated with glass wool. The temperature of the tubing was monitored using a calibrated Pt-100 resistance thermometer, with the temperature displayed on a RKC CB100 digital display.

This was done in order to prevent condensation of the solvent vapours in this line. The condensation was possible due to the high temperatures at which measurements were performed, and therefore the large temperature difference between the carrier gas leaving the pre-saturators and the ambient conditions. The temperature of this transfer line was maintained at the same temperature as the pre-saturator cells.

Krummen et al. (2000) suggested that, for the dilutor cell technique, the lines from the dilutor cells to the detector be heated to 40°C above the temperature at which the dilutor cells were operating to prevent condensation in these lines. This could not be undertaken in the GLC measurements, as the helium entering the column had to be at the temperature at which the measurement was being made. If it were at a greater temperature, the column would be heated by the helium, and the measurements would be incorrect, as solvent would elute from the column.

3.1.4.1 Bubble rise height

An equation to determine the height of a liquid solvent through which a gas had to be bubbled in order for the solvent in the gas phase to be in equilibrium with the solvent in the liquid phase was given by Richon et al. (1980). This calculation was also used by George (2008) for his design of inert gas stripping cells, which are based on the equilibrium between the gas and liquid phases.

Richon and co-workers considered both mass transfer in the liquid phase and diffusion in the gas phase. They showed that, for the case of an infinitely diluted solute in a liquid solvent, the gas phase diffusion could be neglected when compared with the time required for mass transfer in the liquid phase only if the bubbles had radii of less than 1.25mm. For the case being considered here, however, the mass transfer could be considered to be inconsequential, as the liquid was the pure solvent. For this case, the equation derived from those of Crank (1956), and given by Richon et al. applies.

$$\tau_G = 1 - \frac{6}{\pi^2}\sum_{l=1}^{\infty}\frac{1}{l^2}exp\left[-\frac{D_{ij}^G l^2\pi^2 h}{R_b^2 u^\infty}\right] \quad (3\text{–}1)$$

The calculation requires the diffusion coefficient of the solvent in the gas phase, which was calculated using the empirical equation proposed by Fuller et al. (1966), as well as the limiting speed of the bubbles in the solution, which was obtained from the equation for the intermediate law (Richon et al., 1980). The calculation of the diffusion coefficient and the limiting speed of the bubbles in the solution are given in Appendix A.

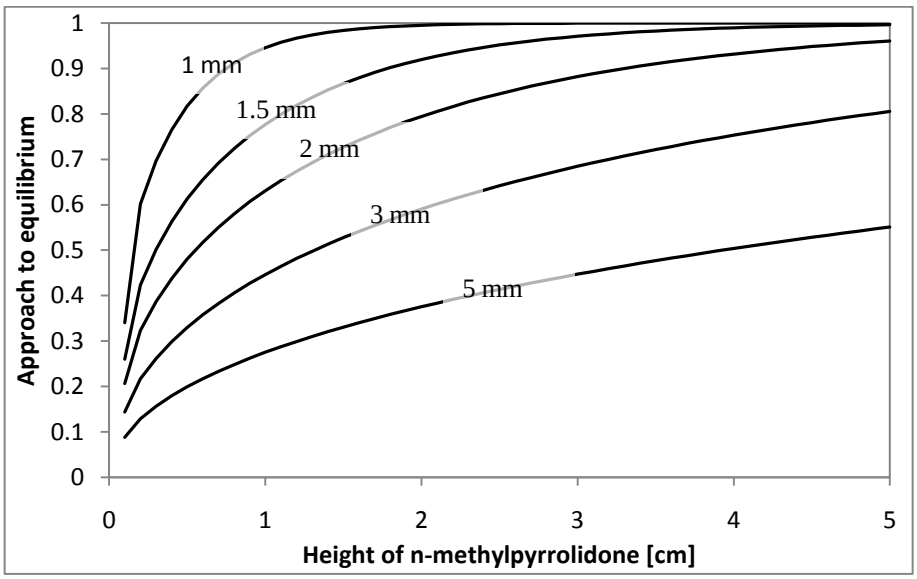

Figure 3-3: Approach to equilibrium in the vapour phase against height of N-methylpyrrolidone as a function of helium bubble diameter

The calculated approach to equilibrium (by Equation 3.1) was plotted against height of liquid for a number of different bubble diameters (Figure 3-3). This plot shows that with increase of the bubble diameter at a given height of NMP, the approach to equilibrium is decreased. This meant that with smaller gas bubble diameters, better saturation of the carrier gas occurred.

3.1.4.2 Gas distribution

Two methods of distribution of the carrier gas through the solvent in the pre-saturators were considered. The first method made use of a length of ¼ inch stainless steel tubing, in which 0.5 mm holes were drilled. The second method made use of 10 evenly spaced 0.05 mm ID capillary tubes immersed in the solvent.

The use of the ¼ inch tubing was found to produce bubbles with diameters of between 4 and 6 mm (Photograph 3-2). The size of the bubbles was determined by comparison with the diameter of the tubing. The bubbles were too large for adequate saturation of the carrier gas. In

order for a bubble of this size to approximately attain equilibrium (99%), it would have to be bubbled through approximately 35 cm of NMP, whereas the pre-saturation cell only had a height of 10 cm. The large height requirement was due to limitations in the mass transfer of the solvent vapour in the gas phase because of the volume of each bubble (see Chapter 3.1.4.1).

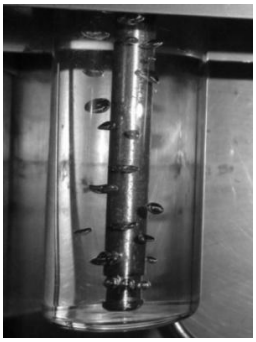

Photograph 3-2: Bubbles from the ¼ inch tubing distributor. Bubbles have a diameter of between 4 and 6mm.

The capillary tube gas distributor provided bubbles with estimated diameters of approximately 1mm (Photograph 3-3). The saturation of the carrier gas was found to be much more complete, with minimal loss of solvent from the column. For these gas bubble sizes, the equation of Crank (1956) was used to show that equilibrium between the gas phase and the liquid phase would theoretically be obtained after the bubbles had bubbled through a height of as little as 2.5 cm of NMP.

Photograph 3-3: Bubbles from the 0.05mm capillary tube distributor. Bubbles have a diameter of approximately 1mm.

3.1.5 Column length

Two column lengths were utilised for the GLC experimental work. Both columns had an internal diameter of 4.1 mm. Initially a column with a length of 1 m was used, but, for the less volatile solutes, the retention time in the column was extremely lengthy, and the solute peaks therefore flattened and became elongated. The carrier gas flow rate could not be increased to overcome this problem, due to the observations of Weidlich et al., (1987) and Knoop et al., (1989) mentioned in Section 2.2.3.

An example of this can be seen in Figure 3-4, which was the recorded output from the detector of the Shimadzu GC-2014 gas chromatography. Figure 3-4 was recorded for the injection of 0.4 µl of propan-1-ol through the longer column. This column contained approximately 1.25 ml of solvent. The peak obtained from this run was spread over a period of 15 minutes, (the tail of the peak is not shown in the figure) with the maximum peak height occurring somewhere between 56 and 57 minutes. This zone of uncertainty produced errors in the calculations, and therefore, a means to reduce this uncertainty was required. It was suggested by Rarey (2011) that to reduce the retention times for these solutes, shorter columns be used.

Figure 3-4: Recorded output from the thermal conductivity detector of the Shimadzu GC-2014, for propan-1-ol in N-methylpyrrolidone at 333.2 K using the 1m column. The peak near the start is the inert component.

To obtain better shaped (sharper) peaks, which in turn would give better accuracy as to the 'mean retention time', the column was shortened to 0.3 m. This substantially reduced the time which the solute remained in the column. It also improved the shape of the peak and gave it a better described maximum.

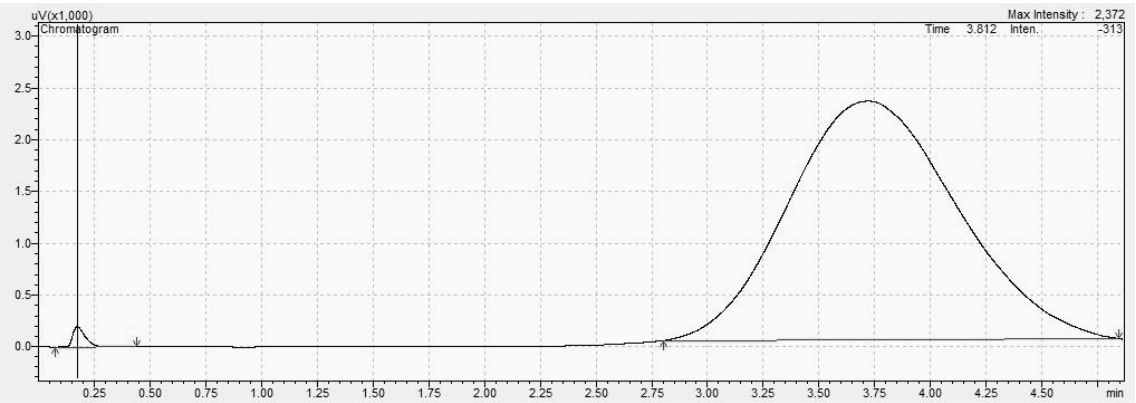

Figure 3-5: Recorded output from the thermal conductivity detector of the Shimadzu GC-2014, for propan-1-ol in N-methylpyrrolidone at 363.2 K, using the 0.3m column. The peak near the start is the inert component.

An example of a better defined peak is given in Figure 3-5. This peak was also for propan-1-ol in N-methylpyrrolidone, but was at 363.15 K. 0.2 µl of solute was injected through the column,

which had a volume of solvent of approximately 0.3 ml. Figures 3-4 and 3-5 are given to illustrate a "sharp" peak, in comparison to a peak that is not "sharp". A number of observations were used to determine whether the decrease in the column length provided better shaped peaks. These observations were supported by calculations performed using Equations 4-6 to 4-9. The figures given above do not provide adequate proof of this, as the retention time was also expected to decrease with an increase in temperature. This approach has been previously practised in the measurement of infinite dilution activity coefficients (Rarey, 2011).

3.1.6 Column preparation

The columns were thoroughly washed prior to packing with the solvent supported on the inert solid (Chromosorb WHP-SP 80/100 mesh). The column had to be packed in such a way as to provide even distribution of the solvent through the column. This was to ensure that no channelling of the solute through the column occurred, as this would have produced erroneous results.

Accurately weighed amounts of Chromosorb WHP-SP 80/100 mesh and solvent were combined. These were measured using a Mettler Toledo AB204S electronic balance with a stated readability of 0.1mg. To obtain an even distribution of the solvent on the inert support, a volume of dichloromethane sufficient to cover the mixture was added. The dichloromethane was slowly evaporated from the mixture in an Ilmvac ROdist digital rotary vacuum evaporator at a temperature of approximately 30°C. Care had to be taken when working with the dichloromethane, due to its toxicity and high volatility. To ensure that all of the dichloromethane was removed from the system, the evaporation was continued until such a time as the mass of prepared packing was equal to that of the solvent and inert support measured prior to the addition of the dichloromethane.

Once installed, the packed columns were conditioned for 2 hours, and were thereafter weighed at regular intervals.

3.1.6.1 Solvents

The solvents were obtained from a number of different sources. N-formylmorpholine and triethylene glycol were both obtained from Sigma-Aldrich Co., and had a stated purity of greater than 99 wt%. The N-methylpyrrolidone was supplied by Merck Schuchardt OHG, with a purity of greater than 99.5 wt%. Diethylene glycol was obtained from Riedel-deHaën with a minimum purity of 99 wt%. The measured refractive indices and purities of these solvents are given in Chapter 6.2.2.1.

The solvents were degassed prior to being used, to ensure the removal of any volatile components, which could have contaminated the solvents. The degassing was performed in the Ilmvac ROdist digital rotary vacuum evaporator. The vacuum pump used for this equipment had the ability to draw a vacuum of up to 95kPa. Due to leaks in the rotary evaporator, the degassing may not have been performed at such low pressures. The solvent was held at 35°C while being degassed.

3.1.6.2 Inert support

Chromosorb WHP-SP 80/100 mesh, supplied by Sigma-Aldrich Co. was used as the inert support for this work. At present, there is no supplier of this type of Chromosorb, and the available reserves are running low. A new inert support needs to be chosen and tested.

3.1.6.3 Packing

The technique for packing the column with the prepared stationary phase has been discussed in literature (Letcher and Reddy, 2005). The stationary phase must be uniform, with no voids or channels, to prevent poor contact between the solvent and the solute. In order to obtain an even compaction, it is usually packed into the column with the aid of a slight vacuum from the injector end of the column.

3.1.7 Operational procedure

a. The pre-saturation cell is filled with the de-gassed solvent and sealed. The column is prepared with the required solvent loading.
b. Helium flow to gas chromatograph is turned on, with an empty column installed in the oven to ensure the flow of carrier gas across the detector while the gas chromatograph is allowed to equilibrate. This is set to 30 ml/min. Thereafter the Shimadzu GC-2014 gas-chromatograph is switched on (TCD current remains off). The injector and detector temperatures are set to 548.15 K and the oven temperature is set to the temperature at which measurements are being made.
c. All other electrical equipment is turned on and set to their respective set-points (heating lines, bath temperature controllers, etc.).
d. The silicon oil bath and the heating lines are allowed to equilibrate at the system temperature. The equilibration of the GC, the silicon oil bath and the heated lines requires approximately 1 hour.
e. The three way valves, V-02 and V-04 are adjusted to allow the carrier gas to flow through the pre-saturation loop.

f. The flow rate is checked by measurement with the bubble flow meter. If there is a large deviation from the set point on the flow controller, a soap water solution is used to check for leaks around the pre-saturators.
g. Once the gas-chromatograph has equilibrated, the prepared column is weighed and the empty column in the oven is replaced with the prepared column.
h. The freshly prepared column is conditioned for at least 2 hours, to ensure that the pressure drop across the column remains steady.
i. After conditioning, the column is removed from the oven and weighed once more. It is then reinserted in the oven, and the detector current is turned on.
j. The retention time of the reference solute is firstly measured. Thereafter the measurement of the retention times of the various solutes is performed. At least three comparable retention times are taken for each solute, with regular measurement of the retention time of the reference solute. The retention times of the different solutes are recorded on the desktop computer. The temperatures, pressures and flow rate are also recorded at regular intervals.
k. Once all the measurements are completed, the detector current is turned off, and the column is removed from the oven and weighed. The three way valves, V-02 and V-04 are switched so as to prevent the carrier gas from flowing to the pre-saturation loop.
l. The bath temperature controllers, the line heating and the heating of the injector, detector and oven of the GC are switched off and allowed to cool.
m. When the temperature of the injector, detector and oven is sufficiently lowered, the flow of helium can be stopped and the gas-chromatograph switched off.

3.1.8 Experimental uncertainties

Table 3-1: Experimental uncertainties for gas-liquid chromatography technique

Process variable	Units	Variability	Uncertainty
Temperature	K	1% of set value [K]	0.1 K
Pressure	Pa	0.2% of set value [Pa]	100 Pa
Carrier gas flow rate	m^3s^{-1}	1% of set value [m^3s^{-1}]	3×10^{-6} m^3s^{-1}
Solvent mass	kg	1×10^{-4} kg per 8 hours	5×10^{-6} kg
Retention time	s	1% of measured [3 runs]	0.6 s

3.2 Dilutor cell technique

The gas-liquid chromatography set up with the pre-saturators, as depicted in Figure 3-1 was installed such that it could easily be modified to be used for the dilutor cell method. The only significant change that was made to convert the GLC apparatus into a dilutor cell set up was the replacement of the packed column by the dilutor cell. The modified set up was shown in Figure 3-6.

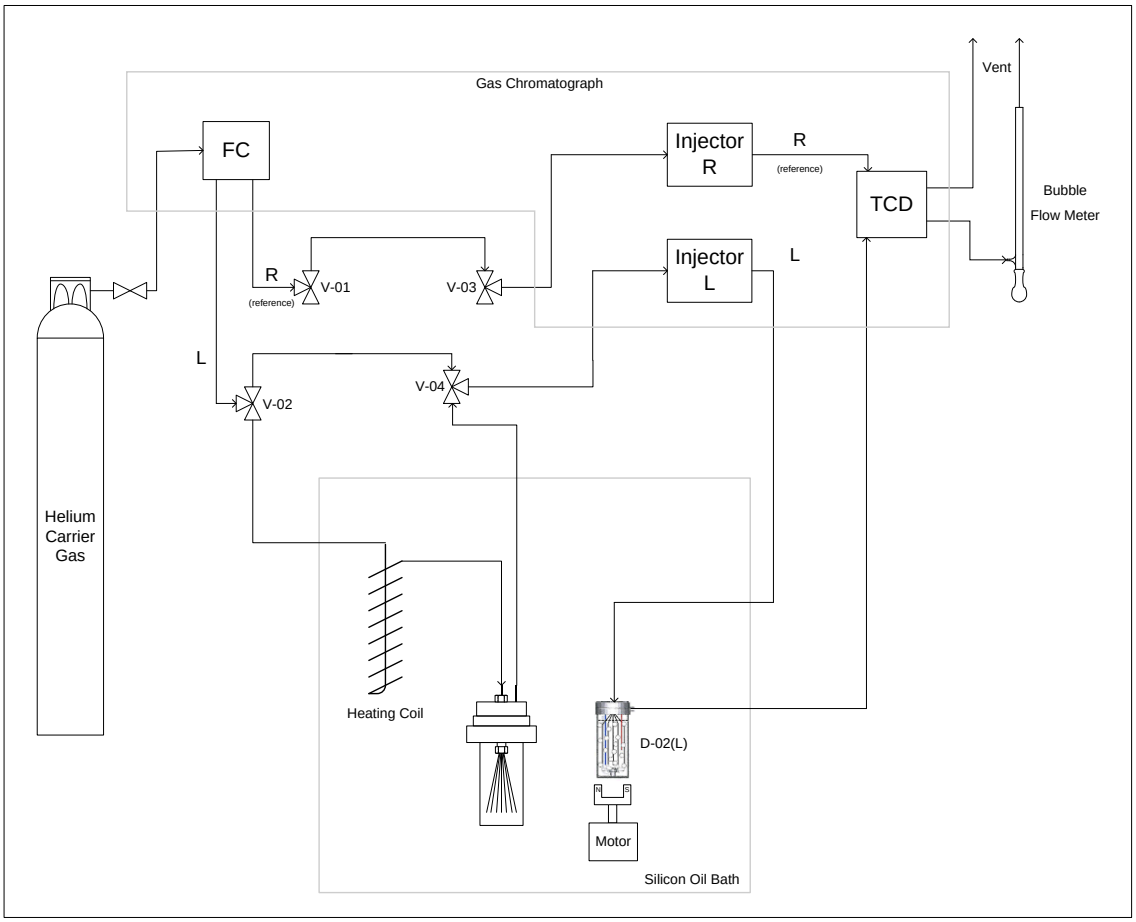

Figure 3-6: Experimental set up for measurement of infinite dilution activity coefficients using inert gas stripping, based upon the experimental set up of Richon (2011a).

The experimental procedure for the measurement of infinite dilution activity coefficients using the dilutor cell technique is far simpler than using the gas-liquid chromatography technique. The novel experimental method is detailed by Richon (2011a).

The dilutor cell was firstly loaded with the degassed solvent, and the mass of solvent in the cell was recorded. The solvents were degassed prior to being used, to ensure that any volatile components, which could have contaminated the solvents, were removed. The degassing was performed in the Ilmvac ROdist digital rotary vacuum evaporator. The vacuum pump used for this equipment had the ability to draw a vacuum of up to 95kPa. Due to small leaks in the

rotary evaporator, the degassing did not occur at such low pressures, but the pressure was low enough to ensure the removal of volatile components. The solvent was held at 35°C while being degassed.

A constant helium gas flow was bubbled through the solvent by means of a number of capillary tubes. The helium gas flow rate was controlled by the flow controller provided in the gas chromatograph (Shimadzu GC-2014). The carrier gas passed through a 3 m long heating coil submerged in a silicon oil bath, and was thereafter bubbled through the solvent in the pre-saturator. The temperature of the silicon oil bath was maintained constant by a Polyscience 8206 heating circulator. The temperature in the bath was monitored using a calibrated Pt-100 resistance thermometer immersed in close proximity to the cell.

From the pre-saturator, the carrier gas passed back to the gas-chromatograph through lines that were maintained at a constant temperature by means of a jacketed nichrome wire wrapped around the tube, along its length. A voltage was applied across the wire using a variable voltage transformer. The voltage was set to maintain the tubing at the system temperature. The temperature of the tubing was monitored using a calibrated Pt-100 resistance thermometer. The temperature was displayed on a RKC CB100 digital display. To prevent heat loss from the tubing, it was insulated with glass wool.

The carrier gas, saturated with solvent, flowed through the injector port of the gas chromatograph and then to the dilutor cell, which was immersed in the silicon oil bath. The transfer line from the injector to the dilutor cell was maintained at the system temperature by the same heating system as used for the line from the pre-saturator to the injector.

To construct the dilutor cell, five 50 μm ID stainless steel capillaries were placed into the end of the $1/8^{th}$ inch stainless steel delivery tubing and cemented into place using a modified polyamine epoxy resin supplied by Pratley. A Teflon cap was machined to fit the glass cell tightly, and the delivery and discharge lines were fitted through this cap. The discharge line removed the vapour phase from the top of the cell.

The carrier gas was bubbled through the solvent in the dilutor cell from the ends of the capillaries. A magnetic stirrer was placed at the base of the dilutor cell to ensure that equilibrium between the gas and the liquid phases was achieved. An external stirrer, turning a magnet at speeds of approximately 400 rpm gave sufficient rotation of the internal magnet. The high speeds were required to cause a vortex to form, which caused a substantial increase in the length of travel of the bubbles through the solvent.

From the dilutor cell, the carrier gas returned to the gas chromatograph, where it passed through the thermal conductivity detector (TCD). The line transferring the carrier gas was heated to

approximately 40 K above the system temperature. This heating was performed by means of a jacketed nichrome wire wrapped around the tube along its length. Across this a voltage was applied, using a variable voltage transformer. The voltage was set to maintain the tubing at the required temperature. The temperature was monitored using a calibrated Pt-100 resistance thermometer, with the temperature displayed on a RKC CB100 digital display. To prevent heat loss from this tubing, it was also insulated with glass wool.

A flat baseline was required prior to the injection of any solutes through the detector and to the dilutor cell. Once this steady baseline was achieved, a small volume of solute was injected using the injector of the gas chromatograph. The volume of solute injected had to be sufficiently small to maintain the mole fraction of solute at less than 10^{-3} (Richon, 2011a). A volume of 1.5µl of solute was therefore used for the measurements.

Once the high purity solute was introduced, the detector signal increased to a peak, after which there was an exponential decay back to the baseline value. The detector signals were recorded for this 'decay' phase, and were used in order to determine the infinite dilution activity coefficient of the particular solute by Equation 4-27. Once the signal returned to the baseline value, a new run could be performed.

The flow rate of carrier gas was measured using a bubble flow-meter, in order to obtain a more accurate value than that given by the flow-controller. The gas flowed through the bubble flow meter upon exiting the TCD of the gas chromatograph. The flow rate measured by the bubble flow meter had to be corrected for the vapour pressure of water, used in the soap solution which generated the bubbles.

3.2.1 Operational procedure

a. The pre-saturation cell is filled with the de-gassed solvent and sealed. The dilutor cell is also filled to the required level with the degassed solvent.
b. Helium flow to gas chromatograph is turned on, with an empty column installed in the place of the dilutor cell. The flow rate is set to 10 ml/min. Thereafter the Shimadzu GC-2014 gas-chromatograph is switched on (TCD current remains off). The injector and detector temperatures are set to 548.15 K and the oven temperature is set to the temperature at which measurements are being made.
c. All other electrical equipment is turned on and set to their respective set-points (heating lines, bath temperature controllers, etc.).

d. The silicon oil bath and the heating lines are allowed to equilibrate at the system temperature. The equilibration of the GC, the silicon oil bath and the heated lines requires approximately 1 hour.
e. The three way valves, V-02 and V-04 are adjusted to allow the carrier gas to flow through the pre-saturation loop.
f. The flow rate is checked by measurement with the bubble flow meter. If there is a large deviation from the set point on the flow controller, a soap water solution is used to check for leaks around the pre-saturators.
g. Once the system has equilibrated, the dilutor cell is weighed and the empty column is replaced with the dilutor cell filled with the solvent. The stirrer for the dilutor cell is turned to a speed which is high enough to force the bubbles into a vortex.
h. The detector current is turned on.
i. The carrier gas is allowed to pass through the dilutor cell until such time as the signal from the detector remains constant. The detector signal is then zeroed.
j. The solutes are then injected one solute at a time, and the output signal from the TCD is recorded on the desktop computer for calculation purposes. At least three repeats were made for each solute. The temperatures, pressures and flow rate are also recorded at regular intervals.
k. Once all the measurements are completed, the detector current is turned off, and the dilutor cell is removed from the oven and weighed. The three way valves, V-02 and V-04 are switched so as to prevent the carrier gas from flowing to the pre-saturation loop.
l. The bath temperature controllers, the line heating and the heating of the injector, detector and oven of the GC are switched off and allowed to cool.
m. When the temperature of the injector, detector and oven is sufficiently lowered, the flow of helium can be stopped and the gas-chromatograph switched off.

3.2.2 Experimental uncertainties

Table 3-2: Experimental uncertainties for dilutor cell technique

Process variable	Units	Variability	Uncertainty
Temperature	K	0.05 K	0.2 K
Pressure	Pa	0.2% of set value [Pa]	100 Pa
Carrier gas flow rate	m^3s^{-1}	1% of set value [m^3s^{-1}]	3×10^{-6} m^3s^{-1}
Solvent mass	kg	1×10^{-4} kg per 8 hours	5×10^{-6} kg
Signal height	V	1×10^{-5} V	1×10^{-6} V

blank page

CHAPTER 4

Theory

In the first section of this chapter, the definition of the infinite dilution activity coefficient, the selectivity and the capacity are given and discussed. Thereafter, the equations for the determination of the infinite dilution activity coefficients from both gas-liquid chromatography and the dilutor cell technique are specified.

4.1 Infinite dilution activity coefficient

The activity coefficient of a species, *i*, in solution was defined by Smith et al. (2005) as

$$\gamma_i \equiv \frac{\hat{f}_i}{x_i f_i} = \frac{\hat{f}_i}{\hat{f}_i^{id}} = \frac{y_i P}{x_i f_i} = \frac{y_i P}{x_i P_i^0} \tag{4–1}$$

and

$$\bar{G}_i^E = RT \ ln\, \gamma_i \tag{4–2}$$

The activity coefficient is used as a measure of the non-ideality of a component, *i*, in the liquid phase.

The infinite dilution activity coefficient was defined by Schult et al. (2001) as

$$\gamma_i^\infty = \lim_{x_i \to 0} \gamma_i \tag{4–3}$$

The selectivity of a solvent for a particular solute over another, $S_{ij,s}^{\infty}$, is the preference of the solvent to form a phase with one solute rather than with the other solute.

$$S_{ij,s}^\infty = \frac{\gamma_i^\infty}{\gamma_j^\infty} \tag{4–4}$$

The capacity of the solvent for a solute, k_i^{∞}, gives a measure of the amount of solute which the solvent would be capable of entraining.

$$k_j^{\infty} = \frac{1}{\gamma_j^{\infty}} \tag{4–5}$$

Observation of the activity coefficient at infinite dilution provides a means of determining the maximum change in the relative volatility that could be obtained.

Selectivity at infinite dilution of greater than one implies that more of solute *i* would be present in the solvent phase than solute *j*. Therefore, in extractive distillation, solute *i* would be removed from the column by entrainment in the solvent and solute *j* would be removed from the top of the column. Conversely, selectivity at infinite dilution of less than one would imply the opposite, with solute *j* being entrained by the solvent.

4.1.1 Prediction

The infinite dilution activity coefficients can be determined experimentally or can be generated utilising models for Gibbs excess energy as was done by van Dyk and Nieuwoudt (2000). Kossack et al. (2007) showed that the values of the selectivity calculated from the Gibbs excess energy differed vastly for different models. Experimentally measured data therefore has superiority over predicted data in terms of accuracy. For this reason, experimental work was undertaken, in order to obtain accurate values.

4.2 Gas-liquid chromatography

Two methods for calculating the infinite dilution activity coefficient from measured gas-liquid chromatography data have been commonly used. These two methods were developed by Everett (1965) and Laub and Pescok (1978) respectively.

The method developed by Everett (1965) and expanded by Cruickshank et al. (1966), has been used by various authors to determine the values of γ^{∞} from experimental data (Letcher and Whitehead, 1997; Olivier et al., 2010). This method was originally thought to apply only when an ideal carrier gas was assumed, but was shown by Cruickshank et al. to extend to non-ideal carrier gases with a fair degree of accuracy. This method made use of virial coefficients to estimate the molar vapour volumes on the assumption of a slightly imperfect gas mixture.

The method which was developed by Laub and Pescok made use of the Soave Redlich-Kwong equation of state (Soave, 1972) to estimate the fugacity coefficient in the saturated state. This

particular method was used by Weidlich et al. (1987) in their measurements of infinite dilution activity coefficients. Sun et al. (2003) also used this method for their determination of γ^{∞} values.

4.2.1 Everett (1965)

The equation used to determine γ^{∞} for an infinitely dilute volatile solute (1) in a solvent (3), carried by an inert carrier gas (2) was given by Everett as:

$$ln(\gamma_{13}^{\infty}) = ln\frac{n_3 RT}{V_N P_1^o} - \frac{(B_{11} - v_1^*)P_1^o}{RT} + \frac{(2B_{12} - v_1^{\infty})J_2^3 P_o}{RT} \tag{4–6}$$

The solute retention volume was calculated using the equation given by Letcher et al. (2001):

$$V_N = (J_2^3)^{-1}\, q_{ov}(t_R - t_{Rg}) \tag{4–7}$$

The use of a bubble flow column for the measurement of the flow rate of the carrier gas meant that the volumetric flow rate of the carrier gas had to be corrected for the vapour pressure exerted by the water that was present in the soap solution (Heintz et al., 2002). This correction was given by Letcher et al. (2001) and Heintz et al. (2002):

$$q_{ov} = q_v\left(1 - \frac{P_w^0}{P_o}\right)\frac{T}{T_f} \tag{4–8}$$

The vapour pressures of the solutes as well as the vapour pressure of the water for the carrier gas flow rate correction (Equation 4-8) were determined using the vapour pressure correlations given by Poling et al. (2000). These equations are given in Appendix B, with the constants for the equations given in Appendix C.

The pressure correction term, J_2^3 was proposed by Everett (1965). It was shown that this pressure correction could only be used at pressures of less than 20 atm and at a ratio of inlet pressure to outlet pressure of less than 5. The pressure correction term was calculated as:

$$J_2^3 = \left(\frac{2}{3}\right)\left[\frac{\left({}^{P_{in}}/_{P_o}\right)^3 - 1}{\left({}^{P_{in}}/_{P_o}\right)^2 - 1}\right] \tag{4–9}$$

4.2.2 Laub and Pecsok

Laub and Pecsok (1978) based their equation for the calculation of the infinite dilution activity coefficient on the relationship between the rate of travel of a solute through the column and the time periods which the solute spent in the mobile (vapour) phase and the stationary (liquid) phase. The amount of time that the solute spent in the stationary phase was itself dependent on the solute activity in that phase.

The derivation of Laub and Pecsok produced the following equation for the determination of the infinite dilution activity coefficient from GLC measurements:

$$\gamma^{\infty} = \frac{273.15R}{V_g^{0°C}\varphi_i^o P_i^o M_L} \tag{4–10}$$

The specific retention volume, which was corrected to 0°C, was calculated using Equation 4-11.

$$V_g^{0°C} = \left(t_R - t_{Rg}\right)\frac{273.15q_v}{T_f w_L}\left[\frac{P_o - P_w^o}{P_o}\right]\frac{3}{2}\left[\frac{\left({}^{P_{in}}/_{P_o}\right)^2 - 1}{\left({}^{P_{in}}/_{P_o}\right)^3 - 1}\right] \tag{4–11}$$

The fugacity coefficient was estimated for the saturated solute from the Soave Redlich-Kwong (SRK) equation of state (Soave, 1972). However, the form of Equation 4-10 allows the use of the fugacity coefficient of the solute in its saturated state as calculated from any equation of state.

The models for the fugacity coefficient from a number of cubic equations of state are given in Appendix D.

4.2.3 Correlations for physical properties

The calculation procedure for the determination of the infinite dilution activity coefficients required a large amount of physical data, such as critical properties and pure component properties. Not all of this data was readily available, and at times, correlations and approximations had to be made.

4.2.3.1 Second virial coefficients

The specific temperatures at which the infinite dilution activity coefficients were determined prevented the use of experimentally determined second virial coefficients for the calculations.

Correlations were therefore used to determine the second virial coefficients. These correlations approximated the second virial coefficients at a given temperature based on the critical properties of the solutes. The two correlations that were utilised were the equation proposed by McGlashan and Potter (1962) and the equation proposed by Tsonopoulos (1974).

McGlashan and Potter correlation

The second virial coefficients could be calculated using the equation proposed by McGlashan and Potter (1962):

$$\frac{B_{ij}}{V_{C,ij}} = 0.43 - 0.886\left(\frac{T_{C,ij}}{T}\right) - 0.694\left(\frac{T_C, ij}{T}\right)^2 - 0.0375\left(N_{ij} - 1\right)\left(\frac{T_{C,ij}}{T}\right)^{4.5} \quad (4\text{–}12)$$

The pure component second virial coefficients calculated from the equation of McGlashan and Potter were compared with experimental data given in the CRC Handbook of Chemistry and Physics (Lide, 2005). The predicted second virial coefficients for non-polar solutes were found to differ from the experimentally measured data by as little as 4%. This can be contrasted to a discrepancy of as much as 80% between the predicted second virial coefficients and the experimentally determined data for alcohols.

The comparisons between the predicted values and the experimentally measured values are given in Figures 4-1, 4-2 and 4-3. These plots were for pure n-hexane, pure benzene and pure methanol respectively.

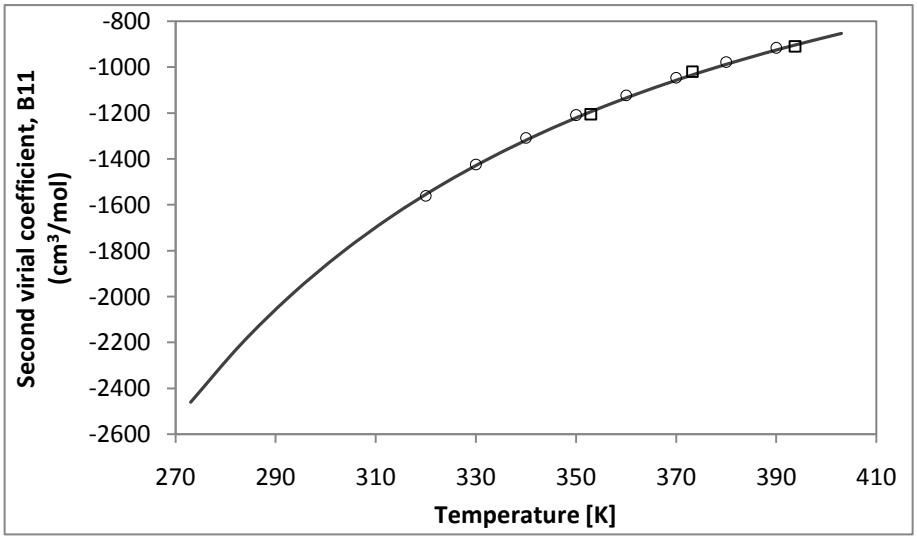

Figure 4-1: The second virial coefficient as a function of temperature for n-hexane: ○, (Lide, 2005); □, (Tsonopoulos, 1974); ——, calculated data using the McGlashan and Potter equation (Equation 4-12).

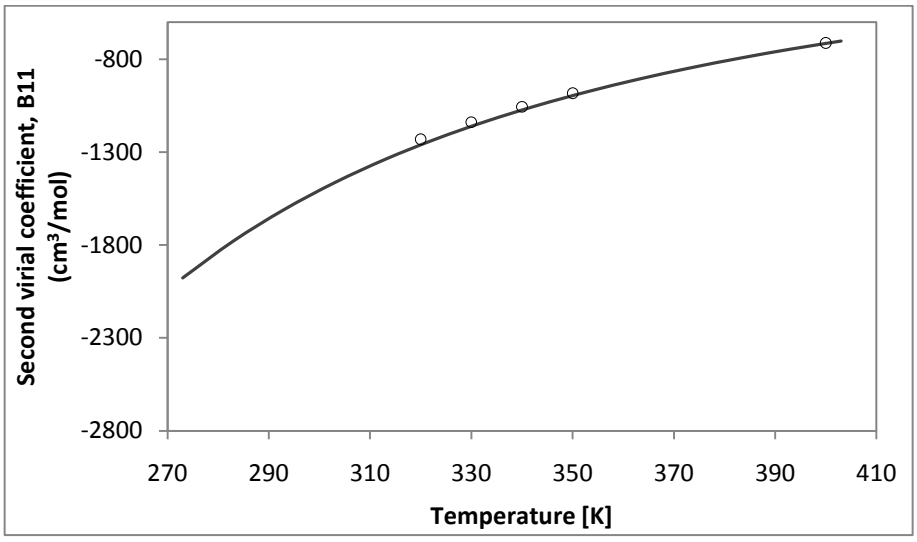

Figure 4-2: The second virial coefficient as a function of temperature for benzene: ○, (Lide, 2005); ──, calculated data using the McGlashan and Potter equation (Equation 4-12).

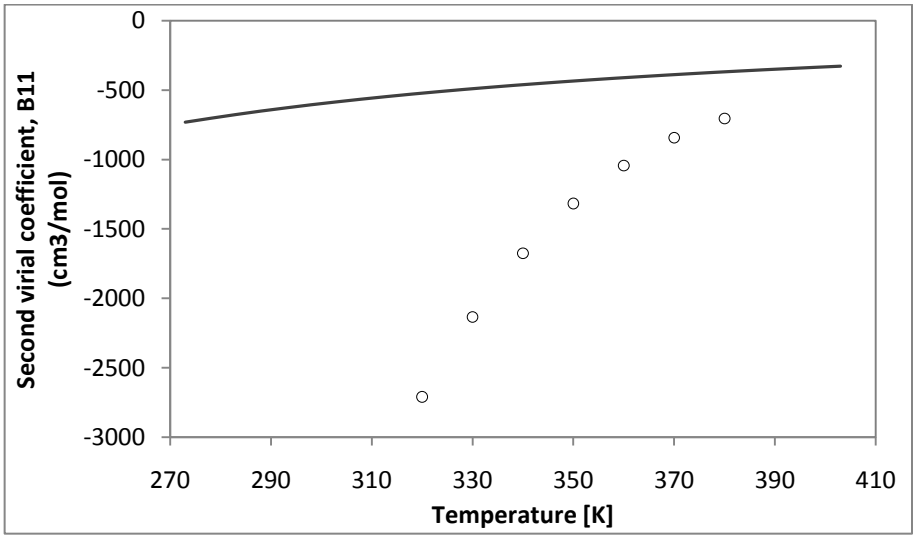

Figure 4-3: The second virial coefficient as a function of temperature for ethanol: ○, (Lide, 2005); ──, calculated data using the McGlashan and Potter equation (Equation 4-12).

The equation of McGlashan and Potter (1962) was originally developed for n-alkanes, and no extension of the equation for other hydrocarbons was alluded to in the study whence the equation was discovered. Equation 4-12 was therefore probably only suitable for the non-polar alkanes, alkenes, alkynes and aromatics. A more suitable pure component second virial coefficient estimation method was required for alcohols.

Tsonopoulos correlation

The Tsonopoulos correlation for determining the second virial coefficient has been the most commonly used correlation because of its reliability (Poling et al., 2000). The parameters used

in the calculation are functions of the reduced temperature and the dipole moment, and are dependent on the class of compound or, in some cases, the actual compound.

$$\frac{BP_c}{RT_c} = f^{(0)} + \omega f^{(1)} + af^{(2)} + bf^{(3)} \tag{4–13}$$

The equations for each of these functions were given by Tsonopoulos (1974) and are listed in Appendix E. The functions $f^{(0)}$, $f^{(1)}$, $f^{(2)}$ and $f^{(3)}$ are functions of the reduced temperature only and '*a*' and '*b*' are either constants or functions of the dipole moment. Tsonopoulos has made several revisions since the initial proposition of the correlation, in which parameters for different families and compounds have been updated by fitting to new data (Poling et al., 2000).

A simplification of the correlation of Tsonopoulos was given by Smith et al. (2005), in which '*a*' and '*b*' were set to zero, and the functions were simplified to be functions of the reduced temperature only. The simplified equation is given by Equation 4-14.

$$B_{ii} = B^0 + \omega_i B^1 = \left[0.083 - \frac{0.422}{T_r^{1.6}}\right] + \omega_i \left[0.139 - \frac{0.172}{T_r^{4.2}}\right] \tag{4–14}$$

The requirements for using this simplification were given by Poling et al. as: $T_r > 0.6$ and $\omega < 0.4$. For this simplification to hold true, Smith and co-authors, who were the first to publish this simplification, gave a plot showing the regions in which the error in B^0 is less than 2%.

For the alcohols for which this study requires the second virial coefficient, the operational point falls outside of the regions in which the simplification can be made, and therefore the original equation proposed by Tsonopoulos had to be utilised to estimate the second virial coefficients.

This correlation still retains a fairly large error, but was found to be a drastic improvement in the predicted second virial coefficient. The predicted data was calculated using the critical and physical properties obtained from both Poling et al. (2000) and the Dortmund Databank software (2011).

The prediction of the Tsonopoulos equation for the second virial coefficient of ethanol is compared to the prediction of the correlation of McGlashan and Potter (1962) as well as experimentally data given by Lide (2005) in Figure 4-4. The correlation of Tsonopoulos was found to predict the second virial coefficient for polar components far more accurately than the correlation of McGlashan and Potter.

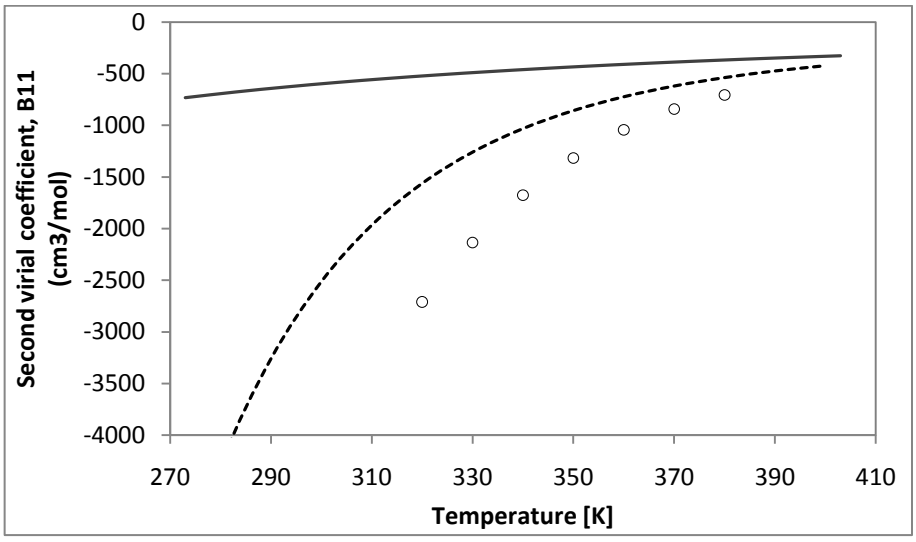

Figure 4-4: The second virial coefficient as a function of temperature for ethanol: ○, (Lide, 2005); ──, calculated data using the McGlashan and Potter equation (Equation 4-12); ····· calculated data using the Tsonopoulous correlation (equation 4-13).

Mixing rules for cross coefficient

The mixed second virial coefficients, B_{12}, were determined using the mixing rules of Hudson and McCoubrey (1960) (Equations 4-15, 4-16 and 4-18) as well as the mixing rule proposed by Lorentz, which was cited by Conder and Young (1979) (Equation 4-17).

$$Tc_{12} = 128(Tc_{11}Tc_{22})^{1/2}(Ic_{11}Ic_{22})^{1/2}V_{c11}\frac{V_{c22}}{Ic_{12}} \tag{4–15}$$

where

$$Ic_{12} = (Ic_{11} + Ic_{22})\left(V_{c11}^{1/3} + V_{c11}^{1/3}\right)^6 \tag{4–16}$$

along with

$$Vc_{12} = \left(V_{c11}^{1/3} + V_{c22}^{1/3}\right)^3/8 \tag{4–17}$$

and

$$N_{12} = \frac{1}{2}(N_1 + N_2) \tag{4–18}$$

In Equation 4-18, N for helium was taken as 1 (Letcher et al., 2001). The above equations allowed for differences in the magnitude of the components, as well as the difference in the diameters of the molecules (Hudson and McCoubrey, 1960). Thus the mixing rules proposed by Hudson and McCoubrey provided more accurate properties for mixtures than could previously be achieved by using the geometric mean of the pure component properties. This was largely due to the fact that the new mixing rules took into effect the interactions between unlike molecules within the system.

It was noted, however, that for some hydrocarbon systems, anomalies do occur, and in these cases, the experimental values have been determined to be closer to those calculated using a geometric mean rather than by using the mixing rules of Hudson and McCoubrey. The corrections that could be obtained by using these mixing rules were discussed in detail in the work of Hudson and McCoubrey (1960).

4.2.3.2 Molar volumes

Molar volume has been shown to be a function of temperature. This was observed when examining the Rackett equation (Equation 4-19) proposed by Rackett (1970).

$$V_L = V_c Z_c^{|(1-T_r)^{2/7}|} \tag{4–19}$$

The Rackett equation is one of the simpler equations for determining saturated liquid volume, as it contains only one right hand term, which itself contains only one component that requires specification (Rackett, 1970). A deviation of up to 5.5% from the experimental data was found to occur for certain organic compounds when predicting the molar volume using the Rackett equation (Spencer and Danner, 1972).

Because of this fairly large deviation, Spencer and Danner put forward the proposition that the critical compressibility factor be replaced with a parameter regressed for each individual compound. The form of the original Rackett equation would still be used, allowing for substitution of the critical compressibility when no regressed parameter was available.

$$V_i = V_c Z_{RA}^{|(1-T_r)^{2/7}|} \tag{4–20}$$

Along with their proposition, which is given by Equation 4-20, Spencer and Danner included recommended regressed parameters for 111 compounds. This database was corrected with parameters based upon new experimental data as well as increased by another 54 components by Spencer and Adler (1978).

The molar volumes of a large number of compounds were given by Poling et al. (2000), but these were at 298.15 K, and could not therefore be used in the calculations, due to the temperature dependency of the molar volume.

4.2.3.3 Partial molar volumes

A partial molar property of species *i* in solution was defined by Smith et al. (2005) as:

$$\bar{M}_i \equiv \left[\frac{\partial(nM)}{\partial n_i}\right]_{P,T,n_j} \tag{4–21}$$

This applies to any molar property, such as Gibbs energy, enthalpy, volume etc.. In this study, for the purpose of calculation, the partial molar volume of the solute at infinite dilution was assumed to be the same as the molar volume of the solute (Letcher and Whitehead, 1997). This assumption was cautioned against by Everett (1965), as the partial molar volume of a hydrocarbon solute at infinite dilution has been found to differ by as much as 10 cm^3/mol from the molar volume. However, the lack of available partial molar volumes for hydrocarbons meant that this assumption could not be avoided.

In order to ascertain whether this assumption could be made, the molar volumes of benzene, methanol and ethanol were compared with their partial molar volumes at infinite dilution in NMP:

For a binary system, the partial molar volumes at infinite dilution could be calculated by extrapolation (Smith et al., 2005).

$$\bar{M}_2 = M - x_1 \frac{dM}{dx_1} \tag{4–22}$$

Using the data provided by Awwad and Farhan (2009), the molar volume of a mixture of N-methylpyrrolidone (1) and benzene (2) was plotted against the molar fraction of N-methylpyrrolidone at various temperatures (Figure 4-5). The partial molar volume of benzene at infinite dilution could be extrapolated from these curves. For benzene, a difference of up to 2.2cm^3/mol between the molar volume and the partial molar volume was observed.

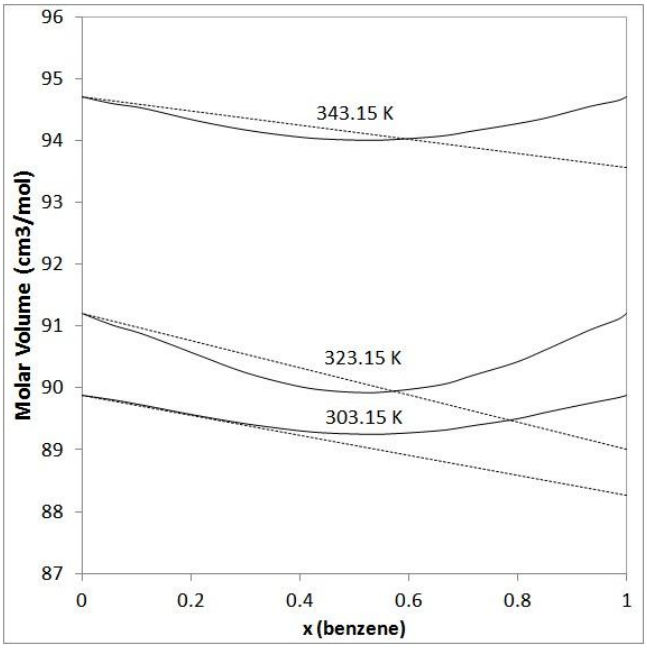

Figure 4-5: Molar volume and extrapolated partial molar volumes at infinite dilution of (2) for the binary system; benzene (1) and N-methylpyrrolidone (2) at various temperatures (calculated from excess volumes and pure component molar volumes given by Awwad and Farhan (2009)).

4.2.3.4 Vapour pressures

The vapour pressures of the solutes were required for the calculation methods of both Everett (1965) and Laub and Pecsok (1978). These were calculated using correlations and parameters given by Poling et al. (2000). In the few cases where the data was not available from Poling et al., the parameters for the Antoine equation (Antoine, 1888) given by the Dortmund Data Bank (2011) were used. The various vapour pressure correlations which are available were discussed by Poling and co-workers. This discussion included accuracies and recommendations as to which equation to use for a specific application.

The equations for the vapour pressure correlations are given in Appendix B and the parameters which were used are given in Appendix C.

4.3 Inert gas stripping

To determine γ^{∞} from the inert gas stripping technique developed by Richon et al. (1980), the equilibrium relationships and the mass balances of the system were used to develop an equation relating the activity coefficient at infinite dilution to the GC peak area, S_i, and the other process variables:

$$\gamma_i^{\infty}(T) = -\frac{NRT}{DP_i^0}\frac{1}{t} ln \frac{S_i}{(S_i)_{t=0}} \tag{4–23}$$

A different equation was developed by Duhem and Vidal (1978) to take into account the influence of the vapour phase volume. Richon (2011a) stated that by minimising the vapour space, by the design of the equipment, this required correction could be relaxed.

$$\gamma_i^{\infty}(T) = -\frac{NRT}{P_i^0\left(D + \frac{V_G}{t}\, ln\frac{S_i}{(S_i)_{t=0}}\right)}\frac{1}{t}\, ln\frac{S_i}{(S_i)_{t=0}}$$

(4–24)

For volatile solvents, Bao and Han (1995) proposed a calculation method which took into account the vapour pressure of the solvent when determining the infinite dilution activity coefficient.

$$ln\left(\frac{S_i}{(S_i)_{t=0}}\right) = \left[\frac{1}{1 + \frac{\gamma_i^{\infty} P_i^0 V_G}{NRT}}\frac{\gamma_i^{\infty} P_i^0}{P_s^0} - 1\right] ln\left[1 - \frac{P_s^0}{P_i - P_s^0}\frac{P_i D}{NRT}t\right]$$

(4–25)

The new method proposed by Richon (2011a) replaced Equations 4–23 and 4–24, and used the signal height rather than the peak area for the calculation. This alteration was possible because, for a linear response, peak area and signal height are proportional. Equations 4–15 and 4–16 are these new equations.

$$\gamma_i^{\infty}(T) = -\frac{NRT}{DP_i^0}\frac{1}{t}\, ln\frac{h_i}{(h_i)_{t=0}}$$

(4–26)

$$\gamma_i^{\infty}(T) = -\frac{NRT}{P_i^0\left(D + \frac{V_G}{t}\, ln\frac{h_i}{(h_i)_{t=0}}\right)}\frac{1}{t}\, ln\frac{h_i}{(h_i)_{t=0}}$$

(4–27)

The use of the height of the signal, rather than the area of the peak, provided Richon with a larger number of samples from a single experiment. This gave an improved and better defined slope, and therefore greater accuracy for the measurements.

CHAPTER 5

Literature data

An extensive literature search was conducted in order to determine the extent to which previous phase equilibria measurements had been performed for the solvents under investigation. A substantial quantity of γ^{∞} values were found for N-methylpyrrolidone and N-formylmorpholine, with most of the previous work being conducted at moderate temperatures (up to 360 K).

5.1 N-formylmorpholine

Although NFM is not a commonly used solvent for extractive distillation, a large amount of infinite dilution activity coefficient data has been measured. Table 5-1 summarises the equipment used and the temperature ranges investigated for previous measurements of γ^{∞} with NFM as the solvent.

Table 5-1: Techniques and temperatures utilised for previous γ^{∞} measurements in NFM

Reference	Technique	T [K]	Comments
(Weidlich et al., 1987)	Gas-liquid chromatography utilising two pre-saturators (wash-bottle type) in an air bath	313 - 373	Reference made to two earlier attempts of the measurement of this system by Gaile and Parlzheva (1974) and van Aken and Broersen (1977) Favourable comparison of the 3 data sets

Reference	Technique	T [K]	Comments
(Knoop et al., 1989)	Gas-liquid chromatography utilising pre-saturators (wash-bottle type)	303 - 353	The pressure drop should be kept to a minimum to prevent excessive elution of the solvent, due to expansion of the carrier gas Tight temperature control on the pre-saturators, to prevent accumulation of solvent in the column
(Park et al., 2001)	Gas-liquid chromatography without pre-saturation of the carrier gas	303 - 323	Lack of pre-saturators could have created substantial errors, especially at higher temperatures
(Krummen & Gmehling, 2004)	Dilutor technique, using pre-saturators for the carrier gas	303 - 413	Pre-saturators used to ensure that solvent was not entrained from the equilibrium cell Stated error of approximately 2.5%

A model of the form of Equation 5-1 below was fitted to the literature data for n-hexane, hex-1-ene, cyclohexane and benzene. The use of such a form was suggested by Heintz et al. (2001). The standard deviations of the literature data from the fitted line were calculated and are given in Table 5-2.

$$\ln(\gamma^{\infty}) = A + B/T \tag{5–1}$$

The slope in Equation 5-1 has the same form as the Gibbs-Helmholtz equation stated by Olivier et al. (2010) (Equation 5-2), and therefore, the slope of the fitted line gives the excess enthalpy, $\Delta H_i^{E,\infty}$.

$$\frac{\partial\left(ln(\gamma_i^{\infty})\right)}{\partial\left({}^{1}/_{T}\right)} = \frac{\Delta {H_i}^{E,\infty}}{R} \tag{5–2}$$

The natural logarithm of the infinite dilution activity coefficients for n-hexane, hex-1-ene, cyclohexane and benzene in NFM are plotted against the inverse of the temperature in Figures 5-1 to 5-4.

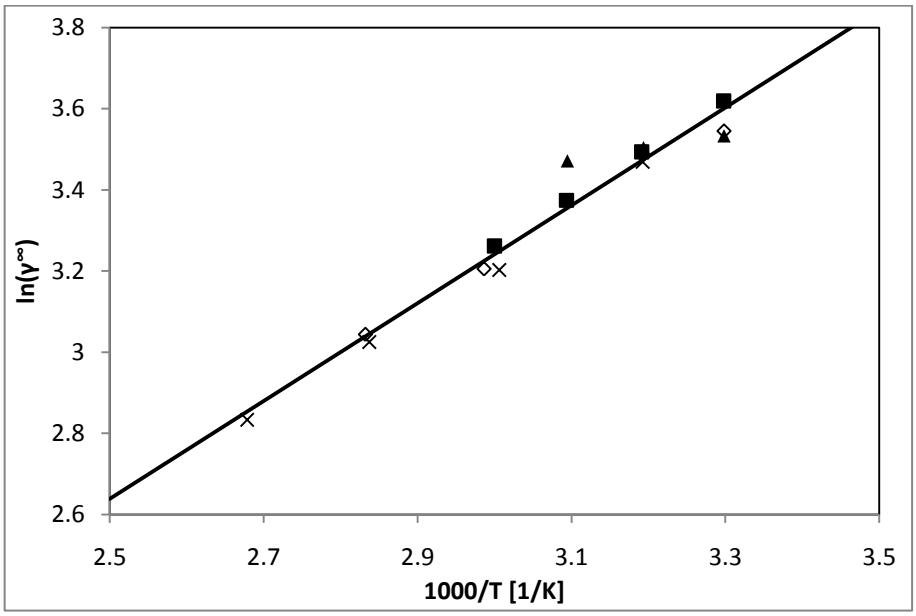

Figure 5-1: Literature ln(γ^{∞}) for n-hexane (1) in NFM (3). ◊, (Knoop et al., 1989); ■, (Krummen and Gmehling, 2004); ▲, (Park et al., 2001); X, (Weidlich et al., 1987); ——, line of best fit for literature data.

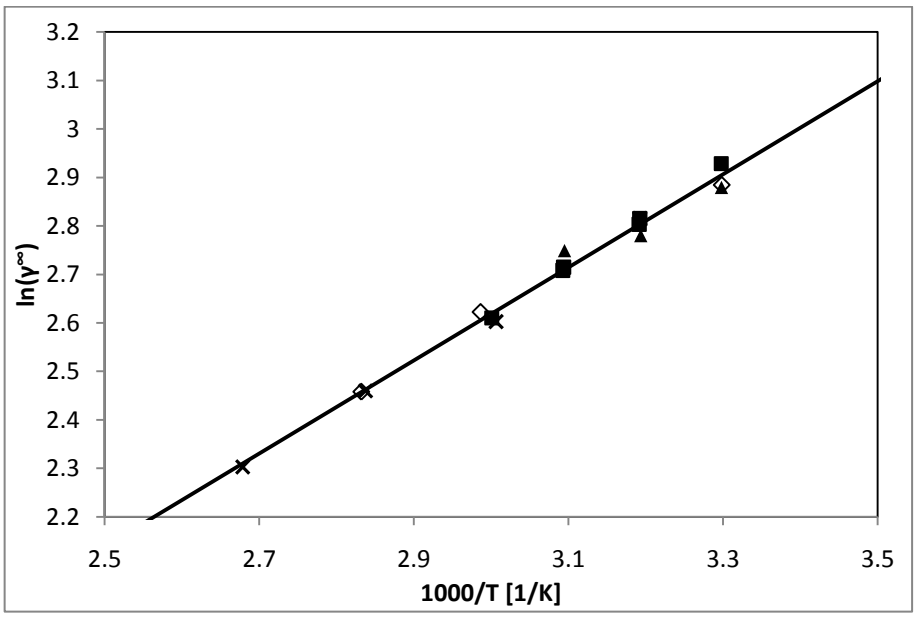

Figure 5-2: Literature ln(γ^{∞}) for cyclohexane (1) in NFM (3). ◊, (Knoop et al., 1989); ■, (Krummen and Gmehling, 2004); ▲, (Park et al., 2001); X, (Weidlich et al., 1987); ——, line of best fit for literature data.

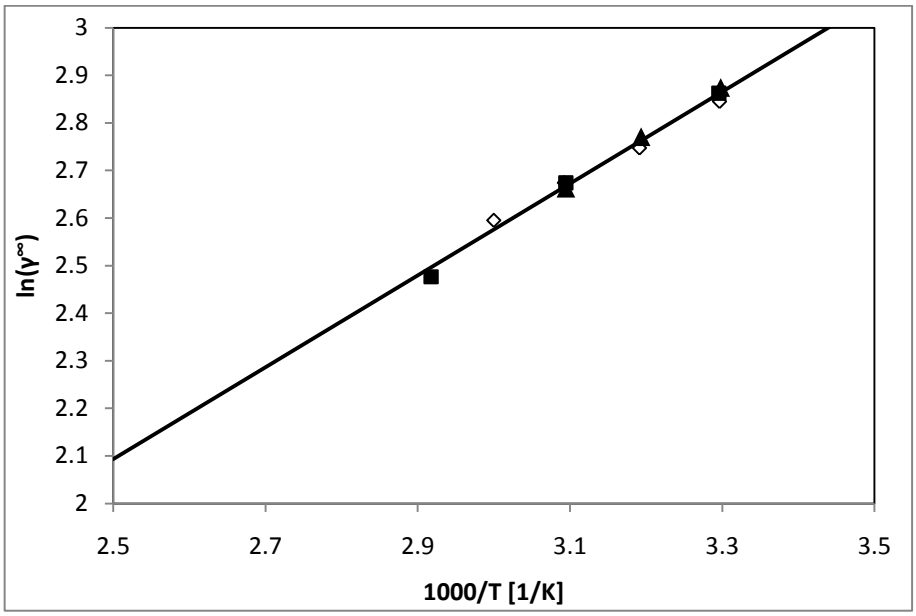

Figure 5-3: Literature ln(γ^{∞}) for hex-1-ene (1) in NFM (3). ◊, (Krummen and Gmehling, 2004); ■, (Weidlich et al., 1987); ▲, (Park et al., 2001); ——, line of best fit for literature data.

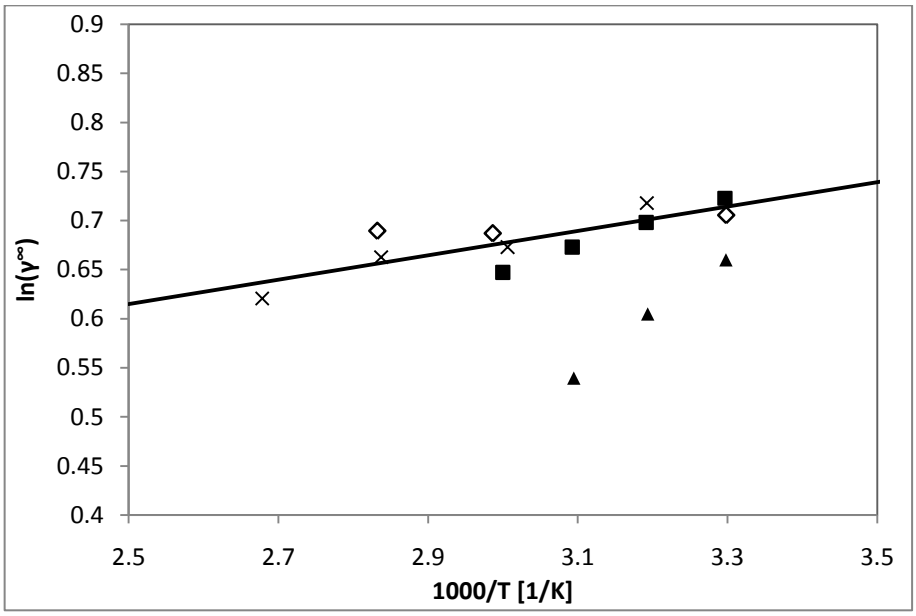

Figure 5-4: Literature ln(γ^{∞}) for benzene (1) in NFM (3). ◊, (Knoop et al., 1989); ■, (Krummen and Gmehling, 2004); ▲, (Park et al., 2001); X, (Weidlich et al., 1987); ——, line of best fit for literature data.

The values measured by Park et al. (2001) did not agree with the values given by the other authors. This could be due to the lack of pre-saturators, which would have allowed a decline in the weight fraction of the solvent in the column packing. This decline may have caused incorrect retention times, and therefore incorrect infinite dilution activity coefficients.

Literature data was available for a number of other components, but the data was not as comprehensive as for these four solutes. The other data sets are provided in Table 5-3.

There was little literature data available for NFM at temperatures above 360 K. This was probably due to the increase in the vapour pressures of NFM with increased temperatures. These higher vapour pressures would have increased the difficulty in maintaining a constant mass of solvent in the column, making steady state more elusive.

Table 5-2: Excess enthalpy and standard deviation of various solutes in NFM from regression of literature data

Solute	Excess Enthalpy, $H_i^{E,\infty}$ [$kJ.mol^{-1}.K^{-1}$)]	Std Deviation
n-pentane	8.69	0.014
n-hexane	10.02	0.046
n-heptane	10.46	0.074
n-octane	11.60	0.012
pent-1-ene	6.61	0.004
hex-1-ene	8.03	0.013
hept-1-ene	6.92	0.005
oct-1-ene	11.35	0.015
cyclopentane	7.03	0.006
cyclohexane	7.99	0.018
methanol	0.63	0.002
ethanol	2.62	0.007
benzene	1.03	0.054
toluene	2.65	0.041
ethylbenzene	1.76	0.014

Table 5-3: Literature Values for γ^{∞} in NFM

n-pentane	T[K]	**303.2**	**303.21**	**303.25**	**313.35**	**313.25**	**323.25**	**332.65**	**333.35**	**352.45**	**373.35**						
	γ^{∞}	25.66[a]	25.679[d]	27.1[b]	24.2[b]	23.6[c]	21.7[b]	19.3[c]	19.6[b]	16.4[c]	13.5[c]						
n-hexane	**T[K]**	**303.2**	**303.21**	**303.25**	**313.13**	**313.25**	**313.35**	**323.12**	**323.25**	**332.65**	**333.35**	**334.86**	**352.45**	**353.09**	**373.35**		
	γ^{∞}	34.64[a]	34.23	37.3[b]	33.25[d]	32.1[c]	32.9[b]	32.193[d]	29.2[b]	24.6[c]	26.1[b]	24.67[a]	20.6[c]	20.99[a]	17[c]		
n-heptane	**T[K]**	**303.2**	**303.21**	**303.25**	**313.13**	**313.25**	**313.35**	**323.12**	**323.25**	**332.65**	**333.35**	**334.86**	**352.45**	**353.09**	**373.35**		
	γ^{∞}	46.68[a]	40.904[d]	50.3[b]	43.211[d]	42.3[c]	43.7[b]	41.378[d]	38.6[b]	31.4[c]	33.9[b]	32.06[a]	26.1[c]	26.62[a]	21.5[c]		
n-octane	**T[K]**	**303.2**	**303.21**	**313.25**	**332.65**	**334.86**	**353.09**	**352.45**	**373.35**								
	γ^{∞}	63.35[a]	63.476[d]	54.2[c]	40.7[c]	41.78[a]	33.43[a]	33.7[c]	26.3[c]								
iso-octane	**T[K]**	**303.2**	**313.25**	**332.65**	**334.86**	**352.45**	**353.09**	**373.35**									
	γ^{∞}	52.42[a]	48.2[c]	36[c]	36.93[a]	30.7	29.87[a]	24.4[c]									
n-decane	**T[K]**	**313.25**	**332.65**	**334.86**	**352.45**	**353.09**	**373.35**										
	γ^{∞}	90.1[c]	65.8[c]	69.78[a]	53.3[c]	52.87[a]	42.2[c]										
cyclopentane	**T[K]**	**303.15**	**303.25**	**313.25**	**313.35**	**323.25**	**323.35**	**332.65**	**333.25**	**352.45**	**373.35**						
	γ^{∞}	12.9[b]	12.8[b]	11.7[c]	11.8[b]	10.9[b]	10.8[b]	9.92[c]	10[b]	8.76[c]	7.6[c]						
cyclohexane	**T[K]**	**303.2**	**303.21**	**303.25**	**313.13**	**313.25**	**313.25**	**313.35**	**323.12**	**323.25**	**323.35**	**332.65**	**333.25**	**334.86**	**352.45**	**353.09**	**373.35**
	γ^{∞}	17.9[a]	17.804[d]	18.7[b]	16.116[d]	16.7[b]	16.7[c]	16.5[b]	15.624[d]	15.1[b]	15[b]	13.5[c]	13.6[b]	13.77[a]	11.7[c]	11.68[a]	10[c]
methyl cyclopentane	**T[K]**	**303.2**	**303.21**	**313.13**	**313.25**	**323.12**	**332.65**	**334.86**	**352.45**	**353.09**	**373.35**						
	γ^{∞}	18.99[a]	18.849[d]	16.785[d]	17.5[c]	14.809[d]	14.2[c]	14.41[a]	12.5[c]	12.51[a]	10.7[c]						
methyl cyclohexane	**T[K]**	**303.2**	**303.21**	**313.13**	**313.25**	**323.12**	**332.65**	**334.86**	**352.45**	**353.09**	**373.35**						
	γ^{∞}	24.11[a]	24.782[d]	23.487[d]	22.8[c]	22.151[d]	18.5[c]	18.36[a]	15.6[c]	15.47[a]	13.2[c]						
ethyl cyclohexane	**T[K]**	**303.2**	**303.21**	**313.25**	**332.65**	**334.86**	**352.45**	**353.09**	**373.35**								
	γ^{∞}	33.25[a]	33.34	29.6[c]	23.3[c]	23.19[a]	19.1[c]	19.32[a]	15.5[c]								
pent-1-ene	**T[K]**	**303.35**	**313.35**	**323.35**	**333.35**												
	γ^{∞}	12.5[b]	11.5[b]	10.7[b]	9.85[b]												
hex-1-ene	**T[K]**	**303.21**	**303.35**	**303.45**	**313.13**	**313.35**	**323.12**	**323.15**	**323.35**	**333.35**	**342.75**						
	γ^{∞}	17.711	17.2[b]	17.5[c]	15.97[d]	15.6[b]	14.331[d]	14.5[c]	14.5[b]	13.4[b]	11.9[c]						
hept-1-ene	**T[K]**	**303.35**	**313.35**	**323.35**	**333.35**												
	γ^{∞}	23.3[b]	20.8[b]	18.9[b]	17[b]												
oct-1-ene	**T[K]**	**303.21**	**303.45**	**313.13**	**323.12**	**323.15**	**342.75**										
	γ^{∞}	32.146[d]	31.5[c]	28.624[d]	24.202[d]	24.6[c]	19[c]										
cyclopentene	**T[K]**	**303.25**	**313.25**	**323.25**	**333.35**												
	γ^{∞}	6.66[b]	6.28[b]	5.99[b]	5.69[b]												
cyclohexene	**T[K]**	**303.21**	**303.25**	**313.25**	**323.25**	**333.35**											
	γ^{∞}	9.761[d]	9[b]	8.07[b]	7.5[b]	6.95[b]											

a (Knoop et al., 1989), b (Krummen and Gmehling, 2004), c (Weidlich et al., 1987), d (Park et al., 2001)

Table 5-3 (cont.): Literature Values for γ^{∞} in NFM

methanol	T[K]	**303.45**	**323.15**	**342.75**													
	γ^{∞}	1.07[c]	1.05[c]	1.04[c]													
ethanol	**T[K]**	**303.45**	**323.15**	**342.75**													
	γ^{∞}	1.52[c]	1.41[c]	1.35[c]													
propan-1-ol	**T[K]**	**323.15**	**342.75**														
	γ^{∞}	1.56[c]	1.46[c]														
propan-2-ol	**T[K]**	**303.45**	**323.15**	**342.75**													
	γ^{∞}	1.94[c]	1.7[c]	1.52[c]													
benzene	**T[K]**	**303.2**	**303.21**	**303.35**	**313.13**	**313.25**	**313.35**	**323.12**	**323.35**	**332.65**	**333.35**	**334.86**	**352.45**	**353.09**	**373.35**		
	γ^{∞}	2.025[a]	1.935[d]	2.06[b]	1.831[d]	2.05[c]	2.01[b]	1.715[d]	1.96[b]	1.96[c]	1.91[b]	1.988[a]	1.94[c]	1.993[a]	1.86[c]		
toluene	**T[K]**	**303.21**	**303.25**	**313.13**	**313.25**	**313.35**	**323.12**	**323.35**	**332.65**	**333.35**	**334.86**	**352.45**	**353.09**	**373.35**			
	γ^{∞}	3.219[d]	2.94[b]	2.986[d]	2.78[c]	2.78[b]	2.896[d]	2.66[b]	2.65[c]	2.56[b]	2.738[a]	2.58[c]	2.7[a]	2.46[c]			
ethylbenzene	**T[K]**	**313.25**	**332.65**	**334.86**	**352.45**	**353.09**	**373.35**										
	γ^{∞}	3.88[c]	3.6[c]	3.619[a]	3.59[c]	3.535[a]	3.44[c]										

a (Knoop et al., 1989), b, (Krummen and Gmehling, 2004), c (Weidlich et al., 1987), d (Park et al., 2001)

5.2 N-methylpyrrolidone

NMP, being a commonly used solvent for extractive distillation in the petrochemical industry, has also been investigated extensively. Table 5-4 summarises the equipment used and the temperature ranges investigated for previous measurements of γ^{∞} with NMP as the solvent.

Table 5-4: Techniques and temperatures utilised for previous γ^{∞} measurements in NMP

Reference	Technique	T [K]	Comments
(Weidlich et al., 1987)	Gas-liquid chromatography utilising two pre-saturators (wash-bottle type) in an air bath	323 – 343	One of the first instances of γ^{∞} measurements at high temperatures
(Fischer & Gmehling, 1996)	Calculation from VLE measurements using Legendre polynomials	363 – 413	Indirect method was used to determine γ^{∞} at high temperatures, in order to avoid inaccuracies due to loss of solvent
(Fischer & Gmehling, 1996)	Gas-liquid chromatography with a pre-saturator cell (wash-bottle type)	343 - 353	Pre-saturators prevented elution of solvent from column
(Letcher & Whitehead, 1997)	Gas-liquid chromatography with a temperature equilibration coil	283 - 298	Pre-saturators were not used due to the low temperatures at which measurements were taken
(Schult et al., 2001)	Gas-liquid chromatography with pre-saturation of the carrier gas using packed columns containing the solvent (similar to main column)	308 - 318	The reference stream passed through a different pre-saturator column. Three pre-saturator column lengths were tested, and it was found that the 1.25m column provided sufficient saturation Error of approximately 6%

Table 5-4 (cont.): Techniques and temperatures utilised for previous γ^{∞} measurements in NMP

Reference	Technique	T [K]	Comments
(Krummen & Gmehling, 2004)	Dilutor technique, using pre-saturators for the carrier gas	303 - 333	Pre-saturators used to ensure that the amount of solvent in the equilibrium cell remained constant Stated error of approximately 2.5%

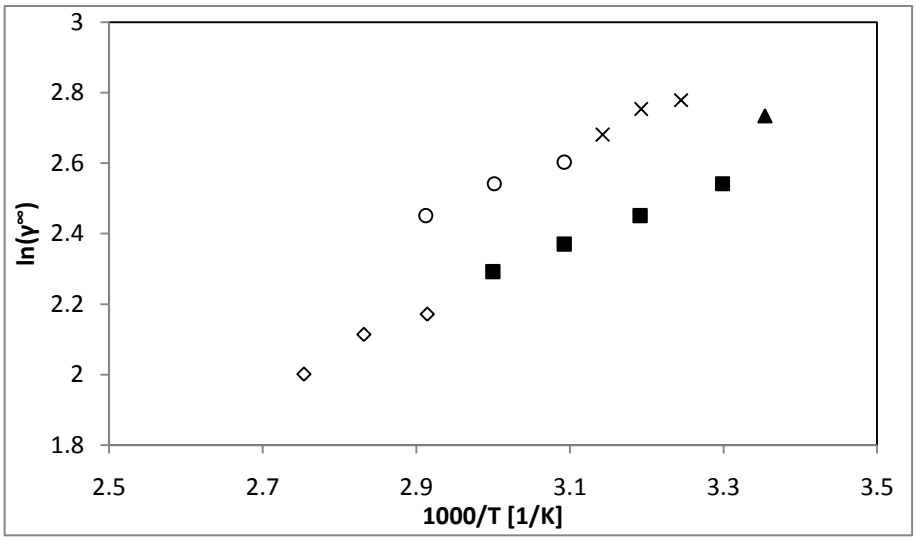

Figure 5-5: Literature $\ln(\gamma^{\infty})$ for n-hexane (1) in NMP (3). ◊, (Fischer & Gmehling, 1996); ■, (Krummen & Gmehling, 2004); ▲, (Letcher & Whitehead, 1997); X, (Schult et al., 2001); ○, (Weidlich et al., 1987).

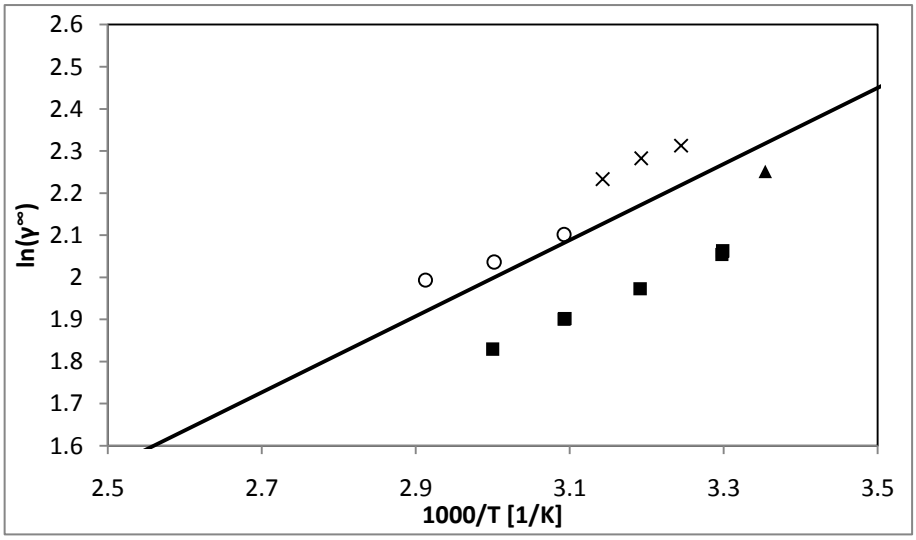

Figure 5-6: Literature $\ln(\gamma^{\infty})$ for cyclohexane (1) in NMP (3). ■, (Krummen & Gmehling, 2004); ▲, (Letcher & Whitehead, 1997); X, (Schult et al., 2001); ○, (Weidlich et al., 1987); ——, line of best fit for literature data.

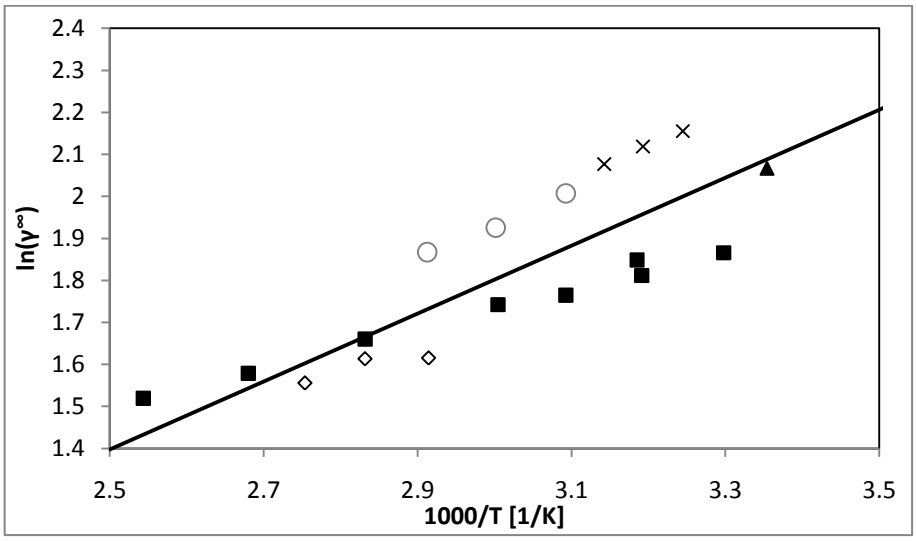

Figure 5-7: Literature ln(γ^{∞}) for hex-1-ene (1) in NMP (3). ◊, (Fischer & Gmehling, 1996); ■, (Krummen & Gmehling, 2004); ▲, (Letcher & Whitehead, 1997); X, (Schult et al., 2001); ○, (Weidlich et al., 1987); ——, line of best fit for literature data.

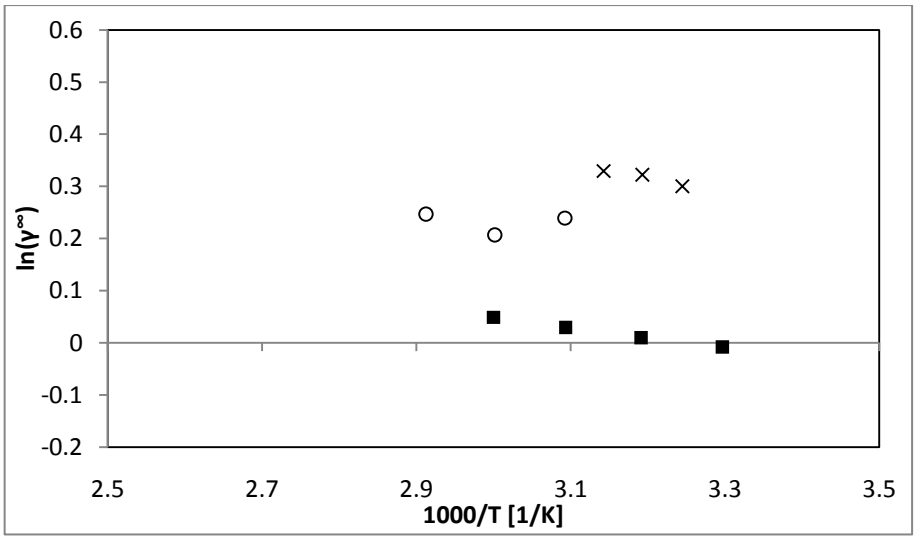

Figure 5-8: Literature ln(γ^{∞}) for benzene (1) in NMP (3). ■, (Krummen & Gmehling, 2004); X, (Schult et al., 2001); ○, (Weidlich et al., 1987); ——, line of best fit for literature data.

Figures 5-5 to 5-8 show the discrepancies between the different literature data points, with two distinct trends appearing for most of the solutes. The values measured by Weidlich et al. (1987) and those given by Schult et al. (2001) show agreement with one another, whereas the values measured by Krummen and Gmehling (2004), Letcher and Whitehead (1997) and Fischer and Gmehling (1996) agree with one another.

Krummen and Gmehling (2004) used the dilutor technique for their measurements, whereas both Fischer and Gmehling (1996) and Letcher and Whitehead (1997) utilised the GLC technique to determine the values of γ^{∞} for various solutes in NMP. Fischer and Gmehling also extrapolated VLE data for several of their values. This made it highly unlikely that the

discrepancies between the two groups were due to the measurement technique. All of the methods of calculation of γ^{∞} from GLC experimental data were based on the method given by Knoop et al. (1989).

The disagreements between different data sources are the cause of the magnitudes of some of the standard deviations, which were obtained from the regression of the literature data. These standard deviations are given in Table 5-5. A few of the deviations were so large as to make the uncertainty of the excess enthalpy extremely large. This was especially the case for benzene and toluene.

The exponential curves plotted against the experimental data for NFM (Figures 5-1 to 5-4) gave a far better representation of the experimental data than the curves plotted against the literature data for NMP (Figures 5-5 to 5-8), largely because of the two trends for NMP. This discrepancy was investigated in this study.

Table 5-5: Excess enthalpy and standard deviation of various solutes in NMP from regression of literature data

Solute	Excess Enthalpy, $H_i^{E,\infty}$ [$kJ.mol^{-1}.K^{-1}$)]	Std Deviation
n-pentane	5.91	0.073
n-hexane	8.01	0.101
n-heptane	6.33	0.133
n-octane	12.11	0.047
pent-1-ene	5.61	0.084
hex-1-ene	6.84	0.122
hept-1-ene	7.64	0.106
oct-1-ene	8.02	0.082
cyclopentane	4.81	0.130
cyclohexane	6.46	0.089
methanol	0.886	0.001
ethanol	2.62	0.007
propan-1-ol	2.16	0.013
benzene	-2.85	0.324
toluene	-2.46	0.140

Table 5-6 contains the literature data for the infinite dilution activity coefficients of a number of solutes in NMP. There was not much literature data freely available for infinite dilution activity coefficients above 360 K. This was probably due to the high vapour pressure of NMP at higher temperatures which would have made such measurements extremely difficult.

Table 5-6: Literature Values for γ^{∞} in NMP

n-pentane	**T [K]**	**303.15**	**308.2**	**313.2**	**313.35**	**318.2**	**323.35**	**323.35**	**333.15**	**333.35**	**343.35**					
	γ^{∞}	10.6[b]	13[a]	12.3[a]	9.79[b]	11.8[a]	9.09[b]	11.5[c]	10.2[c]	8.49[b]	9.35[c]					
n-hexane	**T [K]**	**283.15**	**298.15**	**303.15**	**308.2**	**313.2**	**313.35**	**318.2**	**323.35**	**323.35**	**333.15**	**333.35**	**343.15**	**343.35**	**353.15**	**363.15**
	γ^{∞}	19.4[d]	15.4[d]	12.7[b]	16.1[a]	15.7[a]	11.6[b]	14.6[a]	10.7[b]	13.5[c]	12.7[c]	9.9[b]	8.77[e]	11.6[c]	8.28[e]	7.4[e]
n-heptane	**T [K]**	**283.15**	**298.15**	**303.15**	**308.2**	**313.2**	**313.35**	**318.2**	**323.35**	**323.35**	**333.15**	**333.15**	**343.35**			
	γ^{∞}	24.5[d]	21.3[d]	14.9[b]	19.4[a]	19.5[a]	13.7[b]	17.8[a]	12.4[b]	16.3[c]	11.5[c]	14.7[b]	13.4[c]			
n-octane	**T [K]**	**283.15**	**298.15**	**323.35**	**333.15**	**343.35**										
	γ^{∞}	41.1[d]	25.6[d]	18.9[c]	16.8[c]	16.1[c]										
iso-octane	**T [K]**	**323.35**	**333.15**	**343.35**												
	γ^{∞}	17.9[c]	16[c]	14.4[c]												
cyclopentane	**T [K]**	**303.15**	**308.2**	**313.2**	**313.35**	**318.2**	**323.25**	**323.35**	**333.15**	**333.35**	**343.35**					
	γ^{∞}	6.14[b]	7.37[a]	7.6[a]	5.73[b]	7.29[a]	5.39[b]	6.41[c]	6.07[c]	5.08[b]	5.84[c]					
cyclohexane	**T [K]**	**283.15**	**298.15**	**303.15**	**303.25**	**308.2**	**313.2**	**313.35**	**318.2**	**323.25**	**323.35**	**323.35**	**333.15**	**333.35**	**343.35**	
	γ^{∞}	11.6[d]	9.5[d]	7.87[b]	7.8[b]	10.1[a]	9.8[a]	7.19[b]	9.33[a]	6.7[b]	6.69[b]	8.18[c]	7.66[c]	6.23[b]	7.34[c]	
methyl cyclopentane	**T [K]**	**323.35**	**333.15**	**343.15**	**343.35**	**353.15**	**363.15**									
	γ^{∞}	8.41[c]	7.92[c]	4.02[e]	7.5[c]	3.89[e]	3.81[e]									
pent-1-ene	**T [K]**	**308.2**	**303.25**	**313.2**	**313.35**	**318.2**	**323.05**	**323.35**	**333.35**	**347.75**	**363.15**	**373.15**	**393.15**			
	γ^{∞}	7.04[a]	5.38[b]	6.59[a]	5.21[b]	6.4[a]	5.11[b]	4.93[b]	4.7[b]	4.54[b]	4[e]	4.13[b]	3.82[b]			
hex-1-ene	**T [K]**	**303.25**	**308.2**	**313.2**	**313.35**	**313.95**	**318.2**	**323.35**	**332.85**	**333.35**	**353.15**	**373.15**	**393.15**			
	γ^{∞}	6.46[b]	8.63[a]	8.32[a]	6.12[b]	6.35[b]	7.98[a]	5.84[b]	5.71[b]	5.56[b]	5.26[b]	4.85[b]	4.57[b]			
hept-1-ene	**T [K]**	**283.15**	**298.15**	**303.25**	**308.2**	**313.2**	**313.35**	**318.2**	**323.35**	**333.35**						
	γ^{∞}	11.2[d]	9.5[d]	7.37[b]	10.1[a]	9.89[a]	7[b]	9.7[a]	6.7[b]	6.45[b]						
oct-1-ene	**T [K]**	**283.15**	**298.15**	**303.15**	**313.15**	**323.15**	**323.35**	**333.15**	**333.15**	**343.15**	**343.35**	**353.15**				
	γ^{∞}	18.7[d]	10.9[d]	10.5[a]	9.5	8.59[a]	10.7[c]	9.87[c]	8.08[b]	7.48[b]	9.1[c]	6.96[b]				
cyclopentene	**T [K]**	**303.25**	**308.2**	**313.2**	**313.35**	**318.2**	**323.25**	**333.35**								
	γ^{∞}	3.5[b]	5.03[a]	4.69[a]	3.37[b]	4.59[a]	3.27[b]	3.16[b]								
cyclohexene	**T [K]**	**303.25**	**313.35**	**323.25**	**333.35**											
	γ^{∞}	4.17[b]	3.97[b]	3.82[b]	3.69[b]											
methanol	**T [K]**	**298.15**	**310**	**310.15**	**323.35**	**333.15**	**343.35**									
	γ^{∞}	0.5[f]	0.575[g]	0.58[h]	0.527[c]	0.521[c]	0.517[c]									
ethanol	**T [K]**	**298.15**	**323.35**	**333.15**	**343.35**											
	γ^{∞}	0.67[g]	0.661[c]	0.639[c]	0.643[c]											
propan-1-ol	**T [K]**	**323.05**	**347.95**	**373.15**	**393.15**											
	γ^{∞}	0.582[b]	0.54[b]	0.511[b]	0.507[b]											
propan-2-ol	**T [K]**	**323.35**	**333.15**	**343.35**	**298**											
	γ^{∞}	0.754[c]	0.755[c]	0.737[c]	0.72											
benzene	**T [K]**	**303.35**	**308.2**	**313.2**	**313.35**	**318.2**	**323.25**	**323.35**	**333.15**	**333.35**	**343.35**					
	γ^{∞}	0.992[b]	1.35[a]	1.38[a]	1.01[b]	1.39[a]	1.03[b]	1.27[c]	1.23[c]	1.05[b]	1.28[c]					
toluene	**T [K]**	**303.35**	**313.35**	**323.25**	**323.35**	**333.15**	**333.35**	**343.35**								
	γ^{∞}	1.33[b]	1.33[b]	1.35[b]	1.66[c]	1.67[c]	1.37[b]	1.66[c]								

a (Schult et al., 2001), b (Krummen & Gmehling, 2004), c (Fischer & Gmehling, 1996), d (Letcher & Whitehead, 1997), e (Weidlich et al., 1987), f (Rajeshwar Rao & Bhagat, 1990), g (Sitnyakovskii et al., 1989), h (Rajeshwar Rao & Bhagat, 1991)

5.3 Triethylene glycol

Only a small number of measurements of the γ^{∞} of organic solutes in triethylene glycol (TEG) could be found. Table 5-7 lists the equipment used for these measurements, as well as the temperatures at which they were performed.

Table 5-7: Techniques and temperatures utilised for previous γ^{∞} measurements in TEG

Reference	Technique	T [K]	Comments
(Sun et al., 2003)	Gas-liquid chromatography utilising a pre-saturation vessel placed before the column	323 - 393	Measurements performed for 3 aromatic solutes and 4 alkane solutes
(Arancibia & Catoggio, 1980)	Measurement of the partition coefficient performed using gas-liquid chromatography Infinite dilution activity coefficients calculated from this data	298	A pre-saturator was used to saturate the carrier gas

The natural logarithms of the literature data, and a line of best fit of the form of Equation 5-1, were plotted against the inverse of temperature for n-heptane, n-octane and benzene. These plots are given in Figures 5-9 to 5-11.

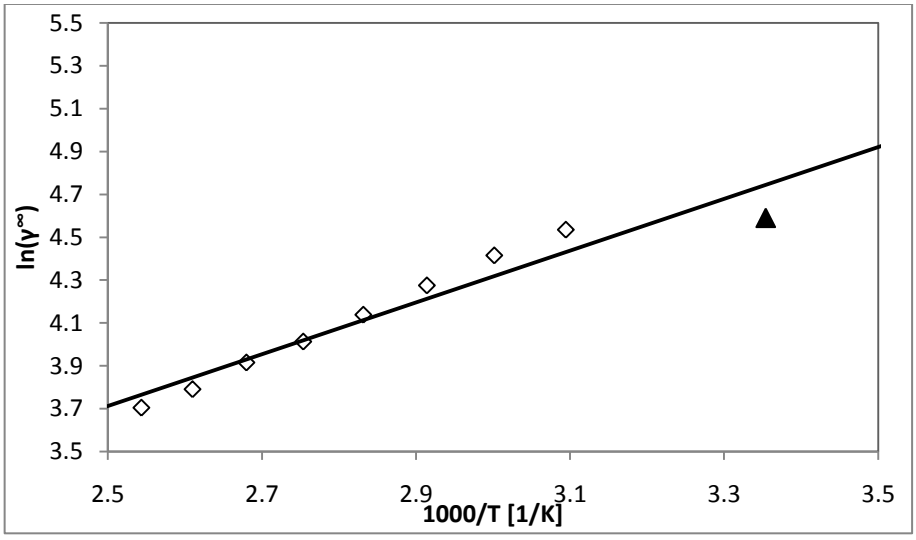

Figure 5-9: Literature ln(γ^{∞}) for n-heptane (1) in TEG (3). ◊, (Sun et al., 2003); ▲, (Arancibia & Catoggio, 1980); ——, line of best fit for literature data.

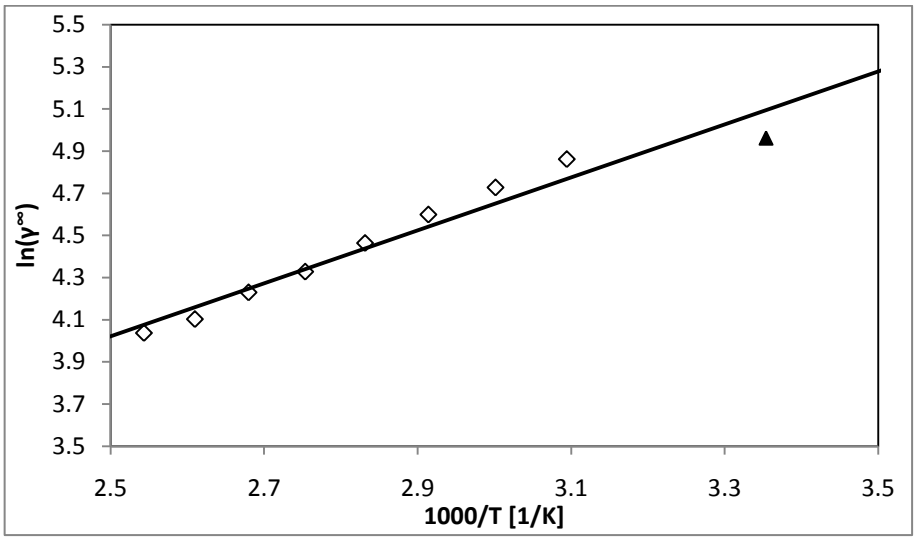

Figure 5-10: Literature ln(γ^{∞}) for n-octane (1) in TEG (3). ◊, (Sun et al., 2003); ▲, (Arancibia & Catoggio, 1980); ——, line of best fit for literature data.

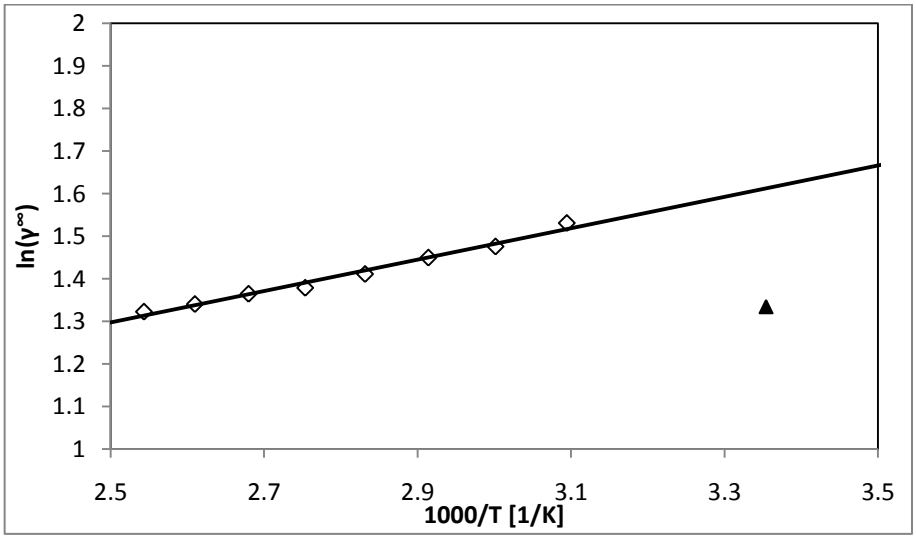

Figure 5-11: Literature ln(γ^{∞}) for benzene (1) in TEG (3). ◊, (Sun et al., 2003); ▲, (Arancibia & Catoggio, 1980); ——, line of best fit for Sun et al..

There was poor agreement between the data given by Arancibia and Cataggio (1980) and that given by Sun and co-workers (2003). This disagreement appeared to be the case for all of the solutes for which values were given by both authors. Literature values for the infinite dilution activity coefficients in TEG are given in Table 5-8.

Table 5-8: Infinite dilution activity coefficient data for various solutes in TEG

Source		Lit.[a]	Lit.[b]							
n-hexane	**T [K]**	**298.15**								
	γ^{∞}	67								
n-heptane	**T [K]**	**298.15**	**323.15**	**333.15**	**343.15**	**353.15**	**363.15**	**373.15**	**383.15**	**393.15**
	γ^{∞}	98.5	93.26	82.73	71.92	62.72	55.34	50.19	44.31	40.65
n-octane	**T [K]**	**298.15**	**323.15**	**333.15**	**343.15**	**353.15**	**363.15**	**373.15**	**383.15**	**393.15**
	γ^{∞}	143	129.34	113.08	99.45	86.86	75.83	68.73	60.54	56.69
n-nonane	**T [K]**	**298.15**	**323.15**	**333.15**	**343.15**	**353.15**	**363.15**	**373.15**	**383.15**	**393.15**
	γ^{∞}	208	182.64	155.99	139.83	119.04	103.05	92.99	81.40	73.91
n-decane	**T [K]**		**323.15**	**333.15**	**343.15**	**353.15**	**363.15**	**373.15**	**383.15**	**393.15**
	γ^{∞}		252.08	219.49	196.39	161.91	140.53	125.21	107.33	95.59
benzene	**T [K]**	**298.15**	**323.15**	**333.15**	**343.15**	**353.15**	**363.15**	**373.15**	**383.15**	**393.15**
	γ^{∞}	3.8	4.62	4.38	4.26	4.10	3.97	3.92	3.82	3.76
toluene	**T [K]**	**298.15**	**323.15**	**333.15**	**343.15**	**353.15**	**363.15**	**373.15**	**383.15**	**393.15**
	γ^{∞}	6.01	7.11	6.80	6.51	6.25	5.99	5.85	5.56	5.51
ethylbenzene	**T [K]**	**298.15**	**323.15**	**333.15**	**343.15**	**353.15**	**363.15**	**373.15**	**383.15**	**393.15**
	γ^{∞}	9.31	10.86	10.28	9.73	9.10	8.72	8.39	7.94	7.72
cyclohexane	**T [K]**	**298.15**								
	γ^{∞}	15.6								
Hept-1-ene	**T [K]**	**298.15**								
	γ^{∞}	49.5								

Lit.[a] (Arancibia & Catoggio, 1980); Lit.[b] (Sun et al., 2003)

5.4 Diethylene glycol

Only one set of literature data could be found for infinite dilution activity coefficients in diethylene glycol (DEG). The equipment that was used by the author and the temperature at which measurements were made are detailed in Table 5-9. The infinite dilution activity coefficients are given in Table 5-10.

Table 5-9: Techniques and temperatures utilised for previous γ^{∞} measurements in DEG

Reference	Technique	T [K]	Comments
(Arancibia & Catoggio, 1980)	Measurement of the partition coefficient performed using gas-liquid chromatography Activity coefficient calculated from this data	298	A pre-saturator was used to saturate the carrier gas

Table 5-10: Infinite dilution activity coefficients for various solutes with DEG at 298.15 K. Data taken from Arancibia and Catoggio (1980)

Solute	γ^{∞}
n-hexane	110
n-heptane	166
n-octane	250
iso-octane	195
n-nonane	372
cyclohexane	50.9
methyl cyclohexane	79.2
ethyl cyclohexane	117
hept-1-ene	83.5
oct-1-ene	128
cyclohexene	26
benzene	6.48
toluene	10.4
ethylbenzene	16.2
o-xylene	15.5
m-xylene	17.6
p-xylene	17.5

CHAPTER 6

Results and discussion

6.1 Calibrations

The Pt-100 resistance thermometers were calibrated to a WIKA CHT 6500 temperature standard. The calibration was performed in a WIKA CTB 9100 silicon oil bath. Three measurements were performed at each temperature, with the temperature increased, then decreased then increased once more. This was to account for any hysteresis that may have occurred. This bath was used as it had a high stability, which allowed for accurate measurements of the temperature readings of both the standard and the Pt-100 resistance thermometers. The calibration plot for the resistance thermometer used to monitor the temperature of the silicon oil bath is provided in Figure 6-1.

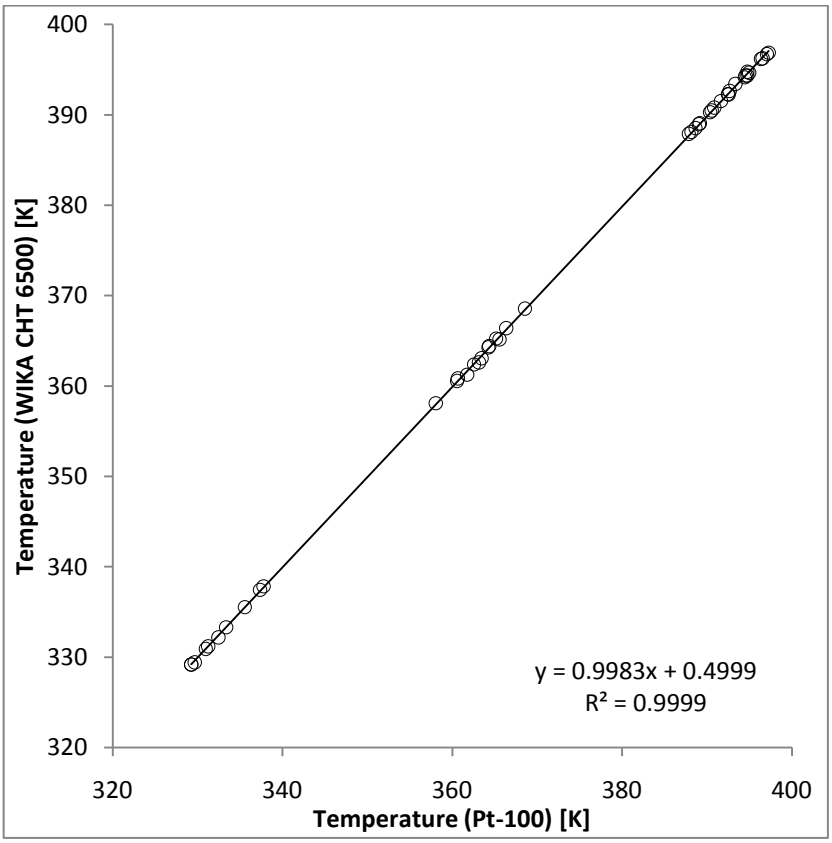

Figure 6-1: Temperature calibration for the Pt-100 measuring the silicon oil bath temperature.

The WIKA CHT 6500 had an accuracy of 0.03 K, and the Pt-100 resistance thermometers provided readings to a resolution of 0.1 K.

The Pt-100 used to monitor the line temperature had an offset of approximately -2.9 K, whereas the Pt-100 used to monitor the bath temperature had an offset of about 0.5 K. Both resistance thermometers exhibited a linear behaviour.

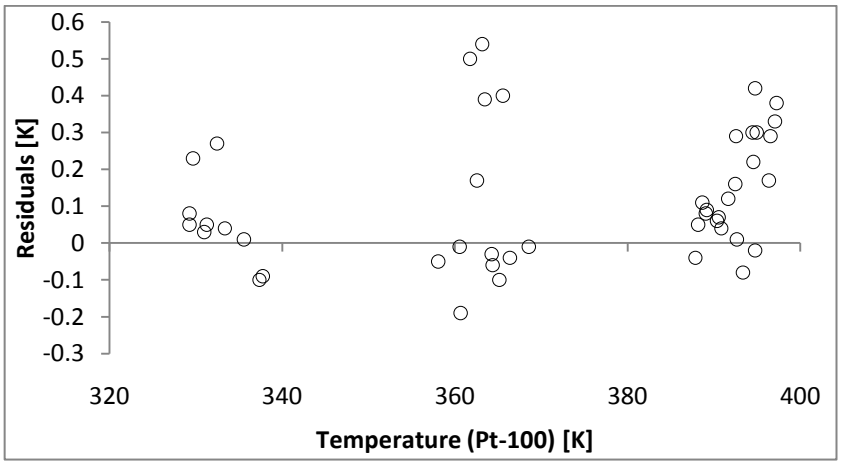

Figure 6-2: Residuals for the calibration of the Pt-100 measuring the silicon oil bath temperature.

The standard error for the calibration of the Pt-100 resistance thermometer measuring the silicon oil bath temperature was 0.11 K.

6.2 Gas-liquid chromatography

The existing gas-liquid chromatography apparatus was modified to allow for pre-saturation of the carrier gas. To provide control of the pre-saturation loop, two Pt-100 resistance thermometers were included. The measurements of the infinite dilution activity coefficients of a number of hydrocarbon solutes in hexadecane were performed prior to the modification, in order to verify the initial procedure (Section 6.2.3)

Once the modification had been completed, the measurements of the infinite dilution activity coefficients of a number of hydrocarbons in N-formylmorpholine were used to verify that the apparatus provided accurate results (Section 6.2.4). After the set up and procedure had been shown to provide accurate results, the infinite dilution activity coefficients in NMP, DEG and TEG were measured.

The method of determining the uncertainty of the results from this GLC set up is discussed in Section 6.2.1. A number of observations were made during the course of the experimental work. These observations and several difficulties that had to be overcome relating to the experimental procedure and set up were discussed in Section 6.2.2.

6.2.1 Uncertainty analysis

It was impossible for an entire set of measurements to be performed at exactly the same conditions, due to fluctuations in ambient pressure and temperature, and other independent variables. There were constantly small disturbances to the process variables during the measurement periods. These variations had to be taken into account during the measurements, and while performing the calculations.

The process conditions were continuously monitored and changes in the process variables were recorded at regular intervals during the entire period of the measurements. From this recorded data, the minimum, average and maximum of each of the variables was obtained.

For each solute-solvent-temperature combination, three repeatable measurements were made. The calculation was then performed for all of the permutations of the process variables. These combinations gave all the possible γ^{∞} values for that particular experimental work. Two outliers were then removed from this set of values. The experimental value for the particular combination was taken as the average of the remaining values, while the error of measurement was calculated by Equation 6-1.

$$measurement\ error\ (\%) = \frac{maximum - minimum}{average} \times 100\% \tag{6–1}$$

The error from literature data was calculated using Equation (6–2.

$$literature\ error\ (\%) = \frac{|measured - literature|}{measured} \times 100\% \tag{6–2}$$

6.2.2 Experimental method

6.2.2.1 Purity of solvents

In order to verify the stated purities of the solvents, the refractive index was initially used. This was, however, not able to confirm whether the purity was greater than the 99 wt % required for the measurements. A Shimadzu GC-2014 gas chromatograph using a Poropak packed column with an 80/100 mesh size was therefore used to check the purity of the solvent after degassing. These measured refractive indices and purities are given in Table 6-1.

Table 6-1: Solvents used; with their refractive index (measured and literature) and their measured purity.

Solvent	CAS Number	$R^I_{meas.}$ (298.15 K)	$R^I_{lit.}$ (298.15 K)	Purity (GC) wt %	Purity (stated) wt %
hexadecane	544-76-3	1.4325	1.4325[a]	99.10	> 99
N-formylmorpholine	4394-85-8	1.4847	1.4850[b]	99.04	> 99
N-methylpyrrolidone	872-50-4	1.4686	1.4681[c]	99.60	> 99.5
triethylene glycol	112-27-6	1.4539	1.4541[d]	99.54	> 99
diethylene glycol	107-21-1	1.4446	1.4447[e]	99.11	> 99

a (Camin et al., 1954), b (Awwad and Al-Dujaili, 2001), c (Blanco et al., 1997), d, (Chiao and Thompson, 1957), e (Aminabhavi and Gopalakrishna, 1995)

6.2.2.2 Preparation of column

Dichloromethane was used to ensure an even distribution of the solvent on the inert support. Dichloromethane is highly volatile, and has a normal boiling point of 39.7°C (Smith et al., 2005). The comparison between the vapour pressure of dichloromethane and water at temperatures between 290 and 320 K is shown in Figure 6-3. The vapour pressure of the solvents was too low to view on this graph. Figure 6-3 shows that at a temperature of 303.15 K, the dichloromethane would boil at an absolute pressure of approximately 60 kPa.

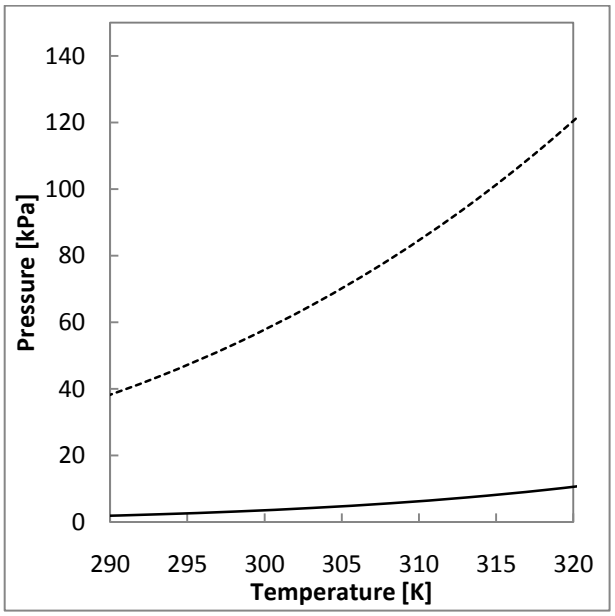

Figure 6-3: Vapour pressure as a function of temperature. Comparison between: -----, dichloromethane (Antoine parameters given by Smith et. al. (2005)); and, ——, water (Antoine parameters given by Smith et. al. (2005)).

6.2.2.3 Column packing

For this work, the stationary phase was packed while the column was vibrated. This ensured that the stationary phase did not form any gaps or channels.

6.2.2.4 Pre-saturator seals

Initially, the pre-saturator cells were sealed by the compression of viton ‘o’-rings. Viton was found to degrade very rapidly when exposed to NFM and NMP, especially at high temperatures, and a replacement seal had to be found.

The viton ‘o’-rings were replaced with machined Teflon ‘o’-rings. These Teflon ‘o’-rings were considerably harder than the viton seals, and therefore had to be heated to approximately 120°C before the pre-saturators could be tightly sealed.

6.2.2.5 Inert component

Air was used as the inert component for all of the measurements, as it was easy to obtain and was not retained by the solvents. A small volume of air was injected with each solute injection in order to improve the accuracy of the measurements. This could be done as interactions between air and the solutes were also negligible.

6.2.2.6 Reference solute

A reference solute was injected at regular intervals, in order to calculate the amount of solvent present in the column. This was preferable to removing the column from the GC and weighing at intervals. For the column to be removed from the GC, the detector had to be turned off, and then turned on again when the carrier gas was flowing again. The direct measurement of the mass of solvent in the column would have wasted lengthy periods of time.

The reference solutes used were either n-hexane or n-octane. Their infinite dilution activity coefficients in the solvent were first measured, and thereafter, the mass of solvent could be determined from the retention time of the reference solute. In the intervals between the estimations of the solvent mass using the reference solute, the mass had to be determined by interpolation. The changes in the mass in these time intervals were, however, usually negligible.

6.2.3 Hexadecane test system

The infinite dilution activity coefficients for a hexadecane test system were measured at 313.2 K, 323.2 K and 333.2 K (Table 6-2). The results were found to correlate with literature data. The measured γ^{∞} values for n-hexane, cyclohexane and benzene are given in Figures 6-4, 6-5 and 6-6 respectively, where they were compared with previously measured data.

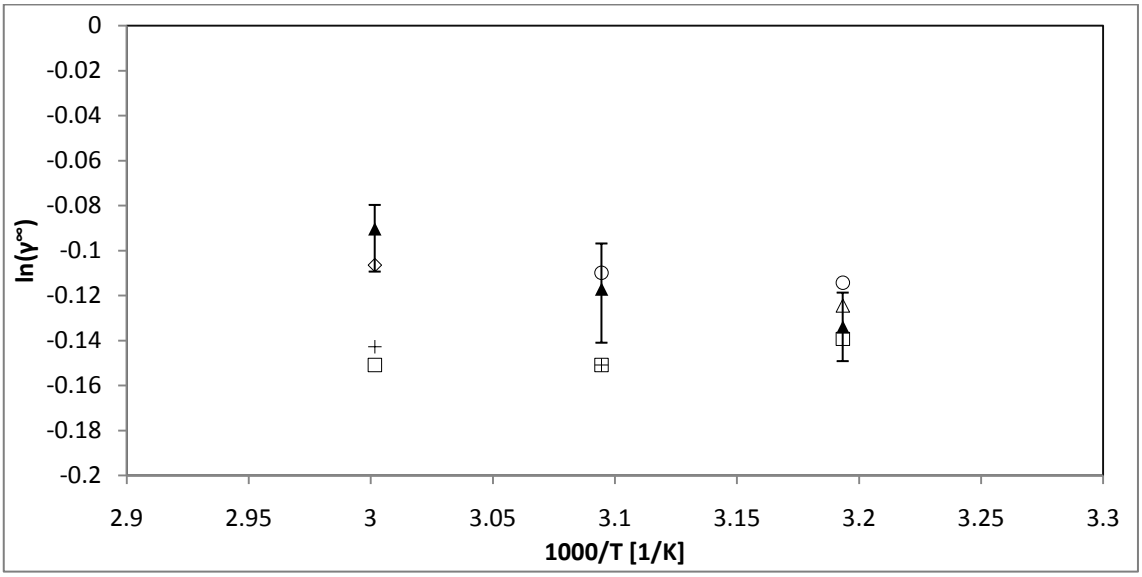

Figure 6-4: Measured $\ln(\gamma^{\infty})$ including error bars and literature $\ln(\gamma^{\infty})$ against 1000/T for n-hexane (1) in hexadecane (3). ▲, this work; □, (Hussey and Parcher, 1973); ◊, (Turek et al., 1979); Δ, (Chien et al., 1981); +, (Schult et al., 2001); ○, (Tumba, 2010).

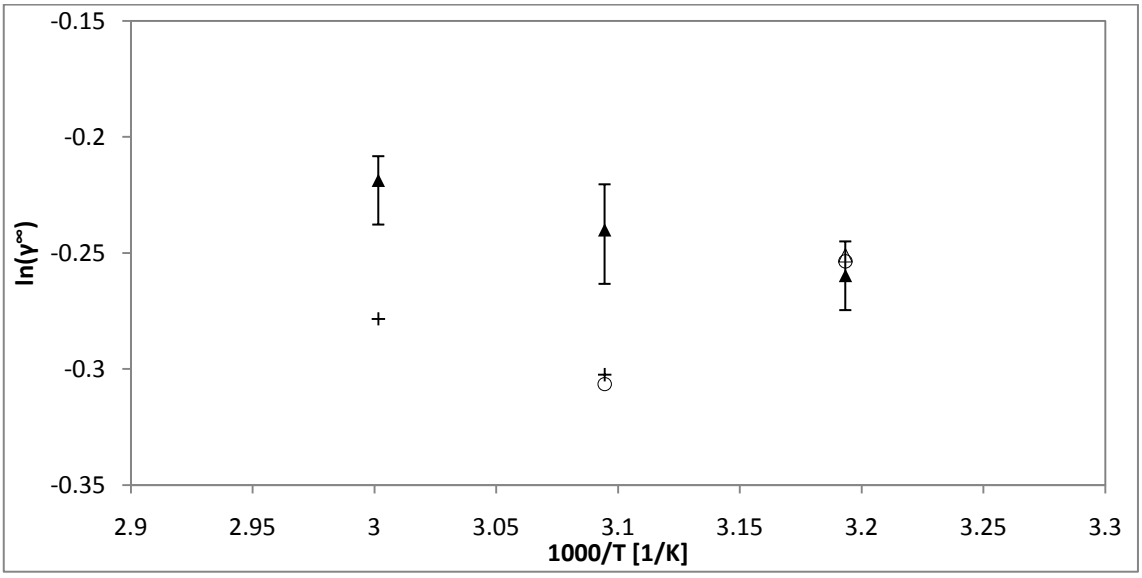

Figure 6-5: Measured $\ln(\gamma^{\infty})$ including error bars and literature $\ln(\gamma^{\infty})$ against 1000/T for cyclohexane (1) in hexadecane (3). ▲, this work; Δ, (Chien et al., 1981); +, (Schult et al., 2001); ○, (Tumba, 2010).

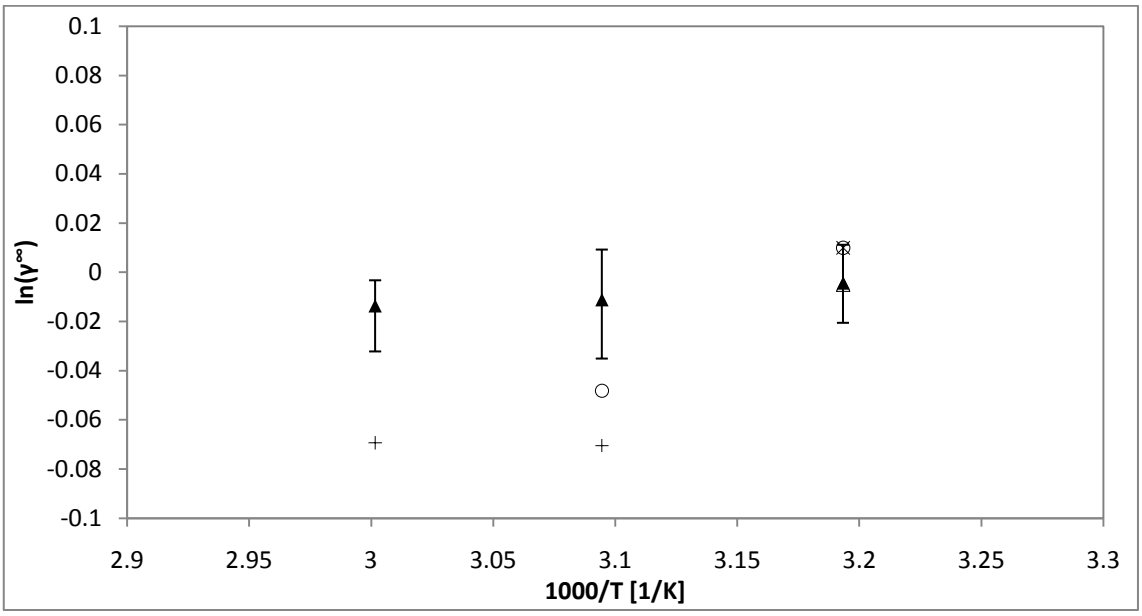

Figure 6-6: Measured ln(γ^{∞}) including error bars and literature ln(γ^{∞}) against 1000/T for benzene (1) in hexadecane (3). ▲, this work; Δ, (Chien et al., 1981); +, (Schult et al., 2001); X, (Heintz et al., 2001); ○, (Tumba, 2010).

All of the measured infinite dilution activity coefficients for the solutes in hexadecane are given in Table 6-2. The differences between the infinite dilution activity coefficients that were found in literature and those that were measured were less than 7.5% for all but the system of benzene in the hexadecane at 333.2 K.

The large errors in the case of benzene could have been due to the use of the measurements of the infinite dilution activity coefficient of the various solutes in hexadecane for the development of an accurate technique for further measurements. These measurements were the first to be undertaken, and were therefore the most prone to errors due to the experimental technique.

The small differences between the experimental data measured here, and those measured by other authors verified that this GLC method provided accurate results.

Table 6-2: Measured γ^{∞} data, literature γ^{∞} data and percentage error with respect to literature data for the systems of several hydrocarbon solutes in hexadecane.

		T [K]	γ^{∞}	Meas. error [%]	Literature	Dif. to Lit. [%]
Alkanes	n-pentane	313.2	0.865	1.68		
		323.2	0.882	2.57	0.839 [a]	4.83
	n-hexane	313.2	0.875	1.53	0.87-0.911 [a, b, c, d, e]	4.15
		323.2	0.890	2.36	0.86-0.905 [a, f]	3.43
		333.2	0.914	1.89	0.867-0.899 [f, g]	5.39
	n-heptane	313.2	0.888	1.49	0.898-0.928 [b, c]	4.47
		323.2	0.905	2.32	0.867-0.921 [a, f]	4.39
		333.2	0.930	1.71	0.879 [f]	5.47
Alkenes	pent-1-ene	313.2	0.881	1.47		
		323.2	0.899	1.87		
		333.2	0.705	1.88		
	hex-1-ene	313.2	0.891	1.47		
		323.2	0.903	2.39	0.862 [a]	4.51
		333.2	0.925	1.91		
	hept-1-ene	313.2	0.902	1.30		
		323.2	0.919	2.31	0.866 [a]	5.78
		333.2	0.943	1.85		
Alkynes	pent-1-yne	313.2	1.230	1.75		
		323.2	1.228	2.56		
		333.2	0.940	1.88		
	hex-1-yne	313.2	1.220	1.62		
		323.2	1.209	2.36		
		333.2	1.206	1.87		
	hept-1-yne	313.2	1.148	1.45		
		323.2	1.139	2.39		
		333.2	1.146	1.91		
Cyclo-alkanes	cyclopentane	313.2	0.720	1.50		
		323.2	0.742	2.36	0.695 [a]	6.33
		333.2	0.566	1.83		
	cyclohexane	313.2	0.771	1.49	0.776-0.778 [a, b]	0.87
		323.2	0.787	2.31	0.736-0.739 [a, f]	6.88
		333.2	0.804	1.89	0.757 [f]	5.80
	cycloheptane	313.2	0.787	1.66		
		323.2	0.803	2.27		
		333.2	0.822	1.94		
Aromatics	benzene	313.2	0.996	1.61	0.995-1.01 [a, b, c]	1.44
		323.2	0.989	2.37	0.932-0.953 [a, f]	6.11
		333.2	0.987	1.84	0.894-0.933 [f, g]	10.35
	toluene	313.2	0.963	1.12		
		323.2	0.968	2.35		
		333.2	0.977	1.92	0.904 [g]	7.48
	ethylbenzene	323.2	1.045	2.49		
		333.2	1.049	1.89		

[a] Tumba, 2010;, [b] Chien et al., 1981; [c] Heintz et al., 2002; [d] Laub et al., 1977; [e] Hussey and Parcher, 1973; [f] Schult et al., 2001; [g] Turek et al., 1979.

6.2.4 N-formylmorpholine test system

The γ^{∞} values of various solutes in N-formylmorpholine, at temperatures of 333.2, 348.2 and 363.2 K, measured using the described gas-liquid chromatography experimental set up, were used to provide verification of the experimental set up and procedure. This verification was done by comparing the results obtained in this work with experimental data obtained from the various literature sources, discussed in Chapter 5.1. Figures 6-7 to 6-10 show the plots of the natural logarithm of γ^{∞} against 1000 divided by temperature for n-hexane, cyclohexane, hex-1-ene and benzene respectively in N-formylmorpholine.

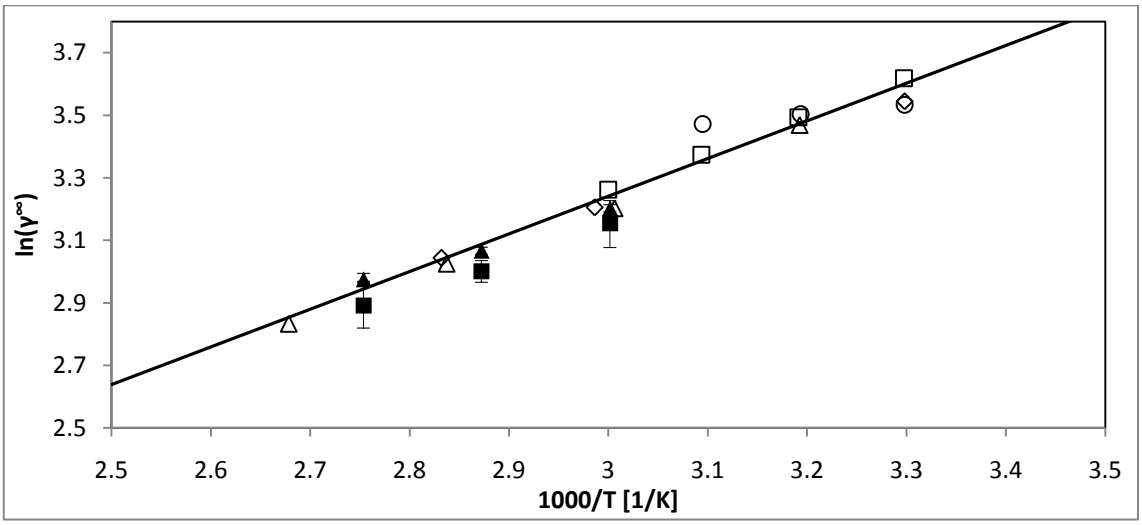

Figure 6-7: Measured ln(γ^{∞}) including error bars and literature ln(γ^{∞}) against 1000/T for n-hexane (1) in N-formylmorpholine (3). ■, this work (calculated using the equation of Laub and Pecsok); ▲, this work (calculated using the equation of Everett); △, (Weidlich et al., 1987); ◊, (Knoop et al., 1989); ○, (Park et al., 2001); □, (Krummen and Gmehling, 2004); ——, line of best fit for literature data.

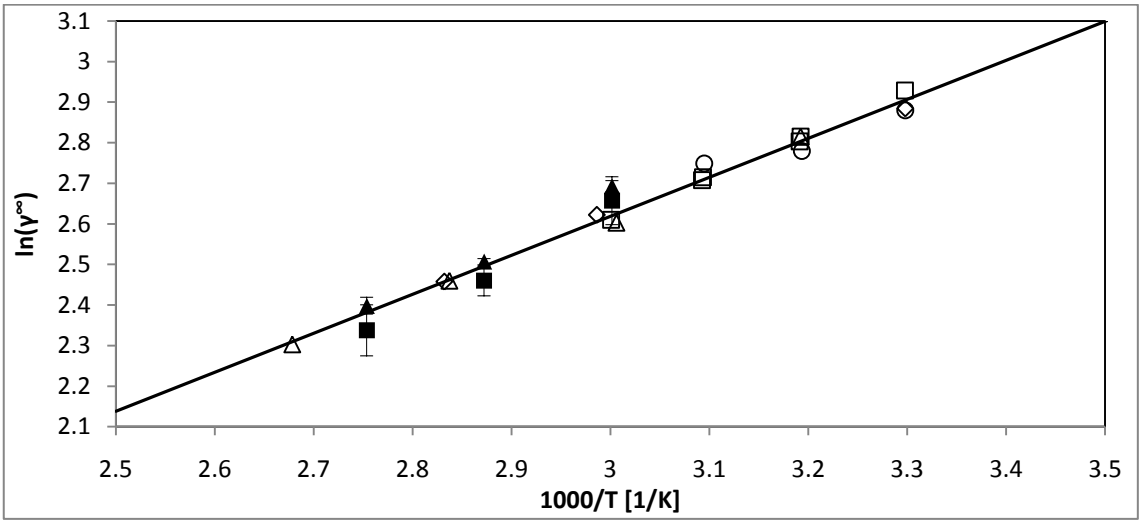

Figure 6-8: Measured ln(γ^{∞}) including error bars and literature ln(γ^{∞}) against 1000/T for cyclohexane (1) in N-formylmorpholine (3). ■, this work (calculated using the equation of Laub and Pecsok); ▲, this work (calculated using the equation of Everett); △, (Weidlich et al., 1987); ◊, (Knoop et al., 1989); ○, (Park et al., 2001); □, (Krummen and Gmehling, 2004); ——, line of best fit for literature data.

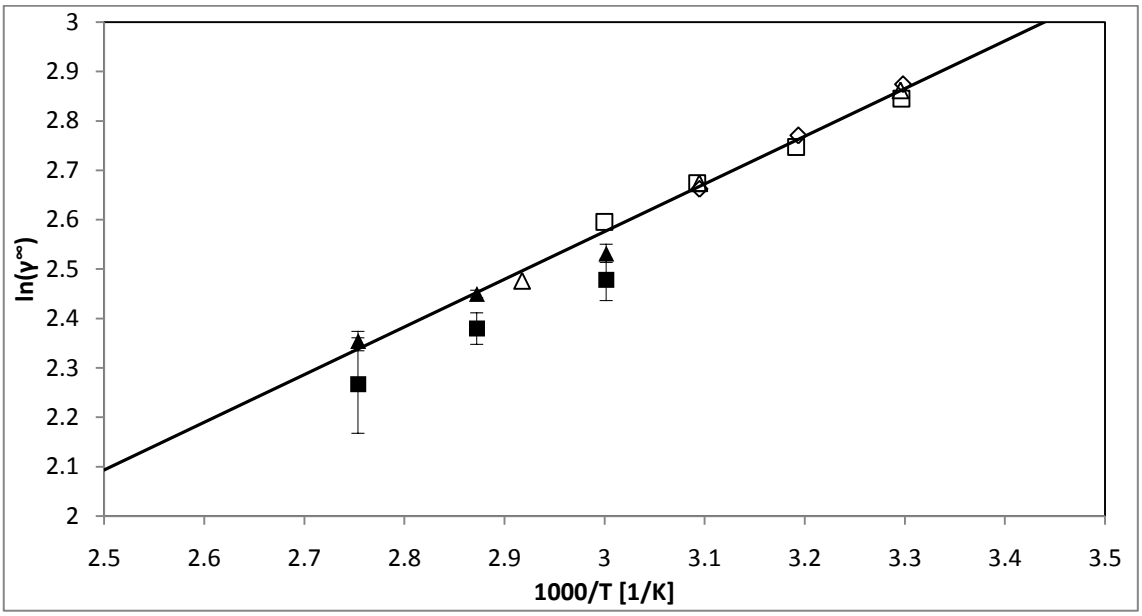

Figure 6-9: Measured ln(γ^{∞}) including error bars and literature ln(γ^{∞}) against 1000/T for hex-1-ene (1) in N-formylmorpholine (3). ■, this work (calculated using the equation of Laub and Pecsok); ▲, this work (calculated using the equation of Everett); △, (Weidlich et al., 1987); ◊, (Park et al., 2001); □, (Krummen and Gmehling, 2004); ——, line of best fit for literature data.

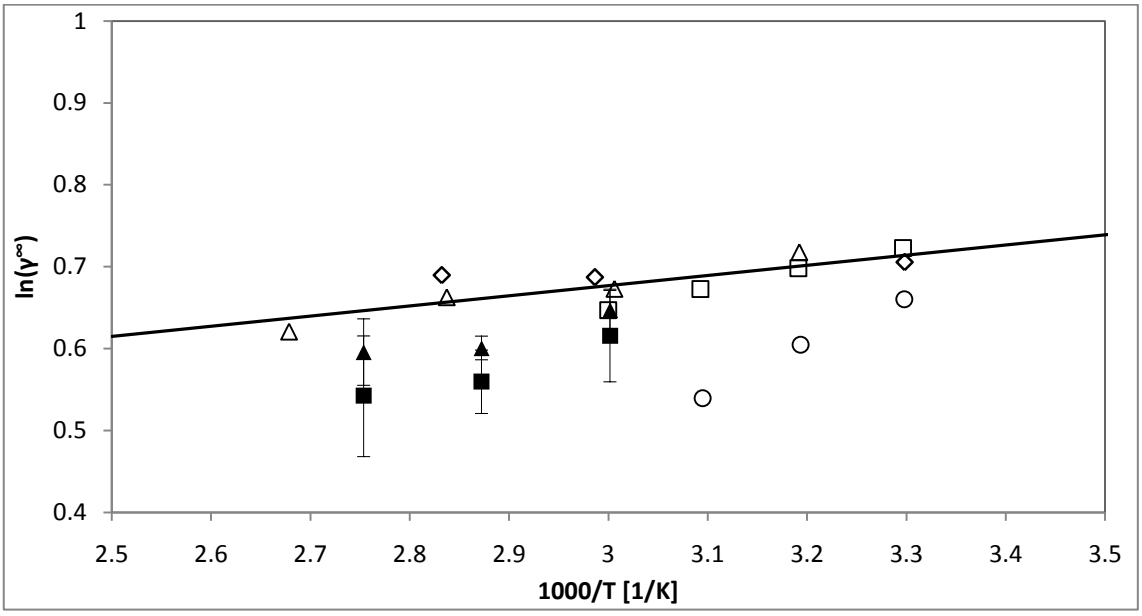

Figure 6-10: Measured ln(γ^{∞}) including error bars and literature ln(γ^{∞}) against 1000/T for benzene (1) in N-formylmorpholine (3). ■, this work (calculated using the equation of Laub and Pecsok); ▲, this work (calculated using the equation of Everett); △, (Weidlich et al., 1987); ◊, (Knoop et al., 1989); ○, (Park et al., 2001); □, (Krummen and Gmehling, 2004); ——, line of best fit for literature data.

Error! Not a valid bookmark self-reference. provides all the measured γ^{∞} values in N-formylmorpholine. For the most part, there is close agreement between the measured data and the literature data, where this is available. The most notable disagreement between literature and experimental data was found for the measurement of the γ^{∞} of alcohols in N-formylmorpholine. The error between the data measured by Weidlich et al. (1987) and the experimental values measured in this work differ by between 10 and 45%. No other data, other than that measured by Weidlich and co-authors could be found, and therefore there was no independent means of verification of the measured γ^{∞} values for the alcohols.

Table 6-3: Measured γ^{∞} and percentage error from literature data for the hydrocarbon solutes in N-formylmorpholine.

		T [K]	γ^{∞}	Meas. error [%] †	Literature	Dif. from Lit. [%] ‡
Alkanes	n-pentane	333.2	19.25	1.34	19.3-19.6 [a, b]	0.26
		348.2	17.30	1.41	16.9 [*]	2.31
		363.2	15.30	3.06	14.9 [*]	2.61
	n-hexane	333.2	24.60	1.19	24.6-26.1 [a, b]	0
		348.2	21.47	1.15	21.9 [*]	2.00
		363.2	19.59	1.98	19.0 [*]	3.01
	n-heptane	333.2	31.26	1.73	31.4-33.9 [a, b]	0.45
		348.2	27.54	1.02	27.8 [*]	0.94
		363.2	25.89	1.4	-	-
	n-octane	333.2	39.45	1.19	40.7-41.8 [a, c]	3.17
		348.2	34.32	1.01	34.9 [*]	1.69
		363.2	30.55	2.21	29.6	3.11
	n-nonane	333.2	50.25	1.88	-	-
		348.2	43.51	2.76	-	-
		363.2	38.18	2.87	-	-
Alkenes	pent-1-ene	333.2	9.97	1.68	9.85 [b]	1.20
		348.2	9.43	0.82	-	-
		363.2	8.61	1.98	-	-
	hex-1-ene	333.2	13.52	2.02	13.4 [b]	0.88
		348.2	11.58	0.82	11.6 [*]	0.17
		363.2	10.53	1.96	10.4 [*]	1.23
	hept-1-ene	333.2	15.98	1.71	17 [b]	6.00
		348.2	14.58	0.88	14.9 [*]	2.14
		363.2	13.27	2.94	13.2 [*]	0.53
	oct-1-ene	333.2	20.51	1.68	21.5 [*]	0.05
		348.2	18.43	1.11	-	-
		363.2	16.71	1.42	-	-
Alkynes	pent-1-yne	333.2	2.56	2.37	-	-
		348.2	2.58	1.12	-	-
		363.2	2.38	1.43	-	-
	hex-1-yne	333.2	3.25	1.85	-	-
		348.2	3.19	0.91	-	-
		363.2	2.78	3.04	-	-

Table 6-4 cont.: Measured γ^{∞} and percentage error from literature data for the hydrocarbon solutes in N-formylmorpholine.

		T [K]	γ^{∞}	Meas. error [%] †	Literature	Dif. from Lit. [%] ‡
Alkynes	hept-1-yne	333.2	3.85	1.71	-	-
		348.2	3.83	0.93	-	-
		363.2	3.68	2.23	-	-
	oct-1-yne	333.2	5.15	1.98	-	-
		348.2	4.90	0.87	-	-
		363.2	4.65	1.73	-	-
Cyclo-alkanes	cyclopentane	333.2	10.22	1.87	9.92-10 [a, b]	2.15
		348.2	8.75	1.17	9.0 [*]	2.86
		363.2	7.59	2.29	-	-
	cyclohexane	333.2	13.77	1.49	13.5-13.77 [a, b, c]	0
		348.2	12.27	0.9	12.1 [*]	1.39
		363.2	11.00	2.20	10.8 [*]	1.82
Cyclo-alkanes	cycloheptane	333.2	15.43	1.59	-	-
		348.2	12.72	1.29	-	-
		363.2	10.46	1.50	-	-
	cyclooctane	333.2	17.68	2.63	-	-
		348.2	14.47	1.26	-	-
		363.2	11.89	1.26	-	-
Alcohols	methanol	333.2	0.852	1.60	1.05 [*]	23.12
		348.2	0.847	0.89	1.04 [*]	22.79
		363.2	0.706	3.94	1.03 [*]	45.89
	ethanol	333.2	1.204	2.55	1.38 [*]	14.62
		348.2	1.141	1.27	1.33 [*]	16.56
		363.2	0.914	3.06	1.28 [*]	40.04
	propan-1-ol	333.2	1.246	0.58	-	-
		348.2	1.153	1.57	-	-
		363.2	0.913	2.24	-	-
	propan-2-ol	333.2	1.460	1.19	-	-
		348.2	1.289	1.59	-	-
		363.2	0.933	4.90	-	-
Aromatics	benzene	333.2	1.91	2.65	1.91-1.99 [a, b, c]	0
		348.2	1.82	1.56	1.94 [*]	6.59
		363.2	1.81	3.96	1.91 [*]	5.52
	toluene	333.2	2.71	1.57	2.56-2.74 [a, b, c]	0
		348.2	4.04	0.75	2.60 [*]	35.64
		363.2	2.55	1.49	2.51 [*]	1.57
	ethylbenzene	333.2	3.46	2.74	3.60-3.62 [a, c]	4.05
		348.2	3.41	1.35	3.57	4.69
		363.2	3.21	1.89	3.48	8.41

[a] (Weidlich et al., 1987); [b] (Krummen and Gmehling, 2004); [c] (Knoop et al., 1989); [*] calculated from line of best fit to all collected literature data (see Table 5-3); † calculated by Equation 6-1; ‡ calculated by Equation 6-2.

Weidlich and co-workers made use of the calculation procedure of Laub and Pecsok (1978), which used the Soave equation of state. The Soave-Redlich-Kwong EOS was proposed for non-polar substances (Soave, 1972). The fugacity coefficient of alcohols would therefore not be described very accurately by the Soave EOS, due to the polarity of alcohols. This could have been one of the factors leading to the disparity between the values measured by Weidlich and co-workers and in this study.

The measured γ^{∞} value for toluene at 348.2 K also appeared to be incorrect when compared with the γ^{∞} values of toluene at other temperatures, as well as when compared with literature data. This was most likely due to a change in the process conditions under which the measurements were made. An example of this could have been a change in the flow rate of the carrier gas, or a fluctuation in the temperature of the column.

An interesting observation was made for hept-1-ene in NFM. The literature data consisted only of the data measured by Krummen and Gmehling (2004). When the excess enthalpies of the various alkenes in NFM were examined (See Table 5-2), the excess enthalpy of hept-1-ene differed substantially from that of both hex-1-ene and oct-1-ene. This could mean that the hept-1-ene measurements of Krummen and Gmehling and the data presented here were incorrect. This would have to be verified by further measurement.

6.2.4.1 Method of calculation

For this work, the method of calculation that gave values that fitted the literature data with better consistency and accuracy had to be chosen. From Figures 6-7 to 6-10, it can be seen that the calculation method of Everett (1965), given by Equation 4-6, and the calculation of Laub and Pecsok (1978), given by Equation 4-10, produced very similar results. The values determined using both calculation techniques are given in Table 6-5.

Table 6-5: Comparison of results calculated using the equation of Everett (1965) and the equation of Laub and Pecsok (1978) for selected solutes in N-formylmorpholine

			Everett Eqn. (4–6)		Laub and Pecsok Eqn. (4-10)		
		T [K]	γ^{∞}	Meas. error [%] †	γ^{∞}	Meas. error [%] †	Literature
Alkanes	n-pentane	333.2	19.25	1.34	17.73	4.72	19.3-19.6 [a, b]
		348.2	17.30	1.41	15.55	3.88	16.9 *
		363.2	15.30	3.06	13.38	7.52	14.9 *
	n-hexane	333.2	24.60	1.19	23.43	7.58	24.6-26.1 [a, b]
		348.2	21.47	1.15	20.10	3.48	21.9 *
		363.2	19.59	1.98	18.02	8.1	19.0 *
Alkenes	pent-1-ene	333.2	9.97	1.68	9.08	3.94	9.85 [b]
		348.2	9.43	0.82	8.36	3.26	8.79 *
		363.2	8.61	1.98	7.41	10.85	7.91 *
	hex-1-ene	333.2	13.52	2.02	11.92	4.43	13.4 [b]
		348.2	11.58	0.82	10.80	3.26	11.6 *
		363.2	10.53	1.96	9.65	9.86	10.4 *
Cyclo-alkanes	cyclopentane	333.2	10.22	1.87	9.66	5.69	9.92-10 [a, b]
		348.2	8.75	1.17	8.13	5.53	9.0 *
		363.2	7.59	2.29	6.90	4.91	8.1 *
	cyclohexane	333.2	13.77	1.49	13.30	6.12	13.5-13.77 [a, b, c]
		348.2	12.27	0.9	10.92	3.77	12.1 *
		363.2	11.00	2.20	9.01	6.54	10.8 *
Aromatics	benzene	333.2	1.91	2.65	1.85	5.76	1.91-1.99 [a, b, c]
		348.2	1.82	1.56	1.75	4.01	1.94 *
		363.2	1.81	3.96	1.67	7.69	1.91 *
	toluene	333.2	2.71	1.57	2.50	6.68	2.56-2.74 [a, b, c]
		348.2	4.04	0.75	3.93	6.06	2.60 *
		363.2	2.55	1.49	1.96	4.06	2.51 *

[a] (Weidlich et al., 1987); [b] (Krummen and Gmehling, 2004); [c] (Knoop et al., 1989); * calculated from line of best fit to all collected literature data (see Table 5-3); † calculated by Equation 6-1.

The difference between the infinite dilution activity coefficients obtained using the two different calculation methods was between 2 % and 10 % of the value determined using the equation of Everett. The equation proposed by Laub and Pecsok gave much larger experimental errors than that of Everett, even though the same measured data was used in both calculations. The value determined using Equation 4-6 usually fell inside of the area of uncertainty given by Equation 4-10.

This difference between the two values was due to the different means of estimating the behaviour of the solute in the vapour phase. The equation of Everett used a truncated virial equation of state (EOS) to determine this behaviour, whereas that of Laub and Pecsok used the Soave Redlich-Kwong (SRK) equation of state to describe this behaviour. Both the SRK EOS and the virial EOS are dependent only on the critical properties and the temperature. Therefore

the larger disparity between the calculated value from Equation 4-10 and the literature data, in comparison with that between the calculated value from Equation 4-6 and the literature data is most likely due to the accuracy of the prediction given by the equation of state.

As a result of the better fit of the values calculated using the equation of Everett (Equation 4-6), as well as the smaller experimental error calculated, the equation proposed by Everett was preferred and used to calculate the subsequent infinite dilution activity coefficients.

6.2.4.2 Sensitivities

The sensitivity of the infinite dilution activity as calculated from the equation of Everett (1965) (Equation 4-6), was tested for the solutes in N-formylmorpholine at 333.2K. The sensitivity of the results for this wide range of solutes was investigated because each individual combination (solvent-solute) has its own unique physical properties, and therefore its own sensitivity to errors in the physical properties.

The results for the four most poorly defined properties; the pure and partial molar volumes, and the pure and mixed second virial coefficients; are given in Figure 6-11. The equation was, however, found to be most sensitive to changes in the number of moles of solvent and the vapour pressure of the solute. A change of 10% in the vapour pressure caused a change of approximately 10% in the infinite dilution activity coefficient. A change of 10% of the number of moles of solvent caused the infinite dilution activity coefficient also to change by 10%.

The calculation of the infinite dilution activity coefficient was directly dependent on the number of moles of solvent, and therefore, the accuracy of the determined value was highly dependent on accurate measurement of the mass of the column. Errors in the calculated vapour pressure also greatly affected the accuracy of the results, and it was therefore imperative that the vapour pressure correlations were as accurate as possible.

Second virial coefficient

The dependency of the calculations on the pure second virial coefficients was found to be very slight. The maximum variation in the infinite dilution activity coefficient with a 10% increase in the second virial coefficient of the pure solute, B_{11}, was 0.8%. The sensitivity of γ^{∞} to B_{11} was found to decrease with a decrease in the volatility of the solute. For the least volatile solute, propan-1-ol, γ^{∞} changed by only 0.05% with a 10% change in B_{11}.

The γ^{∞} values for the solutes with higher vapour pressures were most sensitive to the changes in the pure component second virial coefficient. This was probably due to the arrangement of the parameters in Equation 4-6, as the second virial coefficients for the pure components were found in the same term as the vapour pressure.

The sensitivity to changes in the mixed second virial coefficient (solute-carrier gas) was even less than the sensitivity to changes of the pure component second virial coefficient. The maximum change in the infinite dilution activity coefficient for a 10% change in the mixed second virial coefficient was 0.06%. The error due to the uncertainties in the measurements was significantly larger, and therefore this error could be ignored.

Molar volume

As described in Section 4.2.3.2, the value of the molar volume used for the determination of the infinite dilution activity coefficient was calculated from correlations which have been shown to adequately describe the molar volume with respect to temperature.

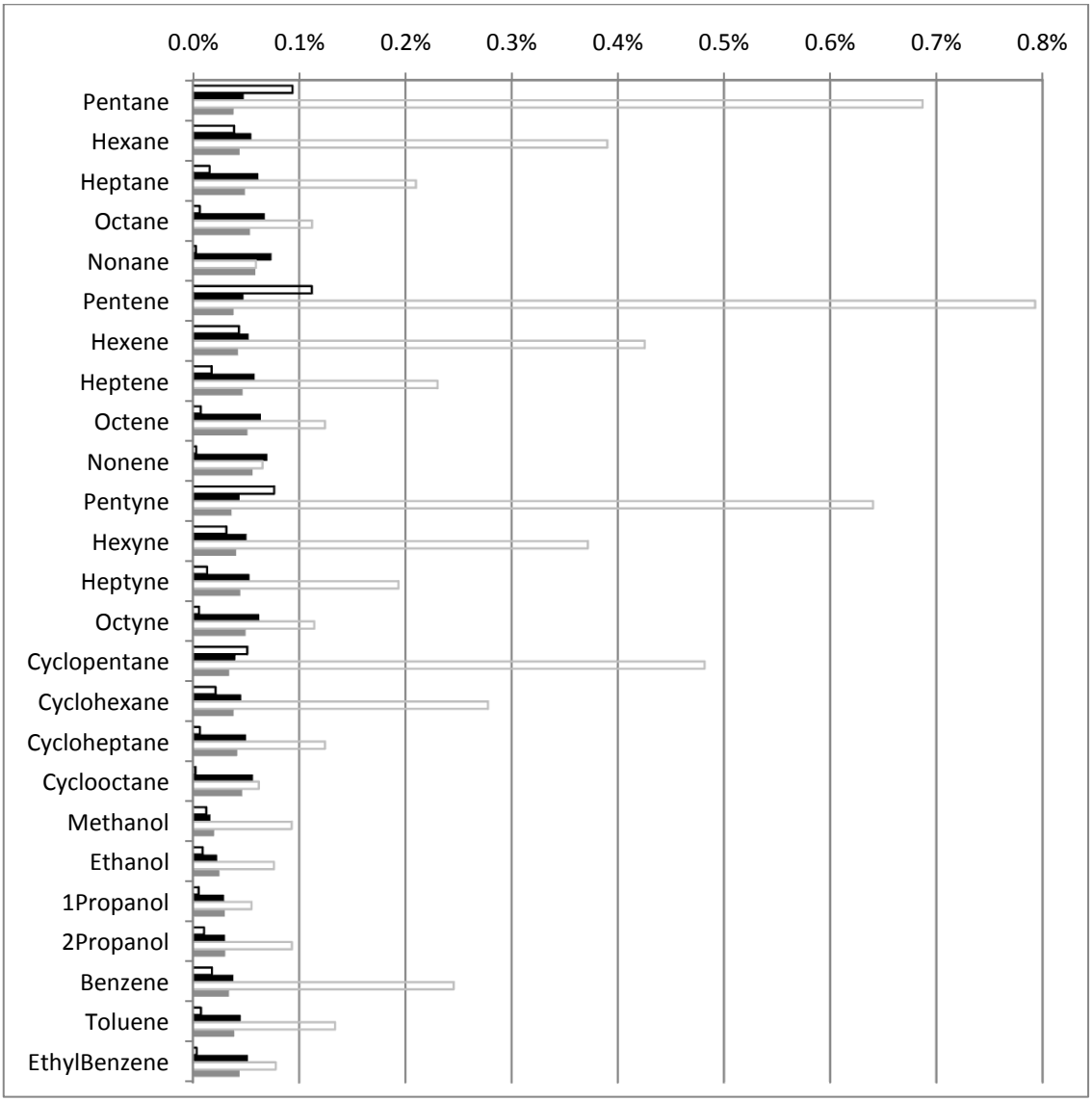

Figure 6-11: Sensitivity of the infinite dilution activity coefficient of various solutes in N-formylmorpholine at 333.2 K to variations of 10% in various parameters when using the equation of Everett (1965). □, sensitivity to a 10% change in molar volume; ■, sensitivity to a 10% change in partial molar volume; □, sensitivity to a 10% change in B_{11}; ■, sensitivity to a 10% change in B_{12}.

The sensitivity of Equation 4-6 to the errors introduced by making use of a correlation, rather than experimentally measured data, was investigated. It was found that for a change of 10% of the molar volume, the maximum deviation of γ^{∞} was 0.1%. This low sensitivity to the molar volume of the pure solutes meant that the correlations described in Chapter 4.2.3.2 could be used for the calculations, as other errors were much larger.

The γ^{∞} values for the components with larger molar volumes were greater affected by changes in the molar volume. They were not, however, affected to the same extent as the γ^{∞} values for changes in the second virial coefficients. This was expected, as a larger molar volume gave the second term in Equation 4-6 a larger weighting.

A worst case scenario of the discrepancy between the molar volume and the partial molar volume at infinite dilution was given as 10 cm^3/mol by Everett (1965). The error introduced by a 10 % change in the partial molar volume was found to be less than 0.04 % for all of the solutes in N-formylmorpholine. Thus, for this solvent, the caution against using the molar volume as the partial molar volume was unfounded. For other solvents, the sensitivity could however be larger, but even if it was ten times as sensitive, the error would still be within the experimental error.

Of course, with the assumption investigated here, the sensitivity of the results to changes in molar volume would increase, because the calculated value would be dependent on the inaccuracies of the molar volume on two occasions.

6.2.5 N-methylpyrrolidone

The γ^{∞} values of the various solutes in N-methylpyrrolidone, at temperatures of 333.2, 348.2 and 363.2 K were measured using the gas-liquid chromatography experimental set up. Prior to these measurements, the range of the literature data for NMP was as much as 30% of the maximum value. Due to the improvement in the accuracy of the experimental technique, an uncertainty of this magnitude has become unacceptable. The plots of the natural logarithm of γ^{∞} against the inverse of temperature for four solutes in NMP are given in Figures 6-12 to 6-15.

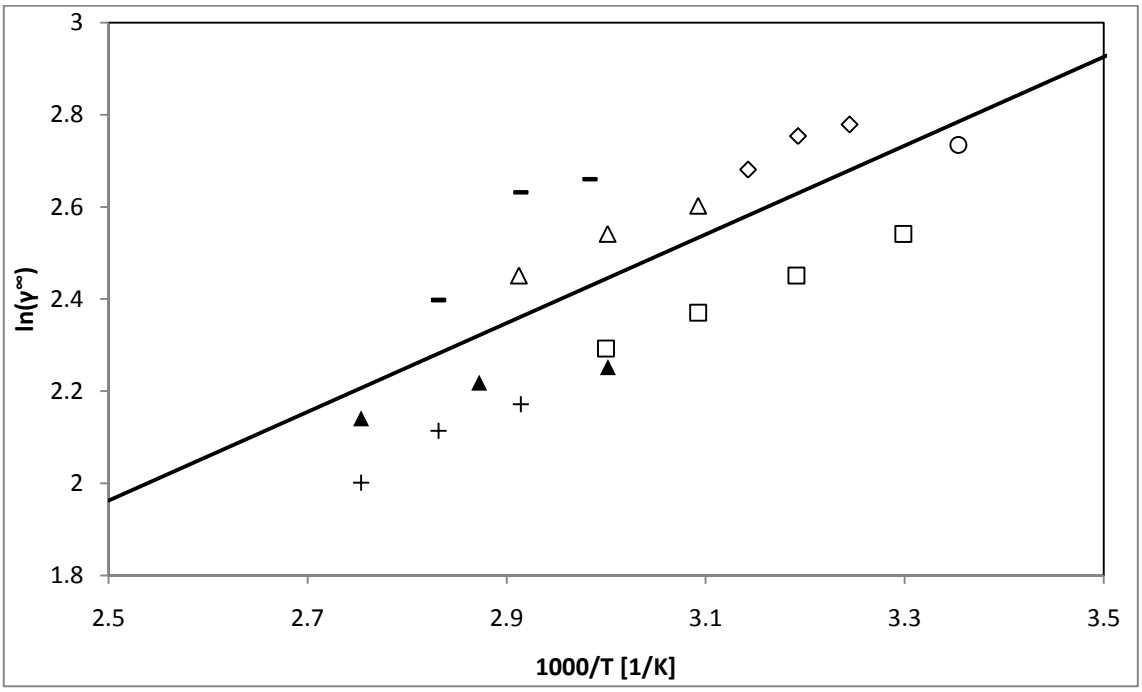

Figure 6-12: Measured ln(γ^{∞}) and literature ln(γ^{∞}) against 1000/T for n-hexane (1) in N-methylpyrrolidone (3). ▲, this work; △, (Weidlich et al., 1987); -, (Ferreira et al., 1987); +, (Fisher and Gmehling, 1996); ○, (Letcher and Whitehead, 1997); ◊, (Schult et al., 2001); □, (Krummen and Gmehling, 2004); ——, line of best fit for literature data.

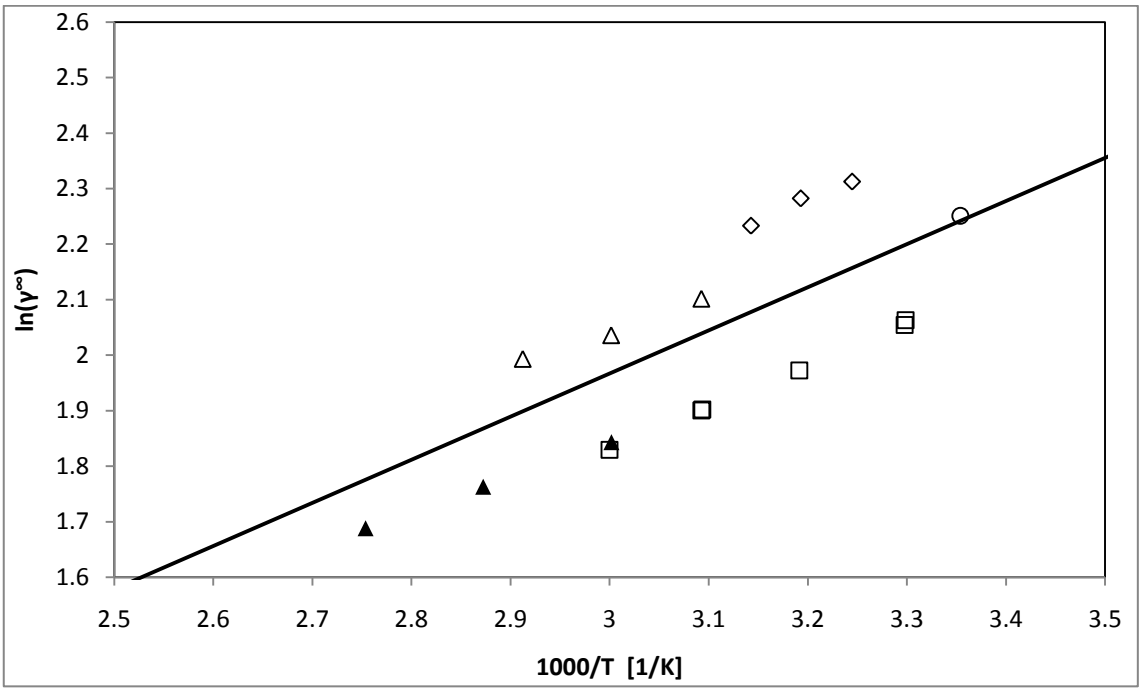

Figure 6-13: Measured ln(γ^{∞}) and literature ln(γ^{∞}) against 1000/T for cyclohexane (1) in N-methylpyrrolidone (3). ▲, this work; △, (Weidlich et al., 1987); ○, (Letcher and Whitehead, 1997); ◊, (Schult et al., 2001); □, (Krummen and Gmehling, 2004); ——, line of best fit for literature data.

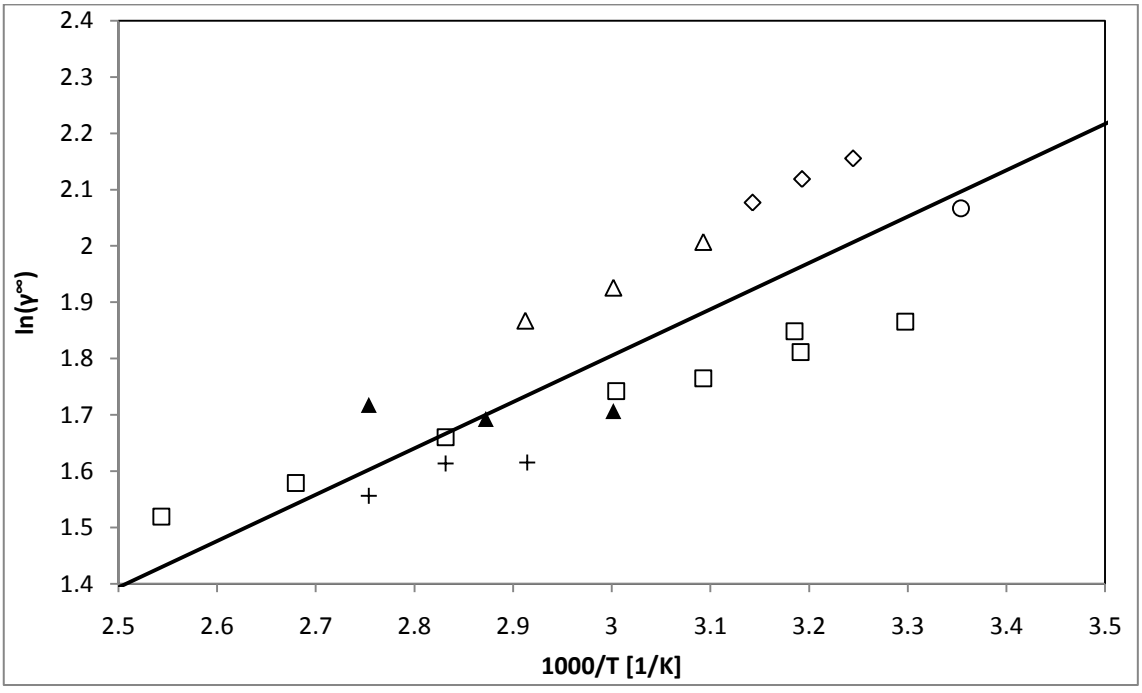

Figure 6-14: Measured ln(γ^{∞}) and literature ln(γ^{∞}) against 1000/T for hex-1-ene (1) in N-methylpyrrolidone (3). ▲, this work; △, (Weidlich et al., 1987); +, (Fisher and Gmehling, 1996); ○, (Letcher and Whitehead, 1997); ◊, (Schult et al., 2001); □, (Krummen and Gmehling, 2004); ——, line of best fit for literature data.

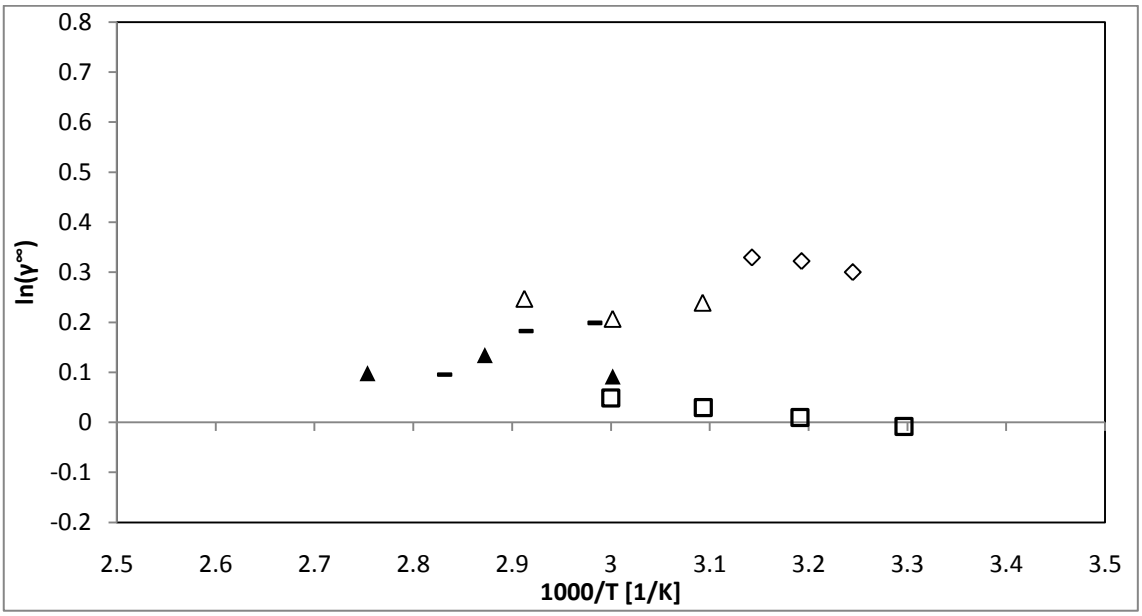

Figure 6-15: Measured ln(γ^{∞}) and literature ln(γ^{∞}) against 1000/T for benzene (1) in N-methylpyrrolidone (3). ▲, this work; △, (Weidlich et al., 1987); -, (Ferreira et al., 1987); ◊, (Schult et al., 2001); □, (Krummen and Gmehling, 2004).

The above figures (Figures 6-12 to 6-15) illustrate that the values measured in this work fitted the data reported by Fischer and Gmehling (1996) and Krummen and Gmehling (2004). The data given by Fischer and Gmehling was determined by extrapolation of vapour-liquid equilibria data and GLC measurement, and the data given by Krummen and Gmehling was measured using the inert gas stripping technique. Since the data obtained from this work, and given in this section, was measured using gas-liquid chromatography, it ruled out the possibility of the method of measurement causing the discrepancy.

The works of Weidlich et al. (1987) and Schult et al. (2001) appear to be inconsistent when compared with the measurements made in this work and those of Fisher and Gmehling, and Krummen and Gmehling. Weidlich and co-workers, however, also measured the infinite dilution activity coefficient in N-formylmorpholine (see Chapter 5.1), and their data for NFM was found to be very similar to other literature sources, including the measurements made by Krummen and Gmehling (2004). It appears peculiar that their measurements in N-methylpyrrolidone differed from what appears to be the correct trend for the n-hexane, cyclohexane and hex-1-ene but not for benzene.

Weidlich and co-workers did not state the purity or source of the solvents used for measurements, and it was therefore not possible to determine the cause of the discrepancy.

All of the measured data for NMP is reported below in Table 6-6. The measured data in this table was compared with the trend-line when no previously measured data was available at the

given temperature. The trend line is discussed in Chapter 5.2. There were large errors for most of the comparisons to the fitted line. When the γ^{∞} from this work was compared with the full range of γ^{∞} values at that specific temperature, the error was, in many cases, smaller than the uncertainty of the measurement.

Table 6-6: Measured γ^{∞} and percentage error from literature data for the hydrocarbon solutes in N-methylpyrrolidone.

		T [K]	γ^{∞}	Meas. error [%] †	Literature	Dif. [%] ‡
Alkanes	n-pentane	333.2	8.32	1.96	8.49-10.2 [a, b]	2.04
		348.2	8.11	1.95	8.86 [*]	9.25
		363.2	7.54	2.10	8.14 [*]	7.96
	n-hexane	333.2	9.51	1.96	9.9-14.4 [a, b, c]	4.10
		348.2	9.19	0.66	10.2 [*]	10.99
		363.2	8.51	1.67	9.1 [*]	6.93
	n-heptane	333.2	11.43	1.11	11.5-17.6 [a, b, c]	0.61
		348.2	10.74	1.03	13.4 [*]	24.77
		363.2	10.00	1.97	12.2 [*]	22.00
	n-octane	333.2	13.76	5.37	16.8 [a]	22.09
		348.2	13.21	1.71	14.2 [*]	7.49
		363.2	10.59	2.85	12.0 [*]	13.31
	n-nonane	333.2	16.67	8.79	-	-
		348.2	14.86	1.79	-	-
		363.2	12.02	2.74	-	-
Alkenes	pent-1-ene	333.2	4.75	1.82	4.7 [b]	1.05
		348.2	4.84	1.34	4.7 [*]	2.89
		363.2	4.99	1.38	4.3 [*]	13.83
	hex-1-ene	333.2	5.51	1.87	5.7-6.9 [a, b]	3.45
		348.2	5.44	1.34	5.5 [*]	1.10
		363.2	5.57	1.69	5.0 [*]	10.23
	hept-1-ene	333.2	6.37	2.05	6.45 [b]	1.26
		348.2	6.24	1.21	6.2 [*]	0.64
		363.2	6.28	1.15	5.5 [*]	12.42
	oct-1-ene	333.2	8.39	1.69	9.87 [a]	17.64
		348.2	7.60	1.54	8.5 [*]	11.84
		363.2	6.70	4.91	7.6 [*]	13.43
Alkynes	pent-1-yne	333.2	1.27	2.01	-	-
		348.2	1.41	2.44	-	-
		363.2	1.63	1.44	-	-
	hex-1-yne	333.2	1.47	1.89	-	-
		348.2	1.57	4.59	-	-
		363.2	1.77	3.09	-	-
	hept-1-yne	333.2	1.72	1.87	-	-
		348.2	1.79	4.94	-	-
		363.2	1.92	8.52	-	-
	oct-1-yne	333.2	2.07	2.09	-	-
		348.2	2.15	5.05	-	-
		363.2	2.16	8.12	-	-

Table 6-5 (cont.): Measured γ^{∞} and percentage error from literature data for the hydrocarbon solutes in N-methylpyrrolidone.

		T [K]	γ^{∞}	Meas. error [%] †	Literature	Dif. [%] ‡
Cyclo-alkanes	cyclopentane	333.2	5.16	1.99	5.08-6.07 [a, b]	0
		348.2	4.68	2.45	5.4 [*]	15.38
		363.2	4.55	3.39	5.1 [*]	12.09
	cyclohexane	333.2	6.32	2.03	6.69-7.66 [a, b]	5.85
		348.2	5.83	2.50	6.5 [*]	11.49
		363.2	5.41	1.54	5.9 [*]	9.06
	cycloheptane	333.2	7.51	1.21	-	-
		348.2	6.71	2.66	-	-
		363.2	6.80	6.57	-	-
	cyclooctane	333.2	8.23	3.69	-	-
		348.2	7.62	3.87	-	-
		363.2	6.06	8.12	-	-
Alcohols	methanol	333.2	0.482	1.24	0.521 [a]	8.09
		348.2	0.556	5.01	0.514 [*]	7.55
		363.2	0.511	7.12	0.508 [*]	0.58
	ethanol	333.2	0.606	1.35	0.639 [a]	5.45
		348.2	0.605	2.10	0.635 [*]	4.96
		363.2	0.618	9.33	0.623 [*]	0.81
	propan-1-ol	333.2	0.537	2.28	0.563 [*]	4.84
		348.2	0.552	4.46	0.54 [a]	2.17
		363.2	0.548	4.63	0.528 [*]	3.65
	propan-2-ol	333.2	0.627	1.97	-	-
		348.2	0.639	2.74	-	-
		363.2	0.632	10.49	-	-
Aromatics	benzene	333.2	1.10	0.67	1.05-1.23 [a, b, c]	0
		348.2	1.14	2.39	1.15 [*]	0.87
		363.2	1.10	6.63	1.20 [*]	9.09
	toluene	333.2	1.39	1.26	1.37-1.67 [a, b, c]	0
		348.2	1.35	3.64	1.53 [*]	13.33
		363.2	1.42	8.97	1.58 [*]	11.27
	ethylbenzene	333.2	1.73	6.28	-	-
		348.2	1.83	4.89	-	-
		363.2	1.61	10.70	-	-

[a] (Weidlich et al., 1987); [b] (Krummen and Gmehling, 2004); [c] (Ferreira et al., 1987); [*] calculated from line of best fit to all collected literature data (see Table 5-6); † calculated by Equation 6-1; ‡ calculated by Equation 6-2.

Most of the measured data agreed well with the literature data with a fair degree of accuracy, although the fit was not quite as good as the fit achieved for NFM. The largest discrepancies occurred when comparing the measured data to the line of best fit obtained from all the available literature values. This was done when there were no direct literature values with which to compare the experimental data.

6.2.6 Triethylene glycol

The γ^{∞} values of the various solutes in triethylene glycol, at temperatures of 333.2, 348.2 and 363.2 K, were measured using the gas-liquid chromatography experimental set up. The semi-logarithmic plots of the experimental values from this work as well as the literature data, given by Arancibia and Catoggio (1980) and by Sun et al. (2003), against 1000/T for n-heptane and benzene in TEG are given in Figures 6-16 and 6-17.

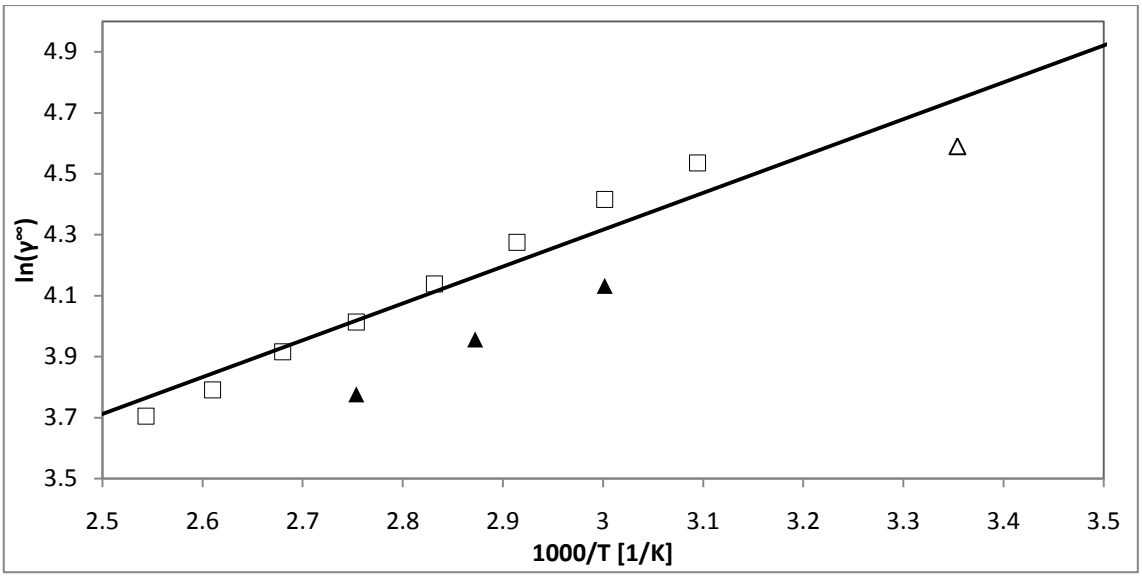

Figure 6-16: Measured ln(γ^{∞}) and literature ln(γ^{∞}) against 1000/T for n-heptane (1) in triethylene glycol (3). ▲, this work; △, (Arancibia & Catoggio, 1980); □, (Sun et al., 2003); ——, line of best fit to literature data.

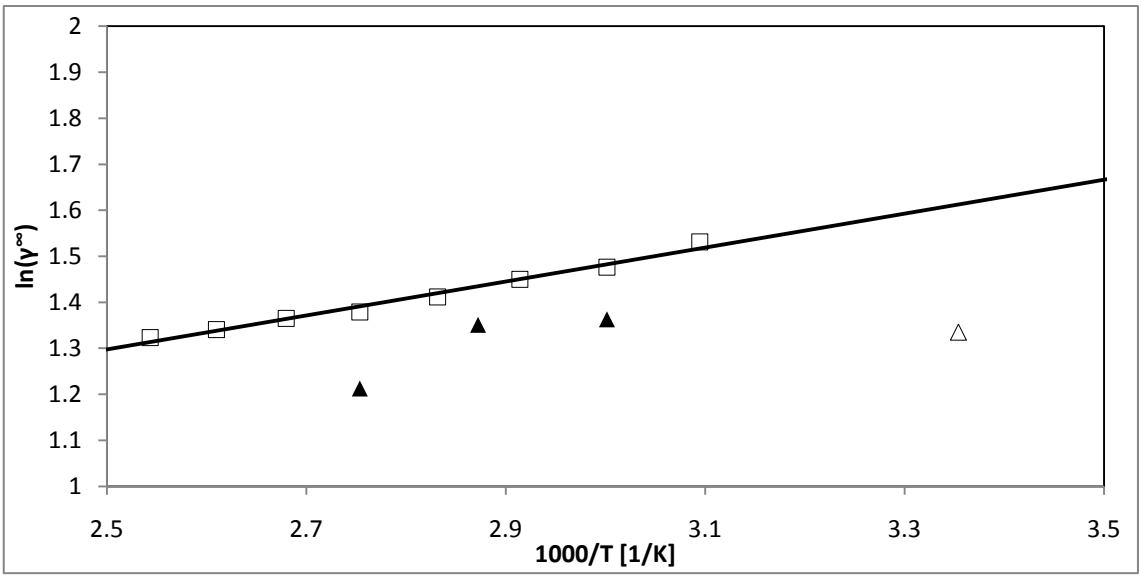

Figure 6-17: Measured ln(γ^{∞}) and literature ln(γ^{∞}) against 1000/T for benzene (1) in triethylene glycol (3). ▲, this work; △, (Arancibia & Catoggio, 1980); □, (Sun et al., 2003); ——, line of best fit to literature data.

All of the measured data points for the solutes in TEG at the three temperatures at which measurements were made are given in Table 6-7. Also included in this table were the errors of measurement, the literature values where these were available and the difference from the literature values.

Table 6-7: Measured γ^{∞} and percentage error from literature data for the hydrocarbon solutes in triethylene glycol.

		T [K]	γ^{∞}	Meas. error [%] †	Literature	Dif. [%] ‡
Alkanes	n-pentane	333.2	33.71	9.15	-	-
		348.2	30.84	10.22	-	-
		363.2	23.18	6.41	-	-
	n-hexane	333.2	45.84	0.79	-	-
		348.2	40.27	1.78	-	-
		363.2	35.15	0.97	-	-
	n-heptane	333.2	62.31	1.83	82.7 [a]	32.72
		348.2	52.28	1.37	64.2 [*]	22.80
		363.2	43.67	1.21	55.3 [a]	26.63
	n-octane	333.2	103.2	0.67	113.1 [a]	9.61
		348.2	73.96	0.77	89.0 [*]	20.34
		363.2	62.86	2.23	75.8 [a]	20.59
	n-nonane	333.2	137.0	0.85	156.0 [a]	13.84
		348.2	98.90	0.82	127.1 [*]	28.51
		363.2	83.12	1.03	103.0 [a]	23.92
Alkenes	pent-1-ene	333.2	17.52	0.96	-	-
		348.2	16.09	0.92	-	-
		363.2	14.83	4.70	-	-
	hex-1-ene	333.2	24.55	0.81	-	-
		348.2	22.73	2.31	-	-
		363.2	20.35	1.49	-	-
	hept-1-ene	333.2	34.38	1.68	-	-
		348.2	30.57	2.25	-	-
		363.2	27.48	1.65	-	-
	oct-1-ene	333.2	55.90	0.57	-	-
		348.2	41.77	1.08	-	-
		363.2	36.81	1.57	-	-
	non-1-ene	333.2	75.39	0.67	-	-
		348.2	57.16	0.85	-	-
		363.2	49.19	1.07	-	-

a, (Sun et al., 2003); [*] calculated from line of best fit to all collected literature data (see Table 5-8) ; † calculated by Equation 6-1; ‡ calculated by Equation 6-2.

Table 6-6 (cont.): Measured γ^{∞} and percentage error from literature data for the hydrocarbon solutes in triethylene glycol.

		T [K]	γ^{∞}	Meas. error [%] †	Literature	Dif. [%] ‡
Alkynes	pent-1-yne	333.2	5.07	0.95	-	-
		348.2	5.11	1.84	-	-
		363.2	5.01	1.68	-	-
	hex-1-yne	333.2	7.01	0.54	-	-
		348.2	7.03	1.85	-	-
		363.2	6.69	1.68	-	-
	hept-1-yne	333.2	10.25	0.38	-	-
		348.2	9.04	0.66	-	-
		363.2	8.99	0.94	-	-
	oct-1-yne	333.2	14.37	0.45	-	-
		348.2	12.75	0.67	-	-
		363.2	12.19	1.60	-	-
Cyclo-alkanes	cyclopentane	333.2	15.19	0.58	-	-
		348.2	13.98	1.94	-	-
		363.2	12.69	1.62	-	-
	cyclohexane	333.2	21.12	0.70	-	-
		348.2	18.64	0.78	-	-
		363.2	16.80	1.43	-	-
	cycloheptane	333.2	29.55	0.68	-	-
		348.2	22.34	0.55	-	-
		363.2	19.83	1.22	-	-
	cyclooctane	333.2	35.31	0.63	-	-
		348.2	27.17	0.36	-	-
		363.2	23.89	1.38	-	-
Alcohols	methanol	333.2	0.788	0.32	-	-
		348.2	0.787	1.10	-	-
		363.2	0.705	1.27	-	-
	ethanol	333.2	1.18	0.41	-	-
		348.2	1.15	0.55	-	-
		363.2	1.12	1.67	-	-
	propan-1-ol	333.2	1.38	0.60	-	-
		348.2	1.34	0.55	-	-
		363.2	1.31	1.62	-	-
	propan-2-ol	333.2	1.45	0.49	-	-
		348.2	1.40	0.55	-	-
		363.2	1.38	1.62	-	-
Aromatics	benzene	333.2	3.91	0.46	4.38 [a]	12.02
		348.2	3.86	0.55	4.20 [*]	8.81
		363.2	3.36	1.26	3.97 [a]	18.15
	toluene	333.2	5.88	0.52	-	-
		348.2	5.73	0.55	-	-
		363.2	5.55	1.72	-	-
	ethylbenzene	333.2	8.63	0.59	-	-
		348.2	8.21	0.55	-	-
		363.2	7.86	1.67	-	-

a, (Sun et al., 2003); [*] calculated from line of best fit to all collected literature data (see Table 5-8) ; † calculated by Equation 6-1; ‡ calculated by Equation 6-2.

The measurement error for most of the solutes was within the accepted range for GLC. The only exceptions were the measurements of n-pentane and pent-1-ene. The errors for n-pentane and pent-1-ene were large because of their short retention times in TEG. The small difference between the retention time of these volatile solutes and the retention time of the inert component caused an exaggeration of any errors.

Only a few literature values were available, and the γ^{∞} values measured here did not agree with this literature data.

6.2.7 Diethylene glycol

The γ^{∞} values of the various solutes in diethylene glycol, at temperatures of 333.2, 348.2 and 363.2 K, were measured using the gas-liquid chromatography experimental set up. Since there were no measurements of this system at temperatures above ambient temperature, there were no values with which to compare the values measured in this work. The measured data is collated in Table 6-8.

Table 6-8: Measured γ^{∞} and calculated error of measurement of hydrocarbon solutes in diethylene glycol.

		T [K]	γ^{∞}	Meas. error [%] †
Alkanes	n-pentane	333.2	70.18	7.68
		348.2	53.76	3.54
		363.2	54.19	2.17
	n-hexane	333.2	95.73	1.79
		348.2	84.01	3.03
		363.2	82.36	4.63
	n-heptane	333.2	131.3	1.88
		348.2	122.2	0.53
		363.2	95.37	1.00
	n-octane	333.2	187.6	0.83
		348.2	168.0	0.93
		363.2	145.6	0.39
	n-nonane	333.2	263.9	1.35
		348.2	230.4	0.76
		363.2	193.4	1.77
Alkenes	pent-1-ene	333.2	35.33	2.25
		348.2	32.92	1.69
		363.2	27.58	5.28
	hex-1-ene	333.2	50.67	0.69
		348.2	47.33	1.99
		363.2	38.87	1.26
	hept-1-ene	333.2	72.28	0.55
		348.2	66.59	1.13
		363.2	60.45	0.39
	oct-1-ene	333.2	100.9	1.62
		348.2	93.51	0.47
		363.2	82.61	2.27
	non-1-ene	333.2	145.1	0.50
		348.2	130.0	1.24
		363.2	114.8	2.24
Alkynes	pent-1-yne	333.2	9.93	3.48
		348.2	10.48	2.50
		363.2	10.15	1.03
	hex-1-yne	333.2	14.07	1.87
		348.2	14.59	1.27
		363.2	13.79	1.23
	hept-1-yne	333.2	20.27	1.18
		348.2	20.83	1.54
		363.2	19.34	1.98
	oct-1-yne	333.2	29.89	1.18
		348.2	29.72	1.32
		363.2	27.04	1.69

Table 6-7 (cont.): Measured γ^{∞} and calculated error of measurement of hydrocarbon solutes in diethylene glycol.

		T [K]	γ^{∞}	Meas. error [%] †
Cyclo-alkanes	cyclopentane	333.2	30.92	1.68
		348.2	27.60	0.15
		363.2	25.92	0.67
	cyclohexane	333.2	42.74	0.70
		348.2	39.19	0.50
		363.2	34.88	1.77
	cycloheptane	333.2	52.38	0.72
		348.2	47.41	0.80
		363.2	42.11	1.66
	cyclooctane	333.2	70.67	1.15
		348.2	61.34	1.47
		363.2	52.21	1.58
Alcohols	methanol	333.2	0.988	1.09
		348.2	1.01	1.74
		363.2	1.024	1.93
	ethanol	333.2	1.47	1.15
		348.2	1.46	1.89
		363.2	1.46	0.47
	propan-1-ol	333.2	1.80	0.68
		348.2	1.77	1.19
		363.2	1.74	3.75
	propan-2-ol	333.2	1.79	1.06
		348.2	1.77	1.05
		363.2	1.74	1.36
Aromatics	benzene	333.2	7.33	1.29
		348.2	7.21	1.88
		363.2	7.05	1.46
	toluene	333.2	11.22	0.58
		348.2	10.94	1.05
		363.2	10.53	2.55
	ethylbenzene	333.2	16.80	1.29
		348.2	16.12	1.10
		363.2	15.21	3.20

† calculated by Equation 6-1.

For measurements with DEG, a problem similar to the problem experienced with the volatile solutes in TEG, occurred. The measured γ^{∞} values for the C_5 components exhibited far larger errors of measurement than the other solutes. This was most likely due to the exaggeration of the error, caused by the small difference between the retention time of the solute and the retention time of the inert component.

6.3 Dilutor cell technique

The new experimental technique proposed by Richon (2011a) was tested with three solutes; n-hexane, n-heptane and cyclohexane; in N-formylmorpholine and N-methylpyrrolidone at 333 K. Very little work has been performed using this novel method. The work conducted on the dilutor cell in this study was therefore an endeavour to increase the scope for which this novel technique was shown to be applicable.

The three solutes that were selected for the test systems were used by Krummen and Gmehling (2004) as well as more recently by George (2008) for their test systems for the dilutor cell technique.

In this section, the experimental data from this novel dilutor cell technique is firstly presented. Thereafter, the applicability of this method to cases of C_6 and C_7 hydrocarbon solutes in volatile solvents at elevated temperatures is discussed.

6.3.1 Uncertainty analysis

Three experimental γ^{∞} values were measured for each of the three six combinations (solutes: n-hexane, n-heptane and cyclohexane with either NFM or NMP as the solvent). From the three raw data sets, the minimum, maximum and average infinite dilution activity coefficients were calculated. The average of the three values was used as the γ^{∞} value for that solute. The error was calculated in the same manner as in Chapter 6.2.1.

6.3.2 N-formylmorpholine

Measurements of the infinite dilution activity coefficients of the three solutes; n-hexane, n-heptane and cyclohexane; in N-formylmorpholine were performed at 333 K, using the dilutor cell technique described in Chapter 3.2.

The semi-logarithmic plot given by Figure 6-18 was used to calculate the infinite dilution activity coefficient using Equation 4-27.

The logarithm of the initial signal over the signal at time, t, was plotted against time, in order to obtain the slope for use in the calculation. This is shown in Figure 6-18.

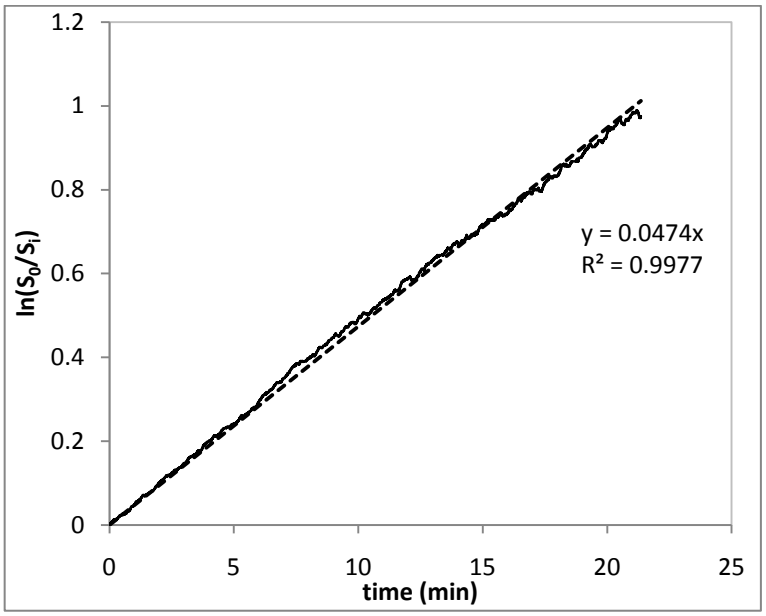

Figure 6-18: Elution of n-hexane from N-formylmorpholine at 333 K; natural logarithm of initial signal over signal as a function of time. Solid black line: experimental values. Dashed black line: trend line for experimental values.

The results obtained from these measurements are shown in Figures 6-19 to 6-21.

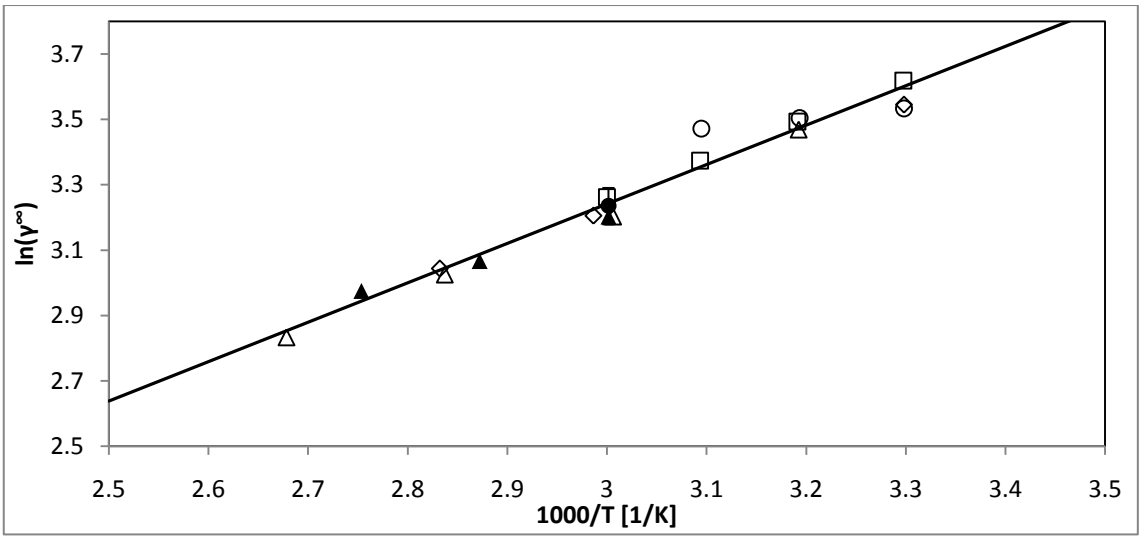

Figure 6-19: $\ln(\gamma^{\infty})$ against 1000/T for n-hexane (1) in N-formylmorpholine (2). ●, this work (dilutor cell technique); ▲, this work (gas-liquid chromatography); Δ, (Weidlich et al., 1987); ◊, (Knoop et al., 1989); ○, (Park et al., 2001); □, (Krummen & Gmehling, 2004); ——, line of best fit for literature data.

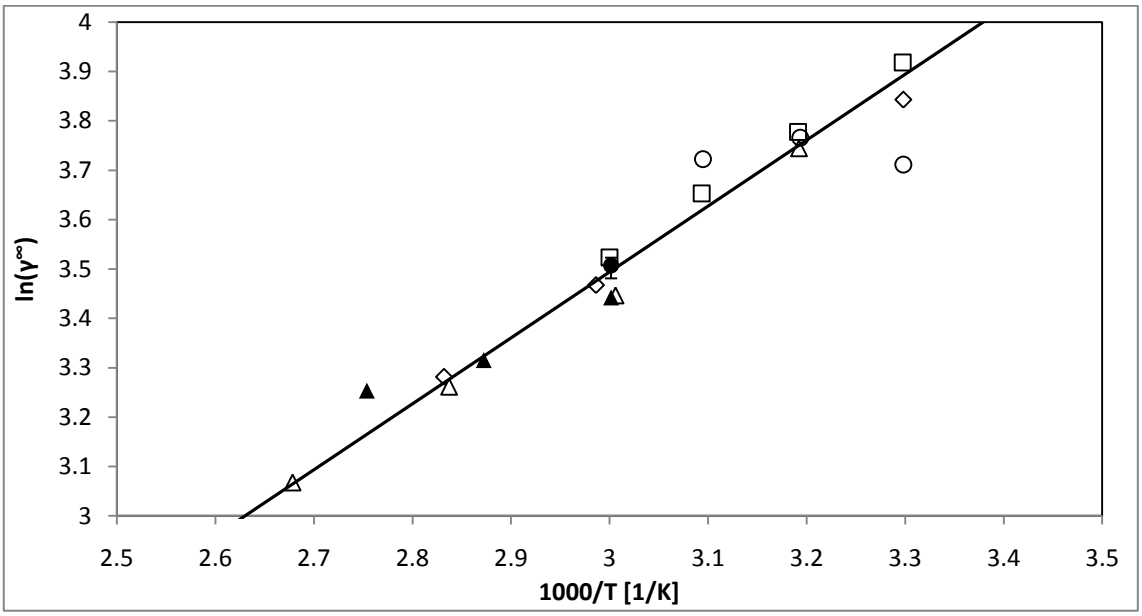

Figure 6-20: ln(γ^{∞}) against 1000/T for n-heptane (1) in N-formylmorpholine (2). ●, this work (dilutor cell technique); ▲, this work (gas-liquid chromatography); Δ, (Weidlich et al., 1987); ◊, (Knoop et al., 1989); ○, (Park et al., 2001); □, (Krummen & Gmehling, 2004); ——, line of best fit for literature data.

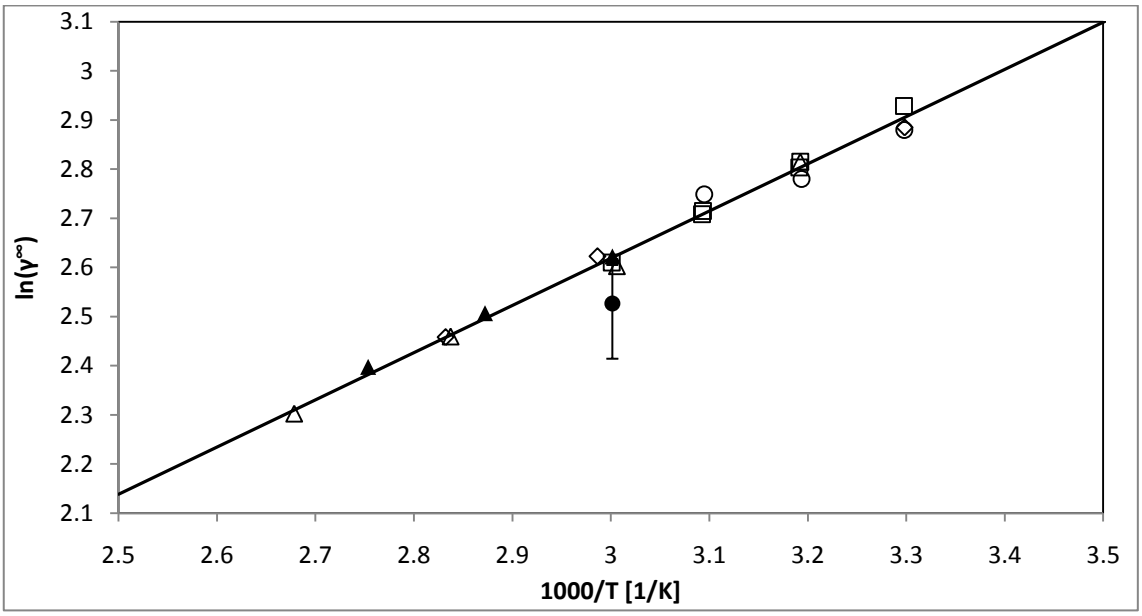

Figure 6-21: ln(γ^{∞}) against 1000/T for cyclohexane (1) in N-formylmorpholine (2). ●, this work (dilutor cell technique); ▲, this work (gas-liquid chromatography); Δ, (Weidlich et al., 1987); ◊, (Knoop et al., 1989); ○, (Park et al., 2001); □, (Krummen & Gmehling, 2004); ——, line of best fit for literature data.

The values obtained by this method are listed in Table 6-9.

Table 6-9: Values of the infinite dilution activity coefficient of three solutes in N-formylmorpholine at 333 K measured utilising the dilutor cell technique.

	T [K]	γ^{∞}	Meas. error [%] †	Literature	Dif. [%] ‡
n-hexane	333	25.42	5.64	24.6-26.1 [a, b]	0
n-heptane	333	33.35	4.17	31.4-33.9 [a, b]	0
cyclohexane	333	13.05	7.57	13.5-13.77 [a, b, c]	3.42

[a] (Weidlich et al., 1987); [b] (Krummen & Gmehling, 2004); [c] (Knoop et al., 1989); † calculated by Equation 6-1; ‡ calculated by Equation 6-2.

From Figures 6-19 to 6-21, it was observed that the results for the three solutes in NFM measured using this new dilutor cell technique were very similar to the results obtained when using the gas-liquid chromatography technique, as well as the results from published literature data. There was a slight discrepancy for the γ^{∞} value of cyclohexane in NFM.

The uncertainties of the measurements were much larger than the uncertainty of measurement for the gas-liquid chromatography method. These large uncertainties were caused by solvent which was present in the vapour phase passing through the detector. The solvent caused 'noise' on the baseline, making it difficult to determine the signal height caused by the solute.

6.3.3 N-methylpyrrolidone

Measurements of the infinite dilution activity coefficients of three solutes; n-hexane, n-heptane and cyclohexane; in N-methylpyrrolidone were also performed at 333 K using the dilutor cell technique described in Chapter 3.2. The values obtained by this method are listed in Table 6-10.

Table 6-10: Values of the infinite dilution activity coefficient of three solutes in N-methylpyrrolidone at 333 K measured utilising the dilutor cell technique.

	T [K]	γ^{∞}	Meas. error [%] †	Literature	Dif. [%] ‡
n-hexane	333	15.69	4.85	9.9-14.4 [a, b, c]	8.22
n-heptane	333	29.27	9.65	11.5-17.6 [a, b, c]	39.87
cyclohexane	333	4.61	29.01	6.69-7.66 [a, b]	45.12

[a] (Weidlich et al., 1987); [b] (Krummen & Gmehling, 2004); [c] (Knoop et al., 1989); † calculated by Equation 6-1; ‡ calculated by Equation 6-2.

The results obtained from these measurements are shown in Figures 6-22 to 6-24.

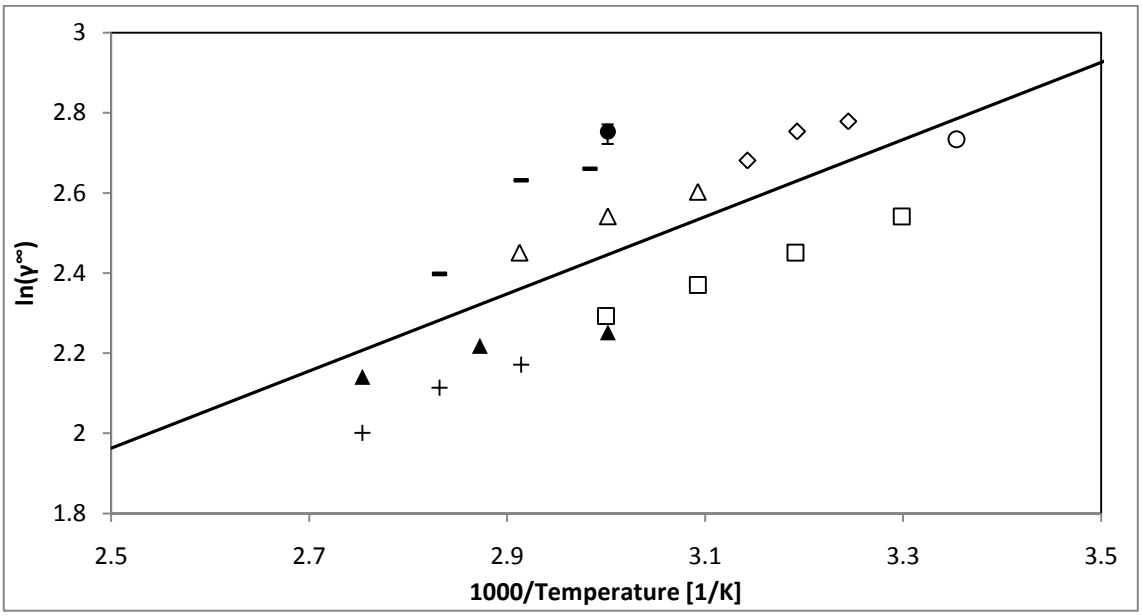

Figure 6-22: ln(γ^{∞}) against 1000/T for n-hexane (1) in N-methylpyrrolidone (2). ●, this work (dilutor cell technique); ▲, this work (gas-liquid chromatography); Δ, (Weidlich et al., 1987); -, (Ferreira et al., 1987); +, (Fischer & Gmehling, 1996); ◊, (Schult et al., 2001); ○, (Letcher & Whitehead, 1997); □, (Krummen & Gmehling, 2004); ——, line of best fit for literature data.

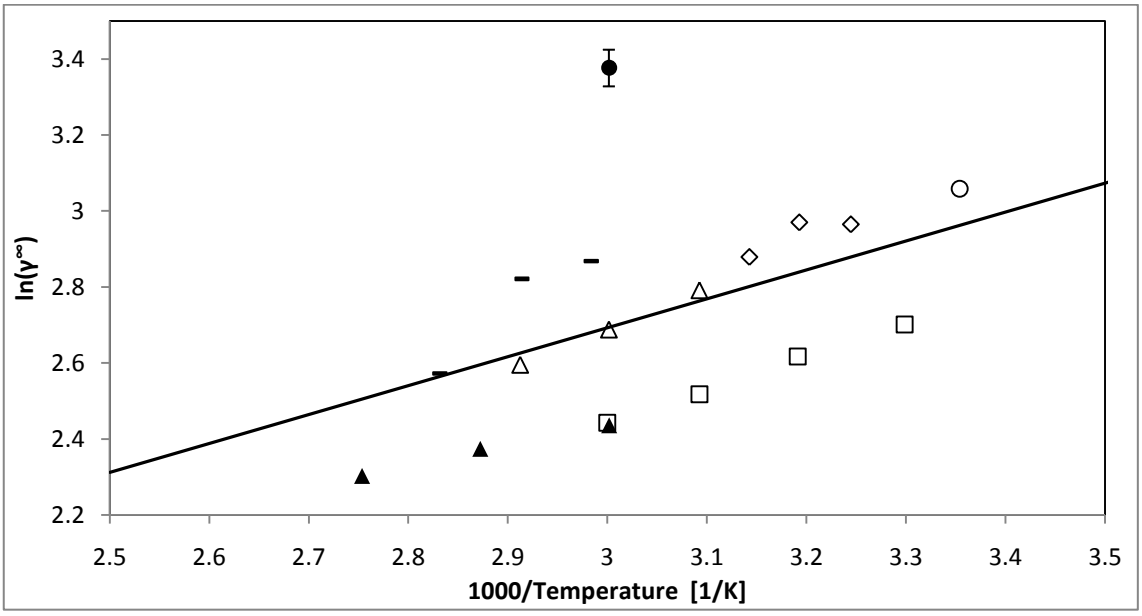

Figure 6-23: ln(γ^{∞}) against 1000/T for n-heptane (1) in N-methylpyrrolidone (2). ●, this work (dilutor cell technique); ▲, this work (gas-liquid chromatography); Δ, (Weidlich et al., 1987); -, (Ferreira et al., 1987); ◊, (Schult et al., 2001); ○, (Letcher & Whitehead, 1997); □, (Krummen & Gmehling, 2004); ——, line of best fit for literature data.

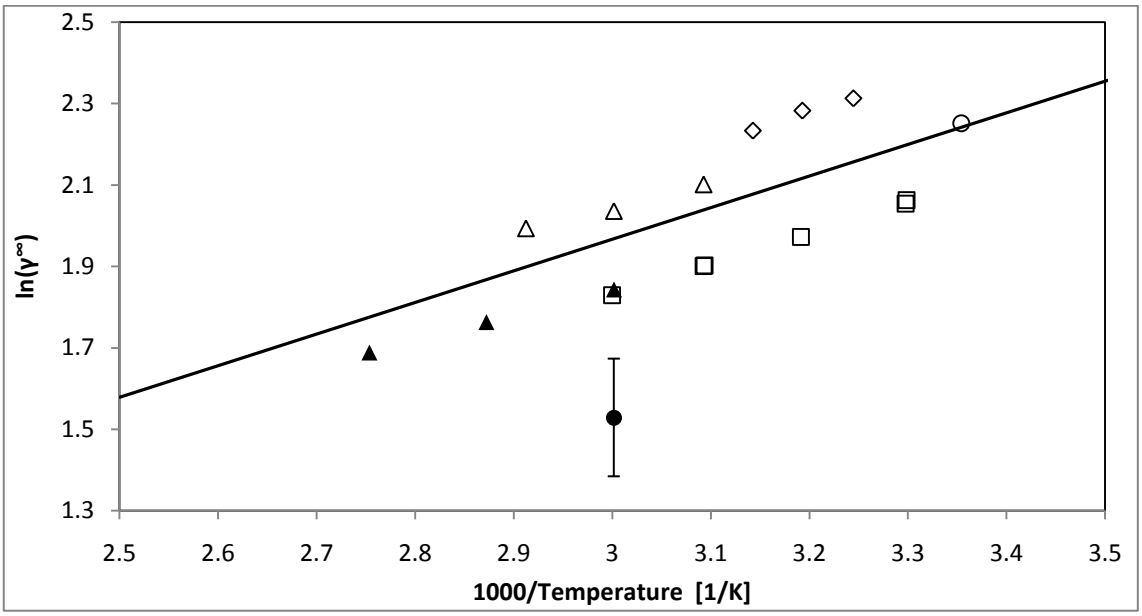

Figure 6-24: ln(γ^{∞}) against 1000/temperature for cyclohexane (1) in N-methylpyrrolidone (2). ●, this work (dilutor cell technique); ▲, this work (gas-liquid chromatography); Δ, (Weidlich et al., 1987); ◊, (Schult et al., 2001); ○, (Letcher & Whitehead, 1997); □, (Krummen & Gmehling, 2004); ——, line of best fit for literature data.

The results for the three solutes in N-methylpyrrolidone were very poor, with very large errors from the literature data. The γ^{∞} values of n-hexane and the n-heptane had positive offsets from the literature data, whereas the γ^{∞} value for cyclohexane in both NFM and NMP had a negative offset. The γ^{∞} value measured for n-hexane had a smaller measurement uncertainty than the γ^{∞} values for n-heptane and cyclohexane. The difference from the literature data was substantially smaller for n-hexane than for the other two solutes.

The uncertainties of the measurements were far too large for the results for this method to be acceptable, as the corresponding uncertainties from the gas-liquid chromatography method were less than 2 % (see Table 6-5).

6.3.4 Experimental method

Richon (2011b) stated that this dilutor cell technique was at present only suitable for the measurement of the infinite dilution activity coefficients of solutes in non-volatile solvents. The reason for this limit on the method was probably due to the interference of the solvent concentration on the detector signal height. The solvent would cause the height of the signal to appear to be greater than was actually the case, which would be translated into erroneous values. The solvent passing through the detector also caused fluctuations in the baseline, and this would also have occurred during the measurements.

Two observations of the experimental work performed here substantiated the belief that the measured infinite dilution activity coefficients were affected by the volatile solvent.

Firstly, the γ^{∞} values in NFM were far closer to previously measured data than was the case in the NMP. The NMP was more volatile than the NFM, and therefore, the fraction of NMP in the vapour phase would have been larger than the fraction of NFM in the vapour phase. The detector signal would therefore have been affected to a greater extent by the NMP than by the NFM. This in turn would have affected the infinite dilution activity coefficients in NMP to a greater extent than in NFM.

The second observation was the fact that n-hexane, which had a greater vapour pressure, and therefore a faster elution from the cell, had the smallest error from literature data. The faster that the solute eluted from the cell, the greater would be the slope of the decaying portion of the peak. Peaks with a greater slope would in turn be less vulnerable to small deviations of the baseline. Because of this, n-hexane was therefore assumed to be less affected by the fraction of solvent in the vapour phase.

6.3.4.1 Effect of vapour volume

The volume of the vapour phase, which was taken into account by Equation 4-27, was sighted as a possible cause of the deviations of the measured data from literature data. This was because the vapour volume of helium and the solute would decrease by the addition of solvent to the vapour phase.

It was found, however, that, for solutes with relatively low vapour pressures, the vapour volume had only a small effect on the infinite dilution activity coefficient. This can be seen in Table 6-11.

Table 6-11: Effect of vapour volume on the infinite dilution activity coefficient for n-hexane and n-heptane in NMP.

	V_G [cm^3]	γ^{∞}_{min}	γ^{∞}_{ave}	γ^{∞}_{max}	Meas. Error [%] †
n-hexane	0	15.21	15.68	15.95	4.72
	1	15.25	15.71	16.00	4.77
	2	15.31	15.75	16.05	4.70
n-heptane	0	27.85	29.24	30.67	9.64
	1	27.91	29.3	30.74	9.66
	2	27.97	29.36	30.81	9.67

† calculated by Meas. Error = $100\% \times (\gamma^{\infty}_{max} - \gamma^{\infty}_{min}) / \gamma^{\infty}_{ave}$

6.3.5 Viability of technique

This technique, in its present unrefined state, did not provide satisfactory results for hydrocarbon solutes in volatile solvents, as the measured γ^{∞} values differed vastly from the published literature data. The uncertainty of the experimental data was also a concern, as three subsequent measurements differed by as much as 29 % from each other. In contrast to this, the GLC method produced uncertainties in measurement of as little as 2%.

It appears that this technique could become feasible for measurement of infinite dilution activity coefficients of hydrocarbon solutes in volatile solvents, but a number of refinements would need to be made prior to this being the case. The major refinement would be a means of accounting for the effect of the solvent in the vapour phase on the signal output from the detector.

Even if this new technique were to become feasible for measurement in volatile solvents, a major setback to its use would be the time required for each measurement. This method required as much as 2 hours from the time of injection of the solvent to the time at which the baseline returned to steady state. The GLC method, in contrast required less than 5 minutes per measurement for the same solvent-solute-temperature combination.

6.4 Selectivities and capacities

The selectivities and capacities of the combinations that are listed in Table 1-2 were compared at temperatures of 333.2, 348.2 and 363.2 K. The selectivities of the solvents for these combinations are given in Tables 6-11 to 6-13 and are further discussed in the sections following. The capacities of the solvents for some solutes are given in Tables 6-14 to 6-19.

The selectivities given below were calculated directly from experimental data, and experimental errors in the measured values meant that at times, the trends were difficult to discern.

Table 6-12: Selectivities of NFM, NMP, TEG and DEG for several hydrocarbon combinations at 333.2K.

Solute (1)	Solute (2)	S_{12} [NFM]	S_{12} [NMP]	S_{12} [TEG]	S_{12} [DEG]
cyclohexane	benzene	7.21	5.76	5.40	5.83
n-heptane	cyclohexane	2.27	1.81	2.95	3.07
n-heptane	toluene	12.24	8.22	10.61	11.70
n-hexane	hex-1-ene	1.96	1.72	1.87	1.89
hex-1-ene	cyclohexane	0.91	0.87	1.16	1.19
hex-1-ene	hex-1-yne	3.87	3.76	3.50	3.60
n-hexane	benzene	12.88	8.67	11.73	13.06
benzene	methanol	2.24	2.27	4.96	7.41

Table 6-13: Selectivities of NFM, NMP, TEG and DEG for several hydrocarbon combinations at 348.2K.

Solute (1)	Solute (2)	S_{12} [NFM]	S_{12} [NMP]	S_{12} [TEG]	S_{12} [DEG]
cyclohexane	benzene	6.27	5.10	4.83	5.44
n-heptane	cyclohexane	2.41	1.84	2.80	3.12
n-heptane	toluene	-	7.98	9.13	11.17
n-hexane	hex-1-ene	1.85	1.69	1.77	1.78
hex-1-ene	cyclohexane	1.01	0.93	1.22	1.21
hex-1-ene	hex-1-yne	3.63	3.45	3.23	3.24
n-hexane	benzene	11.77	8.04	10.43	11.65
benzene	methanol	2.15	2.06	4.91	7.17

Table 6-14: Selectivities of NFM, NMP, TEG and DEG for several hydrocarbon combinations at 363.2K.

Solute (1)	Solute (2)	S_{12} [NFM]	S_{12} [NMP]	S_{12} [TEG]	S_{12} [DEG]
cyclohexane	benzene	6.64	4.90	5.00	4.95
n-heptane	cyclohexane	2.70	1.85	2.60	2.73
n-heptane	toluene	12.73	7.06	7.86	9.06
n-hexane	hex-1-ene	1.86	1.53	1.73	2.12
hex-1-ene	cyclohexane	1.10	1.03	1.21	1.11
hex-1-ene	hex-1-yne	3.79	3.14	3.04	2.82
n-hexane	benzene	13.58	7.71	10.45	11.68
benzene	methanol	2.04	2.16	4.77	6.88

The capacity of the solvent for solute (2) was of importance, as this would be the component that would be entrained by the solvent, and removed from the bottom of the extractive distillation column, with the solvent.

6.4.1 Cyclohexane/benzene

Figure 6-25 is a plot of the selectivities of the different solvents for cyclohexane (1) over benzene (2) against temperature.

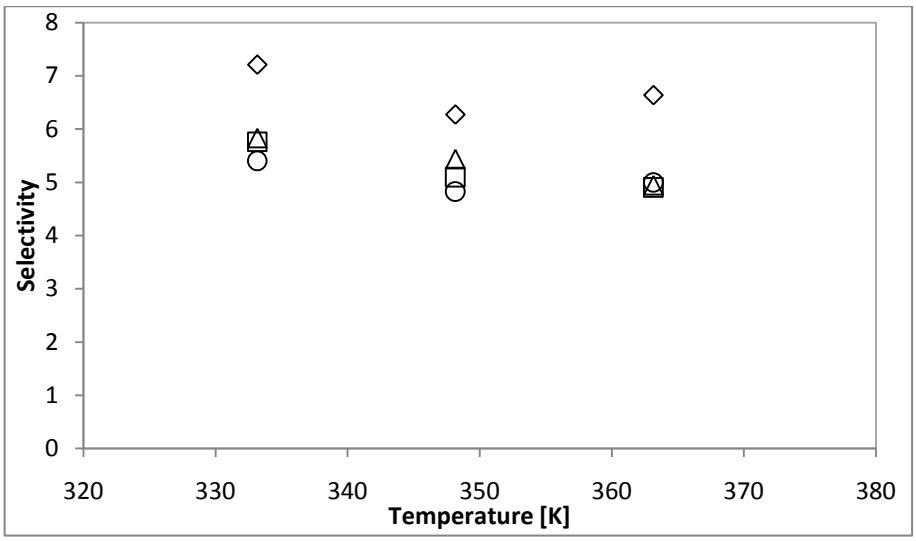

Figure 6-25: Selectivities of various solvents against temperature for the combination of cyclohexane (1) and benzene (2). □, NMP; ◊, NFM; ○, TEG; Δ, DEG.

For the combination of cyclohexane and benzene, N-formylmorpholine had a considerably better performance, in terms of selectivity than the other three solvents. Up to the present, N-methylpyrrolidone has been one of the solvents used for this system industrially, even though N-formylmorpholine has a better selectivity.

Table 6-15: Capacities, k_i, of the various solvents for benzene (2) at 333.2, 348.2 and 363.2 K.

Temperature [K]	**k_2 [NFM]**	**k_2 [NMP]**	**k_2 [TEG]**	**k_2 [DEG]**
333.2	0.524	0.912	0.256	0.136
348.2	0.548	0.874	0.256	0.136
363.2	0.693	0.906	0.297	0.142

From Table 6-15, it can be seen that NMP had the highest capacity for benzene, followed by NFM. The best solvent for this separation would either be NMP or NFM. To choose between the two solvents, further investigation (in the form of more detailed VLE measurements) would be required.

One of the reasons that NMP has been used in industry rather than NFM may have been due to less NMP being required for the separation. The decision would therefore most likely have been based upon the economics of the process.

6.4.2 n-Heptane/cyclohexane

Figure 6-26 is a plot of the selectivities of the different solvents for n-heptane (1) over cyclohexane (2) against temperature.

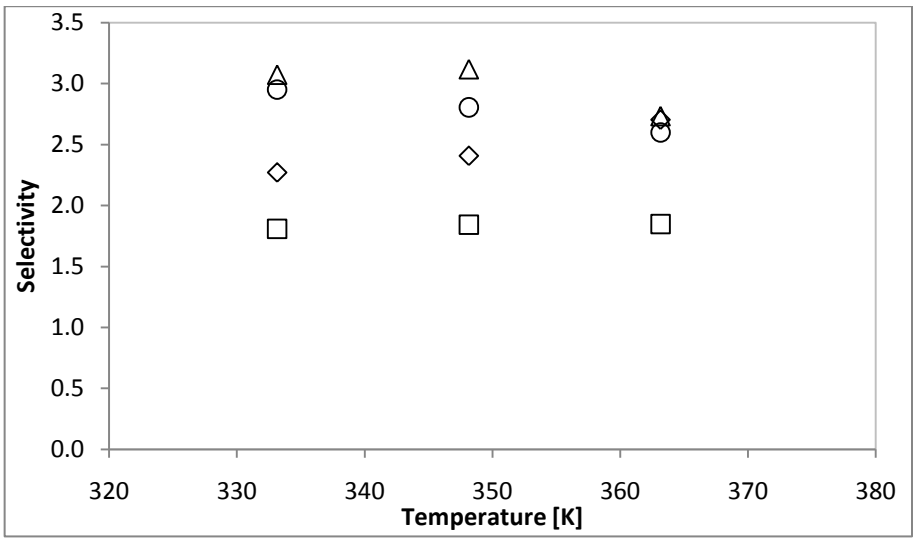

Figure 6-26: Selectivities of various solvents against temperature for the combination of n-heptane (1) and cyclohexane (2). □, NMP; ◊, NFM; ○, TEG; Δ, DEG.

For the combination of n-heptane and cyclohexane, it appeared that, at temperatures of under 350K, the ethylene glycols would exhibit better performance for this separation problem. At higher temperatures, however, NFM would provide a similar selectivity, and by observation of the trend, it appears that, if the temperature were to be increased further, NFM would have the best selectivity.

Table 6-16: Capacities of the various solvents for cyclohexane (2) at 333.2, 348.2 and 363.2 K.

Temperature [K]	**k_2 [NFM]**	**k_2 [NMP]**	**k_2 [TEG]**	**k_2 [DEG]**
333.2	0.073	0.158	0.047	0.023
348.2	0.104	0.185	0.060	0.029
363.2	0.104	0.185	0.060	0.029

Table 6-16 presents the capacities of all the solvents for cyclohexane. These capacities are all low, but with NMP once again having the best capacity. Even though the ethylene glycols had a far greater selectivity for n-heptane over cyclohexane, their low capacities for cyclohexane meant that their use would require much more solvent than if NMP or NFM were used. The use of either of the ethylene glycols would therefore only be justified if they could be obtained at significantly lower prices than the other two solvents.

6.4.3 n-Heptane/toluene

Figure 6-27 displays the selectivities of the different solvents for the combination of n-heptane (1) and toluene (2).

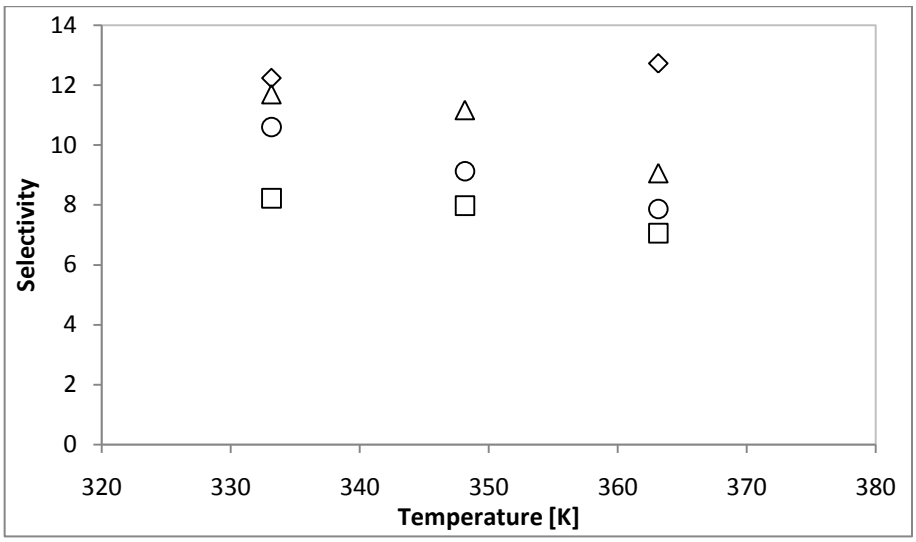

Figure 6-27: Selectivities of various solvents against temperature for the combination of n-heptane (1) and toluene (2). □, NMP; ◊, NFM; ○, TEG; Δ, DEG.

The selectivity of NMP for this combination had the lowest value of the solvents investigated; with the ethylene glycols performing slightly better. NFM had the highest selectivity for this combination of the solvents investigated. Only two selectivities were available for the n-heptane-toluene separation using NFM, as the γ^{∞} value for toluene at 348.2 K was erroneous. It was therefore difficult to verify whether NFM did provide a superior performance at higher temperatures or not.

Table 6-17: Capacities of the various solvents for toluene (2) at 333.2, 348.2 and 363.2 K.

Temperature [K]	**k_2 [NFM]**	**k_2 [NMP]**	**k_2 [TEG]**	**k_2 [DEG]**
333.2	0.391	0.720	0.170	0.089
348.2	0.248	-	0.170	0.089
363.2	0.492	0.706	0.180	0.095

The capacity of NMP for toluene is once more the largest, but the capacity of NFM is just greater than half of the capacity of NMP (Table 6-17). NFM would therefore probably have been the best solvent for this separation problem, as it had the best selectivity, as well as having a good capacity.

6.4.4 n-Hexane/hex-1-ene

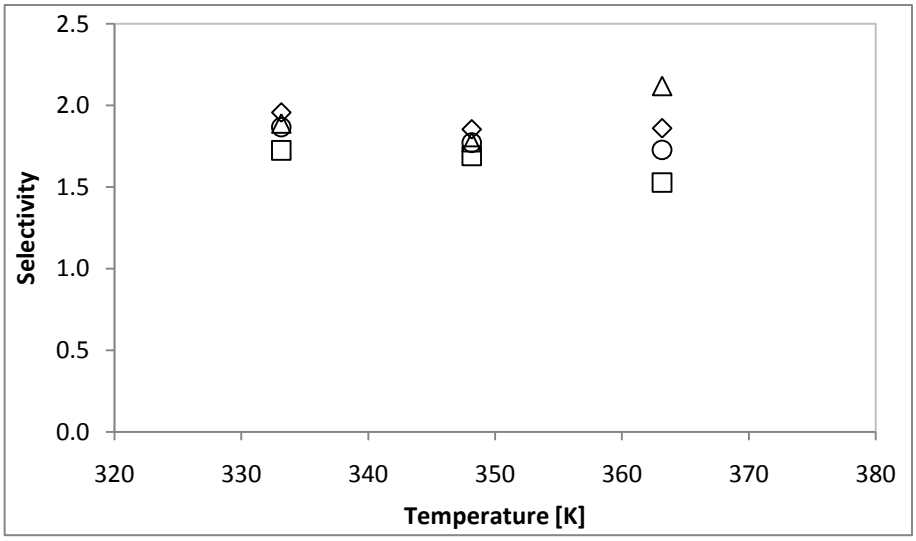

Figure 6-28: Selectivities of various solvents against temperature for the combination of n-hexane (1) and hex-1-ene (2). □, NMP; ◊, NFM; ○, TEG; Δ, DEG.

All of the solvents give very similar selectivities for this system (see Figure 6-28). With selectivities of less than 2, none of these solvents would improve the separation of n-hexane from hex-1-ene by a sufficient quantity to recommend the use of extractive distillation for this system.

The higher selectivity of DEG for n-hexane over hex-1-ene at 363.2 K did not seem correct, as the trend of the other two points pointed downwards. The trend of TEG also appeared to slope downwards with temperature.

Table 6-18: Capacities of the four solvents for hex-1-ene (2) at 333.2, 348.2 and 363.2 K.

Temperature [K]	**k_2 [NFM]**	**k_2 [NMP]**	**k_2 [TEG]**	**k_2 [DEG]**
333.2	0.080	0.181	0.041	0.020
348.2	0.086	0.184	0.041	0.020
363.2	0.095	0.179	0.049	0.026

The capacities of the four solvents for hex-1-ene are given in Table 6-18. The only solvent that provided a reasonable capacity for the separation of n-hexane from hex-1-ene was NMP. The capacity of NFM for hex-1-ene was less than half that of NMP for hex-1-ene, with the other solvents performing far poorer. Even when using NMP, a large amount of solvent would be required to provide an adequate separation.

6.4.5 Hex-1-ene/hex-1-yne

The selectivities of the various solvents for hex-1-ene (1) and hex-1-yne (2) are displayed in Figure 6-29.

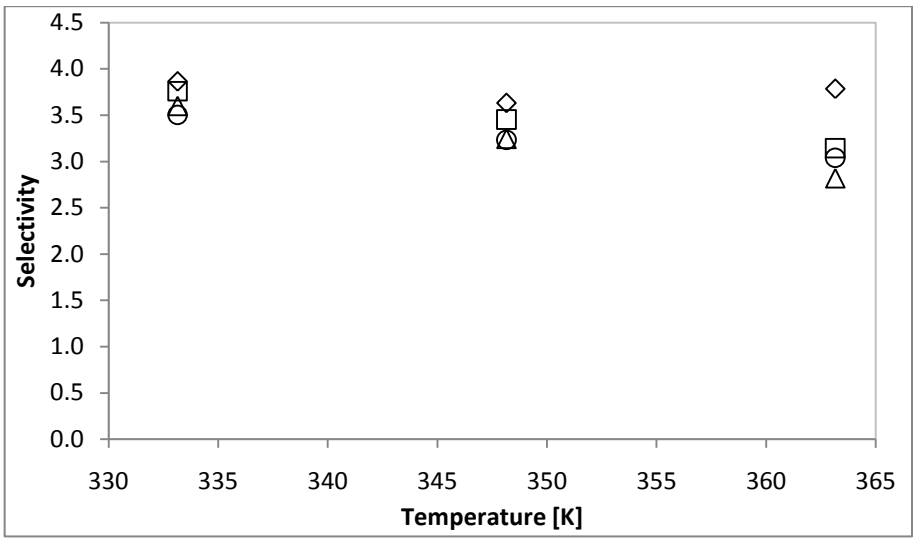

Figure 6-29: Selectivities of various solvents against temperature for the combination of hex-1-ene (1) and hex-1-yne (2). □, NMP; ◊, NFM; ○, TEG; Δ, DEG.

For this combination, the selectivities of all four solvents were very similar, with a greater range occurring with an increase in temperature. The deciding factor for this combination would be the capacity of the different solvents for hex-1-ene, the ease of recovery of the solvent and the economics of the process.

The selectivity of N-formylmorpholine for hex-1-ene over hex-1-yne did not show a decrease with an increase in temperature.

Table 6-19: Capacities of the four solvents for hex-1-yne (2) at 333.2, 348.2 and 363.2 K.

Temperature [K]	**k_2 [NFM]**	**k_2 [NMP]**	**k_2 [TEG]**	**k_2 [DEG]**
333.2	0.307	0.682	0.143	0.071
348.2	0.314	0.635	0.143	0.071
363.2	0.360	0.564	0.149	0.073

When observing the capacities of the solvents for hex-1-yne (Table 6-19), it was noticeable that NMP had the best performance in terms of capacity once again in this separation problem. There was a notable increase in the capacity of NFM for hex-1-yne with temperature, in comparison with the decrease in the capacity of NMP for hex-1-yne with increase in temperature. Therefore, if the separation were to be performed at high temperatures, NFM would be a better performing solvent.

6.4.6 n-Hexane/benzene

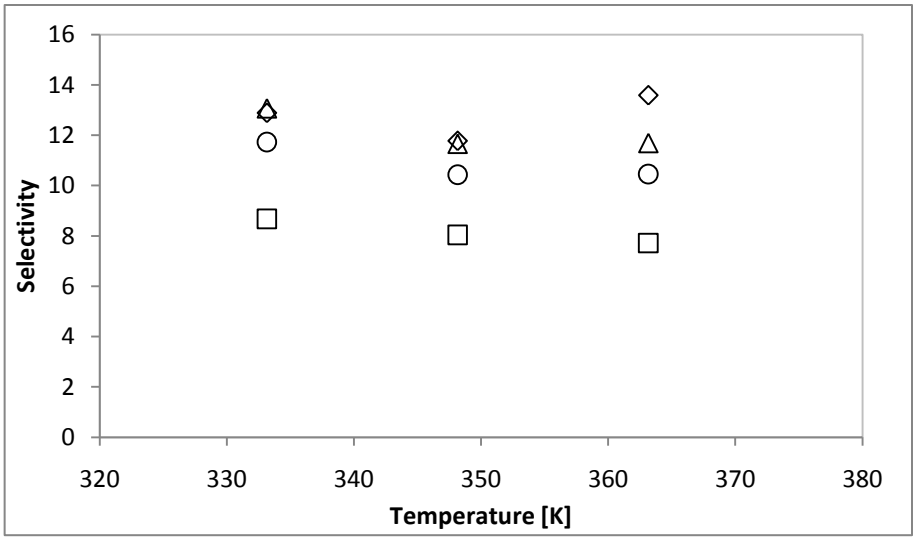

Figure 6-30: Selectivities of various solvents against temperature for the combination of n-hexane (1) and benzene (2). □, NMP; ◊, NFM; ○, TEG; Δ, DEG.

Figure 6-30 shows that NMP had a substantially lower selectivity for n-hexane (1) over benzene (2) than did NFM, TEG or DEG.

Table 6-15 provides the capacities of the four solvents for benzene at temperatures of 333.2, 348.2 and 363.2 K. For benzene, NMP had the largest capacity and NFM the next largest. Either NMP or NFM would be the best solvent for this separation. The decision would have to be decided upon based on a trade off between energy usage and solvent costs.

6.4.7 Benzene/methanol

The selectivity of diethylene glycol for the system of benzene (1) and methanol (2) was far superior to the selectivities of both N-methylpyrrolidone and N-formylmorpholine (Figure 6-31). The high selectivity suggested that diethylene glycol would provide a far simpler separation than the separations using the other solvents.

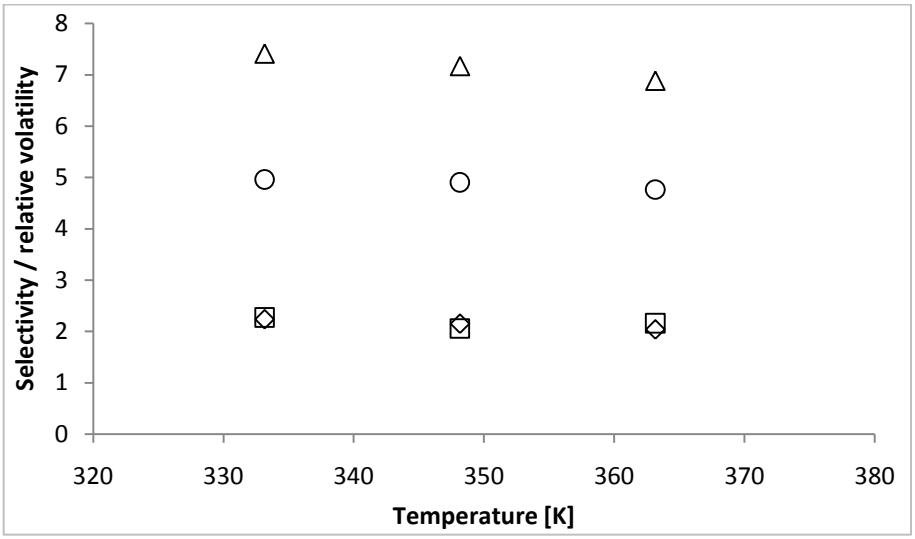

Figure 6-31: Selectivities of various solvents as a function of temperature for the combination of benzene (1) over methanol (2). □, NMP; ◊, NFM; ○, TEG; Δ, DEG.

The capacities of the various solvents for methanol are given in Table 6-20. The capacity of DEG for methanol was low in comparison with the capacities of any of the other solvents, but the selectivity was so much greater, that the use of DEG should be the first choice to effect this separation. The capacity of DEG for methanol was still very high when compared with the capacities of these four solvents for some of the other solutes.

Table 6-20: Capacities of the four solvents for methanol (2) at 333.2, 348.2 and 363.2 K.

Temperature [K]	k_2 [NFM]	k_2 [NMP]	k_2 [TEG]	k_2 [DEG]
333.2	1.173	2.074	1.270	1.012
348.2	1.181	1.800	1.270	1.012
363.2	1.416	1.959	1.417	0.976

CHAPTER 7

Conclusions

An in-depth study of the behaviour of 25 solutes, including alkanes, cycloalkanes, alk-1-enes, alk-1-ynes, alcohols and aromatics, at infinite dilution, was performed using gas-liquid chromatography. Measurements of the infinite dilution activity coefficients were conducted at temperatures of between 333 and 363 K, in four different solvents. These solvents were N-formylmorpholine, N-methylpyrrolidone, triethylene glycol and diethylene glycol. Pre-saturation of the carrier gas was included in the GLC set up, to prevent the elution of the liquid solvent from the column.

The infinite dilution activity coefficients of the various hydrocarbons in N-formylmorpholine were used to verify the experimental set up and procedure, by comparison with previously measured data. The experimental data for NFM from this study was found to be in good agreement with the experimental data of these authors. The uncertainties of the measurements were found to be within the expected uncertainties for gas-liquid chromatography.

Once it was apparent that the experimental set up provided accurate results, the infinite dilution activity coefficients in N-methylpyrrolidone, triethylene glycol and diethylene glycol were also measured. There was a substantial database available in literature of experimental infinite dilution activity coefficients for N-methylpyrrolidone, but there was a severe degree of scatter in this data. The infinite dilution activity coefficients in N-methylpyrrolidone measured in this study were very similar to some of the literature data.

Sun et al. (2003) was the only available source of infinite dilution activity coefficients in triethylene glycol at the temperatures of interest to this study. The experimental data from this study differed by approximately 20% from their data. The measurement of the infinite dilution activity coefficients in diethylene glycol was completely new, with no previous measurements having been made at the temperatures measured in this study.

The infinite dilution activity coefficients of only three solutes; in N-formylmorpholine and in N-methylpyrrolidone; at 333 K were measured using the dilutor cell technique. The technique that was used was a novel technique proposed by Richon (2011a).

The measured data from this study was compared with the literature data reported by the same authors as the GLC experimental data, but the results did not compare very satisfactorily. The difference between the data measured in this study and the data available from literature was unacceptably large, especially for the case of the solutes in N-methylpyrrolidone. It was therefore concluded that, at present, the novel technique cannot be applied to systems with volatile solvents.

The selectivities and capacities at infinite dilution of several systems, which are difficult to separate by conventional methods, were investigated.

- It was difficult to determine whether NFM would provide better separation performance for the combinations of cyclohexane/benzene, n-heptane/cyclohexane and n-hexane/benzene. For these three combinations, the choice of solvent would most likely be a matter of economics.
- For the combinations of n-heptane/toluene and hex-1-ene/hex-1-yne, NFM would provide the best performance, especially were the temperature of operation increased.
- NMP provided the best performance for the separation of n-hexane from hex-1-ene, although this performance remained low.
- The most interesting separation problem was the benzene/methanol case, where the performance of the ethylene glycols was superior to the performance of the other solvents. For the separation of these two components, diethylene glycol had the best performance.

CHAPTER 8

Recommendations

A few minor changes to the gas liquid chromatography set up that could be made in order to improve the accuracy, reliability and ease of use of this technique are listed below.

- By placing the pre-saturators inside the air bath of the gas chromatography, improved control of the temperature can be attained. This would increase the accuracy of the measurements, as the fluctuation of the mass of solvent in the column would be reduced.
- If the measurement of the flow of carrier gas could be automated, the supervision required of the measurements would be greatly reduced, since the injection of the solutes was already automated.
- Stirring of the solvent in the pre-saturators would improve the approach to equilibrium of the solvent in the vapour phase, as it would increase the path length of the bubbles.

The dilutor cell technique required further development in order to render it feasible for the measurement of the infinite dilution activity coefficients in volatile solvents. One modification to the experimental set up is suggested.

- The placement of the dilutor cell inside the air bath of the gas chromatograph would reduce the distance travelled between the cell and the detector, possibly improving accuracy, as well as providing better temperature control.

From the comparisons of the selectivities and capacities of the various solute-solute-solvent combinations, a few notable results were obtained.

- The most interesting result was the superior performance of diethylene glycol for the separation of benzene from methanol. This separation should be further investigated by the measurement of vapour liquid equilibria data.
- On a number of occasions, it appeared that N-formylmorpholine provided similar or better performance than N-methylpyrrolidone. In some of these cases, N-methylpyrrolidone is currently used as the solvent for extractive distillation. These systems should be further investigated.

blank page

References

1. Ahmad, M.I., Zhang, N., Jobson, M., 2010. Molecular component-based representation of petroleum. **Chem. Eng. Res. Des.**, 89, pp.410-20.

2. Ambrosone, L., DÉrrico, G., Sartorio, R., Vitagliano, V., 1991. Analysis of velocity cross-correlation and preferential solvation for the system N-methylpyrrolidone and water. **J. Chem. Soc. Faraday Trans.**, 91(9), pp.1339-44.

3. Aminabhavi, T.M., Gopalakrishna, B., 1995. Density, Viscosity, Refractive Index, and Speed of Sound in Aqueous Mixtures of N,N-Dimethylformamide, Dimethyl Sulfoxide N,N-Dimethylacetamide, Acetonitrile, Ethylene Glycol, Diethylene Glycol, 1,4-Dioxane, Tetrahydrofuran, 2-Methoxyethanol, and 2-Ethoxyethanol at 298.15 K. **J. Chem. Eng Data**, 40, pp.856-61

4. Andrussow, L., 1950. Wärmeleitfähigkeit, Zähigkeit und Diffusion in der Gasphase. **Z. Elektrochem.**, 54, pp.566-71.

5. Antoine, C., 1888. Tensions des vapeurs; nouvelle relation entre les tensions et les températures. **Comptes Rendus des Séances de l'Académie des Sciences**, 107, pp.681–684, 778–780, 836–837.

6. Arancibia, E.L., Catoggio, J.A., 1980. Gas chromatographic study of solution and adsorbtion of hydrocarbons on glycols I. Diethylene glycol and Triethylene Glycol. **Journal of Chromatography**, 197, pp.135-45.

7. Arnold, J.H., 1930. Studies in Diffusion: I. Estimation of Diffusivities in Gaseous Systems. **Ind. Eng. Chem.**, 22, p.1091.

8. Awwad, A.M., Al-Dujaili, A. H., 2001. Density, Refractive Index, Permittivity, and Related Properties for N-formylmorpholine + Ethyl Acetate and + Butanone at 298.15 K. **J. Chem. Eng Data**, 46, pp.1349-50

9. Awwad, A.M., Farhan, A.M., 2009. Volumetric properties of 2-pyrrolidone with aromatic hydrocarbons at T = (293.15, 303.15, 313.15, 323.15, 333.15, and 343.15) K. **J. Chem. Thermodynamics**, 41, pp.205-11.

10. Bao, J., Han, S., 1995. Infinite dilution activity coefficients for various types of systems. **Fluid Phase Equilibria**, 112, pp.307-16.

11. Blanco, B., Beltran, S., Cabezas, J.L., Coca, J., 1997. Phase Equilibria of Binary Systems Formed by Hydrocarbons from Petroleum Fractions and the Solvents N-

methylpyrrolidone and N,N-Dimethylformamide. 1. Isobaric Vapor−Liquid Equilibria. **J. Chem. Eng Data**, 42(5), pp.938-42.

12. Camin, D.L., Forziati, A.F., Rossini, F.D., 1954. Physical Properties of n-Hexadecane, n-Decyclcyclopentane, n-Decylcylcohexane, 1-Hexadecene and n-Decylbenzene. **J. Phys. Chem.**, 58, pp. 440-42

13. Chen, N.H., Othmer, D.F., 1962. New Generalized Equation for Gas Diffusion Coefficient. **J. Chem. Eng Data.**, 7(1), pp.37-41.

14. Chiao, T., Thompson, A.R., 1957. Densities and Refractive Indicies for Glycol-Water Solutions. **Analytical Chemistry.**, 29(11), pp.1678-81.

15. Chien, C.F., Kopecni, M.M., Laub, R.J., Smith, C.A., 1981. Solute Liquid-Gas Activity and Partition Coefficients with Mixtures of n-Hexadecane and n-Octadecane with N,N-Dibutyl-2-ethylhexylamide Solvents. **J. Phys. Chem.**, 85, pp.1864-71.

16. Conder, J.R., Young, C.L., 1979. **Physiochemical Measurement by Gas Chromatography.** Chichester: Wiley.

17. Crank, J., 1956. Chapter VI. In **The mathematics of diffusion.** Oxford: Oxford University Press, p.86.

18. Cruickshank, A.J.B., Windsor, M.L., Young, C.L., 1966. The Use of Gas-Liquid Chromatogrphy to Determine Activity Coefficients and Second Virial Coefficients of Mixtures. I. Theory and Verification of Method of Data Analysis. **Proc. R. Soc. Lond. A**, 295, pp.259-70.

19. Diehl, T., Kolbe, B., Gehrke, H., 2005. Udhe Morphylane Extractive Distillation: Where do we stand? In *ERTC* **Petrochemical Conference.** Prague, Czech Republic, 2005.

20. Dohnal, V., 2005. Measurement of limiting activity coefficients using analytical tools. In Weir, R.D., De Loos, T.W. **Experimental Thermodynamics, Volume 7: Measurement Thermodynamic Properties Multiple Phases.** Elsevier.

21. Dolezal, B., Holub, R., 1985. Approximation relations for determining the activity coefficient at very low concentration by the method of variation of solute concentration. **Collect. Czech. Chem. Comm.**, 50, pp.704-11.

22. Dolezal, B., Popl, M., Holub, R., 1981. Determination of activity coefficients at very low concentrations by the inert gas stripping method. **Journal of Chromatography**, 207, pp.193-201.

23. Dortmund Data Bank Software and Separation Technology GmbH, 2011. **Dortmund Data Bank**. Oldenburg.

24. Duhem, P., Vidal, J., 1978. Extension of the dilutor method to measurement of high activity coefficients at infinite dilution. **Fluid Phase Equilibria**, 2(3), pp.231-35.

25. Everett, D.H., 1965. Effect of Gas Imperfection on G.L.C. Measurements : a Refined Method for Determining Activity Coefficients and Second Virial Coefficients. **Trans. Faraday Soc.**, 61, pp.1637–1645.

26. Ferreira, P.O., Bastos, J.C., Medina, A.G., 1987. Infinite Dilution Activity Coefficients for Aromatic and Nonaromatic Compounds in N-methylpyrrolidone, Ethylene Glycol and Mixtures of the Two Solvents. **J. Chem. Eng Data,** 32, pp.25-31.

27. Fischer, K., Gmehling, J., 1996. Vapour-liquid equilibria, activity coefficients at infinite dilution and heats of mixing for mixtures of N-methyl pyrrolidone-2 with C_5 or C_6 hydrocarbons and for hydrocarbon mixtures. **Fluid Phase Equilibria**, 119, pp.113-30.

28. Fuller, E.N., Schettler, P.D., Giddings, J.C., 1966. A new method for prediction of binary gas-phase diffusion coefficients. **Ind. Eng. Chem.**, 58(5), pp.19-27.

29. Gaile, A.A., Parlzheva, N.V., Proskuryakov, V.A., 1974. **Zh. Prikl. Khim. (Leningrad)**, 47, p.191.

30. George, S., 2008. **Determination of activity coefficients at infinite dilution using the inert gas stripping technique.** MSc. Thesis. University of KwaZulu-Natal.

31. Gilliland, E.R., 1934. Diffusion coefficients in gaseous systems. **Ind. Eng Chem.**, 26, pp.681-85.

32. Gmehling, J., Mollmann, C., 1998. Synthesis of Distillation Processes Using Thermodynamic Models and the Dortmund Data Bank. **Ind. Eng. Chem. Res.**, 37, pp.3112-23.

33. Gruber, D., Langenheim, D., Moolan, W., Gmehling, J., 1998. Measurement of Activity Coefficients at Infinite Dilution Using Gas-Liquid Chromatography. 7. Results for Various Solutes with N-Methyl-2-piperidone as Stationary Phase. **J. Chem. Eng. Data**, 43, pp.226-29.

34. Heintz, A., Kulikov, D.V., Verevkin, S.P., 2001. Thermodynamic properties of mixtures containing ionic liquids. 1. Activity coefficients at infinite dilution of alkanes, alkenes and alkylbenzenes in 4-Methyl-n-butylpyridinium tetrafluoroborate using gas-liquid chromatography. **J. Chem. Eng. Data**, 46, pp.1526-29.

35. Heintz, A., Kulikov, D.V., Verevkin, S.P., 2002. Thermodynamic Properties of Mixtures Containing Ionic Liquids. 2. Activity Coefficients at Infinite Dilution of Hydrocarbons and Polar Solutes in. Using Gas-Liquid Chromatography. **J. Chem. Eng. Data**, 47, pp.894-99.

36. Hirschfelder, J.O., Bird, R.B., Spotz, E.L., 1948. The transport Properties of Non-Polar Gases. **J. Chem. Phys.**, 16 (10), pp.968-981.

37. Hirschfelder, J.O., Bird, R.B., Spotz, E.L., 1949a. Viscosity and Other Physical Properties of Gases and Gas Mixtures. **Trans. ASME**, 71, pp. 921-937.

38. Hirschfelder, J.O., Bird, R.B., Spotz, E.L., 1949b. The transport Properties of Gases and Gaseous Mixtures II. **Chem. Revs.**, 44 (1), pp. 205-231.

39. Holderbaum, T., Gmehling, J., 1991. PSRK: A Group Contribution Equation of State Based on UNIFAC. **Fluid Phase Equilibria**, 70, pp.251-65.

40. Hudson, G.H., McCoubrey, J.C., 1960. Intermolecular Forces Between Unlike Molecules, A more complete form of the combining rules. **Trans. Faraday Soc.**, 56, pp.761–766.

41. Hussey, C.L., Parcher, J.F., 1973. Chromatographic Applications of Wilson's Equation for Excess Free Energy. **Analytical Chemistry**, 45(6), pp.926-29.

42. Johnson, C.D., 2006. **Process Control Instrumentation Technology**. 8th ed. Upper Saddle River, New Jersey: Pearson Education.

43. Knoop, C., Tiegs, D., Gmehling, J., 1989. Measurement of gamma infinite using gas-liquid chromatography. 3. Results for the stationary phases 10-Nonadecanone, N-formylmorpholine, 1-Pentanol, m-Xylene, and Toluene. **J. Chem. Eng. Data**, 34, pp.240-47.

44. Kojima, K., Zhang, S., Hiaki, T., 1997. Measuring methods of infinite dilution activity coefficients and a database for systems including water. **Fluid Phase Equilibria**, 131, pp.145-79.

45. Kossack, S., Kraemer, K., Gani, R., Marquardt, W., 2007. A Systematic Synthesis Framework for Extractive Distillation Processes. In **Proceedings of European Congress of Chemical Engineering (ECCE-6)**. Copenhagen, 2007.

46. Krummen, M., Gmehling, J., 2004. Measurement of activity coefficients at infinite dilution in N-methyl-2-pyrrilodine and N-formylmorpholine and their mixtures with water using the dilutor technique. **Fluid Phase Equilibria**, 215, pp.283–294.

47. Krummen, M., Gruber, D., Gmehling, J., 2000. Measurement of Activity Coefficients at Infinite Dilution in Solvent Mixtures, using the Dilutor Technique. **Ind. Eng. Chem. Res.**, 39, pp.2114-23.

48. Kwantes, A., Rijinders, G.W.A., 1958. **Gas Chromatography 1958**. 1st ed. London: Butterworths.

49. Laub, R.J., Martire, D.E., Purnell, J.H., 1977. Prediction of Infinite Dilution Activity Coefficients in Binary n-Alkane Mixtures. **Faraday Transactions 1**, 73, pp.1686-90.

50. Laub, R.J., Pecsok, R.L., 1978. **Physicochemical applications of gas chromatography.** New York: Wiley.

51. Leroi, J., Masson, J.C., Renon, H., Fabries, J.F, Sannier, H., 1977. Accurate Measurement of Activity Coefficients at Infinite Dilution by Inert Gas Stripping and Gas Chromatography. **Ind. Eng. Chem., Process Des. Dev.**, *Vol 16, No. 1*, pp.139-44.

52. Letcher, T., 1975. Chapter 2. *In* Le Neindre, B., Vodar, B. **Experimental Thermodynamics.** London: Butterworths.

53. Letcher, T.M., Harris, R.A., Ramjugernath, D., Raal, J.D., 2001. Activity coefficients of hydrocarbon solutes at infinite dilution in monoethanolamine from gas-liquid chromatography. **J. Chem. Thermodynamics**, 33, pp.1655–1662.

54. Letcher, T., Reddy, P., 2005. Determination of activity coefficients at infinite dilution of organic solutes in the ionic liquid, trihexyl(tetradecyl)-phosphonium tris(pentafluoroethyl) trifluorophosphate, by gas–liquid chromatography. **Fluid Phase Equilibria**, 235, pp.11-17.

55. Letcher, T.M., Whitehead, P.G., 1997. The determination of activity coefficients of alkanes, alkenes, cycloalkanes, and alkynes at infinite dilution with the polar solvents dimethyl sulphoxide (DMSO), or N,N-dimethylformamide (DMF), or N-methyl-2-pyrrolidinone (NMP) using a g.l.c. technique. **J. Chem. Thermodynamics**, 29, pp.1261-68.

56. Lide, D.R., ed., 2005. **CRC Handbook of Chemistry and Physics**. 86th ed. Boca Raton, Florida: CRC Press, Taylor and Francis Group.

57. Mahmoudi, J., Lotfollahi, M.N., 2010. (Liquid + liquid) equilibria of (sulfolane + benzene + n-hexane), (N-formylmorpholine + benzene + n-hexane), and (sulfolane + N-formylmorpholine + benzene + n-hexane) at temperatures ranging from (298.15 to 318.15) K: Experimental results and correlation. **J. Chem. Thermodynamics**, 42, pp.466-71.

58. McGlashan, M.L., Potter, D.J.B., 1962. An Apparatus for the Measurement of the Second Virial Coefficients of Vapours; The Second Virial Coefficients of Some n-Alkanes and of Some Mixtures of n-Alkanes. **Proc. R. Soc. Lond. A**, 267, pp.478-500.

59. Mitov, I.P., Petrov, L.A., 1995. Assessment of some possibilities for improving the performance of gas chromatographic thermal conductivity detectors with hot-wire sensitive elements. **Journal of Chromatography A**, 715, pp.287-97.

60. Mokhtari, B., Gmehling, J., 2010. (Vapour and liquid) equilibria of ternary systems with ionic liquids using headspace gas chromatography. **J. Chem. Thermodynamics** 42, pp.1036-38.

61. Nagata, I., 1969. Vapour-Liquid Equilibrium Data for the Binary Systems Methanol-Benzene and Methyl Acetate-Benzene. **J. Chem. Eng Data**, 14(4), pp.418-20.

62. Olivier, E., Letcher, T.M., Naidoo, P., Ramjugernath, D., 2010. Activity coefficients at infinite dilution of organic solutes in the ionic liquid 1-ethyl-3-methylimidazolium trifluoromethanesulphonate using gas-liquid chromatography at T=(313.15, 323.15, and 333.15)K. **J. Chem. Thermodynamics** 42, pp.78-83.

63. Othmer, D.F., Chen, H.T., 1962. Correlating Diffusion Coefficients in Binary Gas Systems. Use of Viscosities in a New Equation and Nomogram. **Ind. Eng Chem. Process Design Develop**, 1(4), pp.249-54.

64. Park, S., Oh, J., Han, K., Won, D., 2001. **Determination of Infinite Dilution Activity Coefficient using Gas Liquid Chromatography**. [Online] Available at: http://www.cheric.org/proceeding_disk/kiche2001s/cp064.hwp [Accessed 21 February 2011].

65. Peng, D.Y., Robinson, D.B., 1976. A New Two-Constant Equation of State. **Ind. Eng. Chem. Fundam.**, 15(1), pp.59-64.

66. Pescar, R.E., Martin, J.J., 1966. Solution Thermodynamics from Gas Liquid Chromatography. **J. Anal. Chem.**, 38(12), pp.1661-69.

67. Poling, B.E., Prausnitz, J.M., O'Connell, J.P., 2000. **The Properties of Gases and Liquids**. 5th ed. New York: McGraw-Hill.

68. Polyscience, 2011. **8200 Series Heating Circulators.** [Online] Available at: http://www.polyscience.com/lab/8200.html [Accessed 13 September 2011].

69. Rackett, H.G., 1970. Equation of State for Saturated Liquids. **J. Chem. Eng. Data**, 15(4), pp.514-17.

70. Rajeshwar Rao, B., Bhagat, S.D., 1990. Evaluation of Solute-Solvent Interactions of Some Non-electrolytes with N-methylpyrrolidone by Gas-Liquid Partition Chromatography. **Indian J. Chem. Sect. A.**, 29, pp.652-55.

71. Rajeshwar Rao, B., Bhagat, S.D., 1991. Thermodynamics of Solution of Some Nonelectrolyte Solutes at Infinite Dilution in N-methylpyrrolidone Stationary Phase by Gas-Liquid Partition Chromatography. **Indian J. Chem. Sect. A**, 30, pp.751-55.

72. Rarey, J., 2011. Personal communication.

73. Redlich, O., Kwong, J.N.S., 1949. On the thermodynamics of solutions V. An equation of state. Fugacities of gaseous solutions. **Chemical Reviews**, 44(1), pp.233-44.

74. Richon, D., 2011a. New equipment and a new technique for measuring activity coefficients and Henry's constants at infinite dilution. **Review of Scientific Instruments**, 82, 039902.

75. Richon, D., 2011b. Personal Communication.

76. Richon, D., Antoine, P., Renon, H., 1980. Infinite Dilution Activity Coefficients of Linear and Branched Alkanes from C1 to C9 in n-Hexadecane by Inert Gas Stripping. **Ind. Eng. Chem. Process Dev.**, 19, pp.144-47.

77. Riddick, J.A., Bunger, W.B., Sakano, T.K., 1986. **Organic Solvents; Physical Properties and Methods of Purification.** 4th ed. New York: Wiley-Interscience.

78. Ruiz, C., Coca, J., Vega, A., Diez, F.V., 1997. Extractive Distillation with Dimethylformamide: Experimental and Simulation Data. **Ind. Eng. Chem. Res.**, 36, pp.4934-39.

79. Schult, C.J., Neely, B.J., Robinson, R.L., Gasem, K.A.M., Todd, B.A., 2001. Infinite dilution activity coefficients for several solutes in hexadecane and in N-methyl-2-pyrrolidone (NMP): experimental measurements and UNIFAC predictions. **Fluid Phase Equilibria**, 179, pp.117-29.

80. Seader, J.D., Henley, E.J., 2006. **Separation Process Principles**. 2nd ed. Hoboken: John Wiley and Sons, Inc.

81. Shaffer, D.L., Daubert, T.E., 1969. Gas-Liquid Chromatographic Determination of Solution Properties of Oxygenated Compounds in Water. **Anal. Chem.**, 41, pp.1585-89.

82. Shimadzu Asia Pacific Pty. Ltd., 2006. **ThaiRoHs.org**. [Online] Customer Support Centre, Singapore Available at: http://www.thairohs.org/index.php?option=com_docman&task=doc_view&gid=52&Itemid=89 [Accessed 23 November 2011].

83. Shimadzu Scientific Instruments, 2011. **Gas Chromatography - GC-2014 Product Brochure.** [Online] Available at: http://www.ssi.shimadzu.com/products/literature/GC/gc-2014.pdf [Accessed 12 September 2011].

84. Sitnyakovskii, I.B., Gaile, A.A., Semenov, L.V., 1989. **J. Appl. Chem. USSR**, 62(12), pp.2564-66.

85. Slattery, J.C., Bird, R.B., 1958. Calculation of the diffusion coefficient of dilute gases and of the self-diffusion coefficient of dense gases. **A.I.Ch.E. Journal**, 4(2), pp.137-42.

86. Smith, J.M., van Ness, H.C., Abbott, M.M., 2005. **Introduction to Chemical Engineering Thermodynamics**. 7th ed. New York: McGraw Hill.

87. Soave, G., 1972. Equilibrium constants from a modified Redich-Kwong equation of state. **Chemical Engineering Science,** 27, pp.1197-203.

88. Spencer, C.F., Adler, S.B., 1978. A Critical Review of Equations for Predicting Saturated Liquid Density. **J. Chem. Eng Data**, 23(1), pp.82-89.

89. Spencer, C.F., Danner, R.P., 1972. Improved Equation for Prediction of Saturated Liquid Density. **J. Chem. Eng Data**, 17(2), pp.236-41.

90. Steltenpohl, P., Chlebovec, M., Graczova, E., 2005. Simulation of Toluene Extractive Distillation from a Mixture with Heptane. **Chem. Pap.**, 59(6a), pp.421-27.

91. Sun, P., Gao, G., Gao, H., 2003. Infinite Dilution Activity Coefficients of Hydrocarbons in Triethylene Glycol and Tetraethylene Glycol. **J. Chem. Eng. Data**, 48, pp.1109-12.

92. Thomas, E.R., Newman, B.A., Nicolaides, G.L., Eckert, C.A., 1982. Limiting Activity Coefficients from Differential Ebulliometry. **J. Chem. Eng Data**, 27(3), pp.233-40.

93. Tsonopoulos, C., 1974. An empirical correlation of second virial coefficients. **AIChE Journal**, 20(2), pp.263-72.

94. Tsonopoulos, C., Dymond, J.H., Szafranski, A.M., 1989. Second virial coefficients of normal alkanes, linear 1-alkanols and their binaries. **Pure and Appl. Chem.**, 61(8), pp.1387-94.

95. Tumba, A.K., 2010. Infinite Dilution Activity Coefficient Measurements of Organic Solvents in Fluorinated Ionic Liquids by Gas-Liquid Chromatography and the Inert Gas Stripping Method, **MSc Thesis. School of Chemical Engineering, University of KwaZulu-Natal**.

96. Turek, E.A., Arnold, D.A., Greenkorn, R.A., Chao, K.-C., 1979. A Gas-Liquid Partition Chromatograph for the Accurate Determination of Infinite Dilution Activity Coefficients. **Ind. Eng. Chem. Fundam.**, 18(4), pp.426-29.

97. van Aken, A.B., Broersen, J.M., 1977. Selectivity and solvency properties of extraction solvents and their mixtures. In **Conference on Solvent Extraction, ISEC '77**. Toronto, 1977.

98. van Dyk, B., Nieuwoudt, I., 2000. Design of Solvents for Extractive Distillation. **Ind. Eng. Chem. Res.**, 39, pp.1423-29.

99. Villaluenga, J.P., Tabe-Mohammadi, A., 2000. A review on the separation of benzene/cyclohexane mixtures by pervaporation processes. **Journal of Membrane Science**, 169, pp.159-74.

100. Wauquier, J., Trambouze, P., Favennec, J., 1995. **Petroleum Refining: Separation Processes, Volume 2**. Paris: Editions Technip.

101. Weidlich, U., Gmehling, J., 1985. Extension of UNIFAC by Headspace Gas Chromatography. **J. Chem. Eng. Data**, 30, pp.95-101.

102. Weidlich, U., Rohm, H.J., Gmehling, J., 1987. Measurement of gamma infinite using GLC. 2. Results for the Stationary Phases N-formylmorpholine and N-methylpyrrolidone. **J. Chem. Eng. Data**, 32, pp.450-53.

103. Zhang, S., Tsuboi, A., Nakata, H., Ishikawa, T., 2003. Infinite Dilution Activity Coefficients in Ethylene Glycol and Ethylene Carbonate. **J. Chem. Eng. Data**, 48, pp.167-70.

Appendix A

Diffusion coefficient

No diffusion coefficients for NMP or NFM in helium could be found, and therefore in order to determine the height of solvent required to obtain sufficient saturation of the carrier gas, a diffusion coefficient for the system had to be calculated from a generalised correlation.

A number of generalised equations, which would have provided a sufficiently accurate diffusion coefficient, existed. There were two distinct groups of these correlations. The first group could be traced back to the hard sphere model (Fuller et al., 1966), and included authors such as Arnold (1930), Andrussow (1950) and Gilliland (1934). The second group of correlations was based the diffusion coefficients on the critical volumes of the pure components. These correlations included the work of Hirschfelder, Bird and Spotz (1948, 1949a, 1949b), as well as that of Chen and Othmer (1962), Slattery and Bird (1958) and Othmer and Chen (1962).

Fuller and co-workers (1966) reviewed eight of these methods, and compared the calculated data from these methods, as well as their proposed equation, with experimentally measured data. The Fuller-Schettler-Giddings (FSG) equation that they proposed provided the greatest accuracy to the 340 experimental points to which the comparison was made. Another gain that was made with the new equation was that the number of systems for which the predicted values differed by more than 10% from the experimental data was greatly reduced

The equation that was proposed by Fuller et al. (1966) for the calculation of the diffusion coefficient is given by Equation B-1.

$$D_{ij}{}^{G} = 1 \times 10^{-8} \frac{T^{1.75} \left[\frac{1}{M_A} + \frac{1}{M_B}\right]^{1/2}}{P\left[(\sum_A v_t)^{1/3} + (\sum_B v_t)^{1/3}\right]^2} \qquad \text{(A–1)}$$

The values for v_t, the atomic and structural diffusion volumes, were given by Fuller and co-workers and the values required by this study are listed in Table A-1.

The pressure for the calculation was set to an arbitrary value of 1.3 atm. The pressure drop across the long column was approximately 30 kPa, and therefore the pressure in the pre-saturators was approximated as 1.3 atm.

The above calculation gave a diffusion coefficient of 0.0103 cm^2/s at 333.15K.

Table A-1: Special atomic and structural diffusion volumes for use in the FSG equation proposed by Fuller et al. (1966) (Equation A-1).

Atomic/structural unit	Diffusion volume
Carbon	16.5
Hydrogen	1.98
Oxygen	5.48
Nitrogen	5.69
Ring	-20.2
Helium	2.88

Limiting speed of the bubbles

The limiting speed for the bubbles in the solution was calculated using the equation given by Richon et al. (1980) (Equation A-2).

$$(u^{\infty})^{1.4} = 7.2 \times 10^{-2} {\nu_L}^{-0.6} D_b^{1.6} g \qquad \text{(A–2)}$$

For this equation, the kinematic viscosity was obtained from the work of Ambrosone et al. (1991). This value was measured at 298.15 K, but gave a close enough approximation, as no other data could be found.

Appendix B

Vapour Pressure Correlations

The saturated vapour pressure of the pure components was determined using one of the equations given by Poling et al. (2000) (Equations B-1, B-2 and B-4). Equation B-1 was the Antoine equation, which was extended by Equation B-2. The T_C used in these correlations differed from the actual critical temperatures, as they were regressed parameters (Poling et al., 2000).

$$log_{10}\, P_i^0 = A - \frac{B}{T[°C] + C} \tag{B–1}$$

$$log_{10}\, P_i^0 = A - \frac{B}{T[°C] + C} + \ 0.43429(x^n) + \ E(x^8) + \ F(x^{12}) \tag{B–2}$$

Where

$$x = \frac{(T[°C] - \ t_0)}{T_c} \tag{B–3}$$

$$ln\, P_i^0 = \ ln\, P_c + \frac{T_c}{T}[a\,\tau + b\,\tau^{1.5} + \ c\,\tau^{2.5} + \ d\,\tau^5] \tag{B–4}$$

Where

$$\tau = 1 - \frac{T}{T_c} \tag{B–5}$$

blank page

Appendix C

Physical and Critical Properties

Table C-1: Critical properties for the solutes and for helium used for the calculation of the infinite dilution activity coefficients. Sourced from the Dortmund Data Bank Software (2011). Ionisation energies were obtained from Lide (2005).

	P_c [bar]	V_c [cm^3/mol]	T_c [K]	Z_c	ω	I [kJ/mol]	μ [deBye]
n-pentane	33.70	311	469.8	0.268	0.252	998.6	
n-hexane	30.25	368	507.9	0.264	0.299	977.4	
n-heptane	27.40	428	540.2	0.261	0.350	957.1	
n-octane	24.90	492	568.7	0.259	0.399	947.5	
n-nonane	22.90	555	594.6	0.257	0.445	937.8	
cyclopentane	45.08	260	511.6	0.276	0.192	1014.1	
cyclohexane	40.73	308	553.5	0.273	0.211	951.3	
cycloheptane	38.40	359	604.3	0.274	0.242	962.0	
cyclooctane	35.70	410	647.2	0.271	0.254	941.7	
pent-1-ene	35.60	298.4	464.8	0.275	0.237	917.6	
hex-1-ene	31.43	355.1	504.0	0.266	0.281	910.8	
hept-1-ene	29.20	409	537.3	0.267	0.343	910.8	
oct-1-ene	26.80	468	567.0	0.266	0.393	909.9	
non-1-ene	23.30	526	594.0	0.248	0.411	908.9	
pent-1-yne	41.70	277	470.0	0.296	0.394	969.7	
hex-1-yne	37.62	331	539.3	0.277	0.146	960.0	
hept-1-yne	33.40	376.5	551.6	0.274	0.389	960.0	
oct-1-yne	31.01	441	598.5	0.275	0.262	960.0	
methanol	80.97	118	512.6	0.224	0.565	1046.9	
ethanol	61.48	167	513.9	0.240	0.649	1010.2	1.69
propan-1-ol	51.75	219	536.8	0.254	0.629	982.2	1.68
propan-2-ol	47.62	220	508.3	0.248	0.665	981.3	1.66
benzene	48.95	256	562.2	0.268	0.210	892.1	
toluene	41.08	316	591.8	0.264	0.264	851.0	
ethylbenzene	36.09	374	617.2	0.263	0.304	846.2	
helium	2.27	57.5	5.2			2372.6	

Table C-2: Vapour pressure correlation constants

	A	B	C	D	E	F	n	to	Pc [bar]	Eqn	Ref
n-pentane	-7.3070	1.7585	-2.1629	-2.9130	-	-	-	-	33.75	C-3	a
n-hexane	-7.5400	1.8376	-2.5438	-3.1630	-	-	-	-	30.35	C-3	a
n-heptane	-7.7740	1.8561	-2.8298	-3.5070	-	-	-	-	27.35	C-3	a
n-octane	4.0508	1356.36	209.64	-	-	-	-	-	-	C-1	a
n-nonane	4.0736	1438.03	202.69	-	-	-	-	-	-	C-1	a
cyclopentane	4.0678	1152.57	234.51	-	-	-	-	-	-	C-1	a
cyclohexane	3.9300	1182.77	220.62	-	10.0	-127.0	3.4041	25	-	C-2	a
cycloheptane	3.9633	1322.22	215.30	-	-	-	-	-	-	C-1	a
cyclooctane	3.9813	1434.67	209.71	-	-	-	-	-	-	C-1	a
pent-1-ene	3.9691	1044.01	233.45	-	122.9	-4873.4	2.5751	38	-	C-2	a
hex-1-ene	3.9826	1148.62	225.34	-	106.3	-3773.6	2.4592	72	-	C-2	a
hept-1-ene	4.0268	1258.34	219.30	-	-	-	-	-	-	C-1	a
oct-1-ene	4.0599	1355.46	213.05	-	-	-	-	-	-	C-1	a
non-1-ene	4.0792	1436.20	205.69	-	-	-	-	-	-	C-1	a
pent-1-yne	6.9673	1092.52	227.18	-	-	-	-	-	-	C-1	a
hex-1-yne	7.2567	1351.05	237.47	-	-	-	-	-	-	C-1	b
hept-1-yne	6.2447	918.34	173.47	-	-	-	-	-	-	C-1	b
oct-1-yne	6.9384	1352.05	206.92	-	-	-	-	-	-	C-1	b
methanol	-8.6357	1.1798	-2.4790	-1.0240	-	-	-	-	80.92	C-3	a
ethanol	-8.6859	1.1783	-4.8762	1.5880	-	-	-	-	61.32	C-3	a
propan-1-ol	-8.5371	1.9621	-7.6918	2.9450	-	-	-	-	51.68	C-3	a
propan-2-ol	-8.7366	2.1624	-8.7079	4.7793	-	-	-	-	47.63	C-3	a
benzene	-7.0143	1.5526	-1.8479	-3.7130	-	-	-	-	48.98	C-3	a
toluene	4.0504	1327.62	217.63	-	-	-	-	-	-	C-1	a
ethylbenzene	4.0686	1415.77	212.30	-	-	-	-	-	-	C-1	a

a, (Poling et al., 2000); b, (Dortmund Data Bank Software & Separation Technology GmbH, 2011)

Appendix D

The fugacity coefficients can be determined from an equation of state. The three most widely utilised equations of state for VLE calculations are the Redlich-Kwong (RK) equation (Redlich and Kwong, 1949), the Soave Redlich-Kwong (SRK) equation and the Peng-Robinson (PR) equation (Peng and Robinson, 1976).

The performances of two cubic equations of state (RK and PR) and a modification to the Redlich-Kwong equation of state, the SRK, were compared in Table D-1.

Table D-1: Comparison of three equations of state (Redlich-Kwong, Soave Redlich-Kwong and Peng-Robinson)

Equation of state	**Redlich-Kwong (Redlich & Kwong, 1949)**	**Soave Redlich-Kwong (Soave, 1972)**	**Peng-Robinson (Peng & Robinson, 1976)**
Description of P_i^0	Poor, due to poor expression of the influence of temperature	Accurate description of vapour pressure	Accurate description of vapour pressure
Molar volume	Poor prediction, error of similar magnitude to SRK	Predicts values that are greater than measured values Error worsens with bigger molecular size	More accurate than previous equations of state (RK, SRK), especially for large molecules
Enthalpy departure	Not mentioned	Similar reliability to PR EOS	Similar reliability to SRK EOS
Systems	Adequately describes non-polar to slightly polar hydrocarbons (Holderbaum & Gmehling, 1991)	Can account for more polarity than the RK EOS	Developed for hydrocarbons, but with a change in the mixing rules, can be used for polar compound as well as non-hydrocarbons

The equations of state were defined as:

Redlich-Kwong (Redlich & Kwong, 1949)

$$P = \frac{RT}{V^* - b} - \frac{a}{T^{0.5} V^* (V^* + b)} \qquad \text{(D–1)}$$

Where

$$a_i = 0.42748023 \frac{R^2 T_{c,i}^{2.5}}{P_{c,i}}$$

(D–2)

$$b_i = 0.0864035 \frac{RT_{c,i}}{P_{c,i}}$$

(D–3)

The fugacity coefficient from the RK EOS could be calculated from Equation D-4.

$$ln\varphi = Z - 1 - \ln(Z - BP) - \left(A^2/_B\right) ln\left(1 + \frac{BP}{Z}\right)$$

(D–4)

Where

$$A^2 = \frac{a_i}{R^2 T^{2.5}}$$

(D–5)

$$B = \frac{b}{RT}$$

(D–6)

And

$$Z = \frac{PV}{RT}$$

(D–7)

Soave Redlich-Kwong (Soave, 1972)

$$P = \frac{RT}{V^* - b} - \frac{a(T)}{V^*(V^* + b)}$$

(D–8)

'b' had the same definition as for the R-K EOS, with the definition of 'a' being altered to allow for greater temperature dependence (Equation D-9).

$$a(T) = a_{c,i}\alpha_i(T, \omega_i)$$

(D–9)

$$a_{c,i} = 0.42747 \frac{R^2 T_{c,i}^2}{P_{c,i}}$$

(D–10)

$$\sqrt{\alpha_i} = 1 + m_i\left(1 - \sqrt{\frac{T}{T_{c,i}}}\right)$$

(D–11)

$$m_i = 0.480 + 1.574\omega_i - 0.176\omega_i^2$$

(D–12)

For the fugacity coefficient from the SRK EOS:

$$ln\varphi = Z - 1 - \ln(Z - B) - \left(\frac{A}{B}\right) ln\left(\frac{Z + B}{Z}\right)$$

(D–13)

Where

$$A = \frac{a_i P}{R^2 T^2}$$

(D–14)

and

$$B = \frac{bP}{RT}$$

(D–15)

Peng-Robinson (Peng & Robinson, 1976)

$$P = \frac{RT}{V^* - b} - \frac{a(T, \omega_i)}{V^*(V^* + b) + b(V^* - b)}$$

(D–16)

The '$a(T, \omega_i)$ term' is calculated in the same manner as for Soave Redlich-Kwong, with an alteration to the quadratic equation for determining m_i (Equation D-17).

$$m_i = 0.37464 + 1.54226\omega_i - 0.26992\omega_i^2$$

(D–17)

The fugacity coefficient for a pure component is given by Equation D-18. The parameters, A and B, for Equation D-18 were calculated in the same manner as for the SRK EOS.

$$ln\varphi = Z - 1 - \ln(Z - B) - \left(\frac{A}{2\sqrt{2}B}\right) ln\left(\frac{Z + 2.414B}{Z - 0.414B}\right)$$

(D–18)

blank page

Appendix E

Tsonopoulos Correlation

The equations $f^{(0)}(T_r)$, $f^{(1)}(T_r)$, $f^{(2)}(T_r)$ and $f^{(3)}(T_r)$ for use in the Tsonopoulos equation (equation (4–13), which was proposed by Tsonopoulos (1974) are given by Equations E-1 to E-4.

$$f^{(0)}(T_r) = 0.1445 - \frac{0.330}{T_r} - \frac{0.1385}{T_r^2} - \frac{0.0121}{T_r^3} - \frac{0.000607}{T_r^8} \quad \text{(E–1)}$$

$$f^{(1)}(T_r) = 0.0637 + \frac{0.331}{T_r^2} - \frac{0.423}{T_r^3} - \frac{0.008}{T_r^8} \quad \text{(E–2)}$$

$$f^{(2)}(T_r) = \frac{1}{T_r^6} \quad \text{(E–3)}$$

$$f^{(3)}(T_r) = -\frac{1}{T_r^8} \quad \text{(E–4)}$$

The value for 'a' for all alkanols was set to 0.0878 by Tsonopoulos. The value for 'b' was shown to be a weak function of the dipole moment and in conjunction with the value for 'a', was suggested to be 0.056 by Tsonopoulos. This was later revised to a value of 0.064, which gave a slightly better fit of the prediction to later experimental data (Tsonopoulos et al., 1989).

For other alkanols, the value of 'b' was determined from the equation given by Tsonopoulos (Equation E-5).

$$b = 0.00908 + 0.0006957\frac{\mu^2 P_c}{T_c^2} \quad \text{(E–5)}$$